EFFECTS OF MIXING ON SOLVENT ADDITION TREATMENT PROCESSES

by

Aaron Cheung

A thesis submitted in partial fulfillment of the requirements for the degree of

Master of Science

in

Chemical Engineering

Department of Chemical and Materials Engineering
University of Alberta

© Aaron Cheung, 2019

Abstract

In oil sands extraction, the removal of heavy materials from a bitumen feed is often facilitated by solvent addition treatment processes. These processes mix solvent with bitumen feed to cause the precipitation of heavy products. The settling properties of these heavy products as they separate from the feed can be influenced by the mixing parameters used to combine solvent and feed. Since these properties determine the sizing of settlers and deposition velocity in pipelines, they are important to the overall effectiveness of bitumen recovery operations. Two well known solvent addition treatment processes that have been used in industry for many years are paraffinic froth treatment (PFT) and solvent deasphalting (SDA). While mixing plays a key role in both these processes it is rarely studied making the effects of mixing on solvent addition treatment processes not very well understood. Additionally, both mixing intensity (the rate of energy input) and mixing energy (mixing intensity $\times$ mixing time) are major variables in characterizing mixing. Thus, this study aims to to examine how changes to mixing intensity, mixing energy, and mixer configuration influence separation performance in these processes.

Paraffinic froth treatment involves mixing a light paraffinic solvent, such as n-pentane or n-heptane, with bitumen froth to precipitate out asphaltene aggregates leaving a diluted bitumen product. In this study, bitumen froth from the Athabasca oil sands was mixed with n-pentane inside a windowed autoclave at 80 °C and 6 bar. Mixing intensity and energy were varied by varying impeller speeds from 700 to 1500 RPM and mixing duration from 2 to 60 minutes. Asphaltene aggregates were sampled and recorded settling inside the autoclave through the window and as individual aggregates in a glass column. From these tests, it was observed that mixing at higher mixing energies formed larger aggregates that were lower density and settled more rapidly. Due to the differences in shearing forces, aggregates formed at lower mixing intensities were also found to settle faster than ones formed from mixing at high intensity. When mixing intensity was kept constant, aggregate settling rate was still found to increase with higher mixing energy. Therefore, it was concluded that the fastest settling aggregates formed at low mixing intensity high mixing time conditions.

Solvent deasphalting is traditionally used in refining vacuum residue feeds, but recent interest in partial upgrading technologies has led to exploration of its use with bitumen emulsion feeds extracted from steam-assisted gravity drainage (SAGD). The application of SDA to a bitumen emulsion feed has a potential to result in a three phase mixture of deasphalted oil, pitch, and water. This presents a problem as pitch and water need to flow together but do not readily mix upon settling. This study examined the partial mixing of three phase mixtures to produce a mixture of the bottom two phases while not disturbing the top phase. An analogue alcohol-hydrocarbon-brine mixture was used to simulate SDA phases and test various mixer configurations in a horizontal settler geometry. Ultimately, it was determined that a two-impeller system with a smaller top Lightnin A310 impeller at about $0.8\times$ the diameter of a larger bottom Rushton turbine was the best combination to achieve partial mixing. In order to apply these results to a real process, further investigation of partial mixing with the actual SDA reagents is necessary.

Dedicated to my loving mother, Libby,
for always supporting my choices and endeavors.

Acknowledgements

Collaboration is the foundation of success and the completion of this thesis would not have been possible without the assistance of many individuals whom I am indebted to.

I would like to give the utmost thanks to my supervisor, Dr. Sean Sanders, for all his guidance, support, and for the opportunities he has provided to help me develop professionally. Dr. Sanders has taught me what it means to be a great researcher, teacher, and mentor, always challenging me to think more critically.

I wish to give a huge thank you to Dr. David Breakey for all the endless support and feedback he has provided towards my research. His constant friendship and advice were instrumental in the completion of this work and I will always cherish the lessons he has taught me.

I am also incredibly thankful to Ms. Terry Runyon for her administrative support which made everything run as smoothly as possible.

I would like to give a special thanks to CanmetENERGY for allowing me to use their laboratory space and equipment to perform a significant amount of the experiments in this work. I am especially thankful to Mohamed Ali and Derek Chao for their mentorship throughout this endeavor.

I would also like to acknowledge my colleagues in the Pipeline Transport Processes research group for their helpful ideas and advice. In particular, I would like to thank Simon Sun, Nathan Tinga, Abiodun Olayode, Lisheng (Brad) Zhang, and Akash Saxena for their help, advice, and making me feel welcome in the group.

Finally, I am thankful to Nexen and the NSERC Industrial Research Chair for providing the financial support to make all of this possible. Specifically, I would like to acknowledge Nestor Zerpa, Thiago Righi, and Fredy Cabrales for all of their valuable feedback and help throughout the completion of this work.

Contents

List of Figures

List of Tables

List of Symbols

Symbol	Description	Units
ΔH_i	Enthalpy of vaporization	J/mol
δ_i	Component solubility parameter	$(\text{MPa})^{1/2}$
δ_{mix}	Mixture solubility parameter	$(\text{MPa})^{1/2}$
ϵ	Aggregate porosity	—
μ_L	Fluid viscosity	$\text{Pa} \cdot \text{s}$
Ω	Drag correction factor	—
ϕ_i	Component volume fraction	—
ρ	Density	kg/m^3
ρ_a	Aggregate density	kg/m^3
ρ_L	Fluid density	kg/m^3
ρ_p	Primary particle density	kg/m^3
ρ_s	Solid particle density	kg/m^3
ρ_{eff}	Effective density	kg/m^3
σ	Standard deviation	—
σ_m	Standard error	—
ε_{mix}	Mixing intensity	W/kg
C	Particle concentration	—
C_D	Drag coefficient	—
D	Impeller diameter	m
d	Particle diameter	m
d_a	Aggregate diameter	m

Symbol	Description	Units
E	Mixing energy	J/kg
g	Acceleration due to gravity	m/s^2
H_0	Bitumen froth mixture height	cm
H_c	Interface height at consolidation point	cm
m_{total}	Total mixture mass	kg
N	Impeller rotational speed	s^{-1}
n	Richardson-Zaki settling index	—
N_p	Power number	—
$n_{meas.}$	Number of measurements	—
P	Total mixing power	W
R	Universal gas constant	$J/mol \cdot K$
Re_p	Particle Reynolds number	—
T	Temperature	K
t	Mixing time	s
t_c	Time at consolidation point	s
u_∞	Terminal settling velocity	m/s
u_a	Aggregate settling velocity	m/s
u_s	Hindered settling rate	m/s
V_i	Molar volume	m^3/mol

Chapter 1

Introduction

1.1 Background

With approximately 169 billion barrels in reserve, Canada holds the third largest oil reserves in the world today with 97% of it residing within the Alberta oil sands [1, 2]. In 2017, Alberta produced 81% of Canada's total oil delivering 2.8 million barrels per day [3]. This production is expected to rise to 3.9 million barrels per day by 2027 [3]. As such, it seems likely that the Alberta oil sands will play a prominent role in both the Canadian and worldwide energy market for years to come.

In Alberta, the oil sands themselves consist of bitumen, clays, silica sand, and water. Bitumen is a highly viscous mixture of hydrocarbons, making it difficult to flow without being diluted or heated. It must be separated from mineral solids and water and treated in order to raise its quality to the point where it can be upgraded and refined to produce various products like gasoline, diesel, and aircraft fuel [4].

Currently, approximately 46% of Alberta's oil production comes from surface mining with the remainder being from in-situ extraction techniques such as steam-assisted gravity drainage (SAGD) [3]. Typically, bitumen recovery schemes in surface mining operations involve froth treatment as a key step in the separation of bitumen from mineral solids and water. Froth treatment serves to remove fine solids and water from bitumen froth through the addition of solvent leaving a diluted bitumen product. Downstream in bitumen processing, traditional solvent deasphalting (SDA) is a a popular refinery operation used to further separate heavy feedstock into oil and pitch. In recent years, with industry interest in partial upgrading technologies, the use of an SDA step to partially upgrade bitumen extracted through SAGD is a new area of research with great interest [5, 6]. A parallel can be drawn between the use of froth treatment in surface mining and the use of SDA on SAGD operations as steps in bitumen recovery that are both involved in the removal of heavy materials from bituminous feeds.

The Alberta oil sands has always faced the problem of being geographically isolated

from world markets [5]. Today, that problem is compounded with the issue of limited pipeline capacity available for transport of bitumen products to market. Due to the high cost of building new refineries in Canada, bitumen product is currently exported as diluted bitumen (dilbit) to existing refiners outside of Canada. This is problematic as it requires dedicating approximately 30 vol% of existing pipeline capacity to the transport of diluent to meet pipeline transport viscosity requirements [5]. Once it reaches the refinery, the diluent must be separated out and returned to Alberta which inherently discounts the value of dilbit for producers. As this is incredibly unfavorable to Alberta oil producers, significant interest has been placed into the development of partial upgrading technologies that aim to produce a high yield, pipeline transportable product that removes the need for diluent [5].

1.2 Solvent Addition Treatment Processes

Overall, both froth treatment and solvent deasphalting can be considered processes in which a solvent is added to treat a bitumen feed in order to separate oil from unwanted products like solids, water, and asphaltenes. Asphaltenes are the fraction of crude oil that is insoluble in straight-chain alkanes, such as pentane or heptane, but soluble in toluene [4]. In paraffinic froth treatment (PFT), bitumen froth is mixed with a paraffinic solvent which causes asphaltenes to precipitate out of solution removing water and solids with it. Precipitated asphaltenes combine with the water droplets and dispersed solids to form asphaltene aggregates [4]. In traditional SDA, heavy oil feedstock (vacuum residue) is mixed with solvent at high temperatures to promote the separation of asphaltene rich pitch leaving a deasphalted oil (DAO) product [7].

The general flow diagram of solvent addition treatment processes is shown in Figure 1.1. Generally, as seen in Figure 1.1, solvent addition treatment processes involve a bitumen feed being fed into a mixer and mixed with solvents, which results in a precipitation reaction that forms asphaltene aggregates or pitch droplets. The entire mixture is then sent to a settler where time is given for heavier water and solids to settle out to the bottom of the vessel leaving bitumen product on top. Both froth treatment and SDA aim to efficiently remove unwanted water and heavier oils and solids from bitumen feed in order to produce a cleaner light product. Good mixing is necessary in order to facilitate adequate contact between the solvent and feed. As precipitation occurs during mixing, the settling properties of formed aggregates/droplets can be affected by how mixing is performed [8–10]. Ultimately, changes in these products due to mixing influence how they flow downstream of the settler. Thus, by understanding how mixing influences these properties the overall effectiveness of the process can be improved.

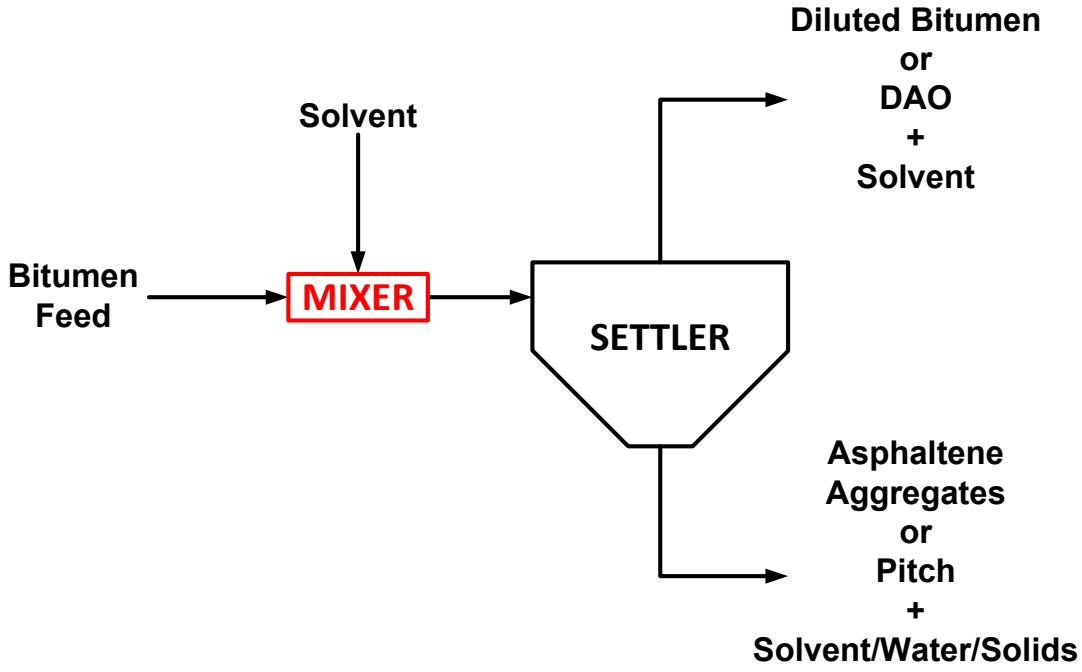

Figure 1.1: High-level overview of solvent addition processes (PFT and SDA)

1.3 Problem Statement

In oil sands extraction, solvent addition treatment processes are typically used to separate heavy materials from a bituminous feed. From Figure 1.1, it can be seen that the mixing parameters used can change the settling properties of heavy products as they separate from the feed. These properties affect the design of settlers and energy requirements to keep solids suspended during pipeline transport and thus have a huge impact on the bitumen recovery process overall.

While many studies into froth treatment processes analyze the effects of temperature [11], solvent choice [12], etc. on aggregate settling properties, few focus on the effects of mixing. Recent studies have shown that changes in mixing can impact the settling properties of heavy products [8–10]. Zawala et al. [9] found that increasing the mixing energy input (mixing intensity x time) in a PFT process led to the formation of higher density aggregates which settled more rapidly. Laplante et al. [8, 13] and Chong et al. [10, 14] discovered that mixing conditions had statistically significant impact on demulsifier performance in naphthenic froth treatment (NFT) applications. They found that changes in mixing conditions could improve demulsifier performance by forming water droplets that settled faster [8, 10]. Changes to aggregate settling properties ultimately affect settler

sizing and the properties of the underflow leaving the settler. As such, better process design in terms of mixer specification and settler sizing can be achieved through improved understanding of the effects of mixing on aggregate settling properties.

Solvent deasphalting holds many parallels to froth treatment processes. However, no studies were found that explore mixing effects in SDA operations. Additionally, recent interest in partial upgrading technologies has sparked new research into the use of SDA on bitumen emulsion feeds coming from SAGD operations [5]. This leads to an interesting challenge as SDA is traditionally performed as part of the refining process with dry bitumen feed in the form of vacuum residue [7]. Feed from SAGD operations comes with water in the form of droplets in emulsion and as free water that conventional SDA has never dealt with. Early studies have found that the application of SDA with a bitumen emulsion feed can result in settling into three phases: water, asphaltene pitch, and DAO [5]. Due to density differences, these phases result in the water phase at the bottom, pitch phase in the middle, and DAO phase on top. In a continuous mixer-settler scheme process, this poses a problem as the pitch layer cannot be drawn out with the water leaving it to accumulate in the settler. A potential solution, that has yet to be investigated in the literature, is installation of a mixer into the settling vessel in order to partially mix the bottom two phases (pitch/water) without entraining the top DAO phase. Successfully accomplishing this would vastly improve the feasibility of the technology.

There is a clearly a knowledge gap present regarding the effects of mixing in solvent addition treatment processes. There is evidence that mixing parameters can effect the settling properties of resulting heavy products. As these properties impact settler design and energy requirements to suspend solids during pipeline transport, understanding how mixing conditions affects these key properties can improve the overall effectiveness of bitumen recovery operations. Therefore, a study of the effects of mixing parameters, such as mixing intensity, mixing duration, and mixer configuration on separation performance of these solvent addition treatment processes is required.

1.4 Objectives

The purpose of this study is to improve the understanding of the effect of mixing on paraffinic froth treatment and partial upgrading solvent deasphalting processes. To this end, the main objectives of this investigation are as follows:

Examine the effects of mixing on aggregate settling in PFT It is necessary to determine how changes in mixing conditions affect the settling properties of asphaltene aggregates formed when bitumen froth and paraffinic solvent are mixed. Asphaltene aggregates will be produced at various mixing conditions and sampled to study the effect of mixing parameters on aggregate settling properties.

Determine the mixing conditions to produce partial mixing in a three-phase system It is important to investigate the type of mixing equipment and conditions necessary to control a three-phase separation to achieve good mixing of the bottom two phases without entraining the top phase. Several mixer types and configurations will be tested over a range of mixing speeds to find combinations that successfully provide partial mixing.

1.5 Thesis Outline

This thesis is organized into six chapters. Chapter 2 reviews the literature and discusses past mixing studies that have been performed on froth treatment applications. Key concepts regarding the characterization of mixing are defined in more detail, and parameters involved in particle and droplet settling are discussed. Chapter 3 provides a more in-depth analysis of past key literature sources that analyzed the effects of mixing on aggregate settling. Data from several sources are combined and analyzed. Chapters 4 and 5 go through the experimental methods, results, and discussion on the studies of mixing in paraffinic froth treatment and the partial mixing of a three-phase system, respectively. Finally, Chapter 6 provides the major conclusions drawn from the investigations performed and gives recommendations for future work.

1.6 Author's Contribution

In this study, the equipment for all PFT testing was provided, calibrated, and commissioned by CanmetENERGY, Devon and Derek Chao. A test matrix and standard operating procedure for the measurement of aggregate settling rates inside and outside of the mixing vessel was developed by the author based on a similar procedure given by Zawala et al. (2012). Safe work procedures for mixing the three-phase analogue solution and testing partial mixing conditions were developed by the author. The author performed all experiments and measurements related to this thesis. A MATLAB program for image processing of video data was written by Dr. David Breakey. Additionally, the design and fabrication of scaled-down clear models of a horizontal settling vessel with a slot for mixers to be installed was performed and overseen by Dr. David Breakey. Interpretation of results including the analysis of the effects of mixing parameters on aggregate size, settling rate, and effective density and the best impeller combination and mixing speed for partial mixing is original work by the author. The author also collapsed the results of various data sources to interpret the trend between mixing energy and settling rate previously observed in the literature. Finally, a comparison of this trend with the results of the current study was also performed by the author.

Chapter 2

Literature Review

2.1 Introduction

Both paraffinic froth treatment (PFT) and solvent deasphalting (SDA) are important processes that are regularly used in bitumen recovery that involve mixing as a key step. While mixing is frequently used in the oil sands extraction industry, it is rarely the focus of study. In the case of froth treatment, studies typically will characterize mixing but focus on the effects of changing other variables such as temperature or solvent-to-bitumen (S/B) ratio instead. No studies were found that characterized mixing in SDA. Mixing can influence the properties of products formed in these solvent addition treatment processes. These properties include aggregate/droplet size, density, and settling rate [8–10]. In turn, these properties are important for the sizing of settlers and deposition velocity in pipelines. Since the deposition velocity is defined as pipeline velocity that must be exceeded to prevent solids from settling out and accumulating at the bottom of the pipe, this influences the power required by pumps to keep aggregates suspended during transport. Thus, the settling properties can influence the overall effectiveness of oil sands extraction.

This chapter reviews some of the more mixing-focused work performed to date. It begins with a more detailed description of solvent addition treatment processes, specifically PFT and SDA. Afterwards, key concepts typically involved in defining mixing and settling are reviewed. Finally, the effects of mixing on solvent addition treatment processes are discussed based on observations in the available literature.

2.2 Solvent Addition Treatment Processes

Paraffinic froth treatment and solvent deasphalting are both solvent addition treatment processes that share various characteristics of operation. Both processes involve precipitation reactions that cause mixing-dependent aggregate/droplet formation which can affect the sizing of settlers and deposition velocity in pipelines. This can impact the overall

effectiveness of bitumen recovery. The goal of both technologies is to separate and remove heavier components from a bitumen feed by taking advantage of the insolubility of these components in the added solvent. In that sense, PFT and SDA are similar in that they can be broken down into one major solvent addition mixing step and one major separation step. However, key differences in PFT and the use of SDA in partial upgrading exist such that there are mixing problems unique to each technology. This section provides in detail discussion of each technology followed by a comparison of the mixing problems identified for each one.

2.2.1 Paraffinic Froth Treatment (PFT)

Figure 2.1 shows a typical surface mining oil sands extraction process. Surface-mined oil sands are fed into crushers that reduce the size of the shoveled sands to small lumps. From here, hot water, surfactant, and pH modifiers are added to the oil lumps to liberate bitumen droplets from the sand grains. This process forms a slurry which is then pumped from the mine to the extraction plant through a hydrotransport pipeline and into gravity separation vessels. In the gravity separation vessels, liberated bitumen droplets are aerated and float to the top where they are removed as bitumen froth. Bitumen froth produced from surface mining operations is typically 60 wt% bitumen, 30 wt% water, and 10 wt%

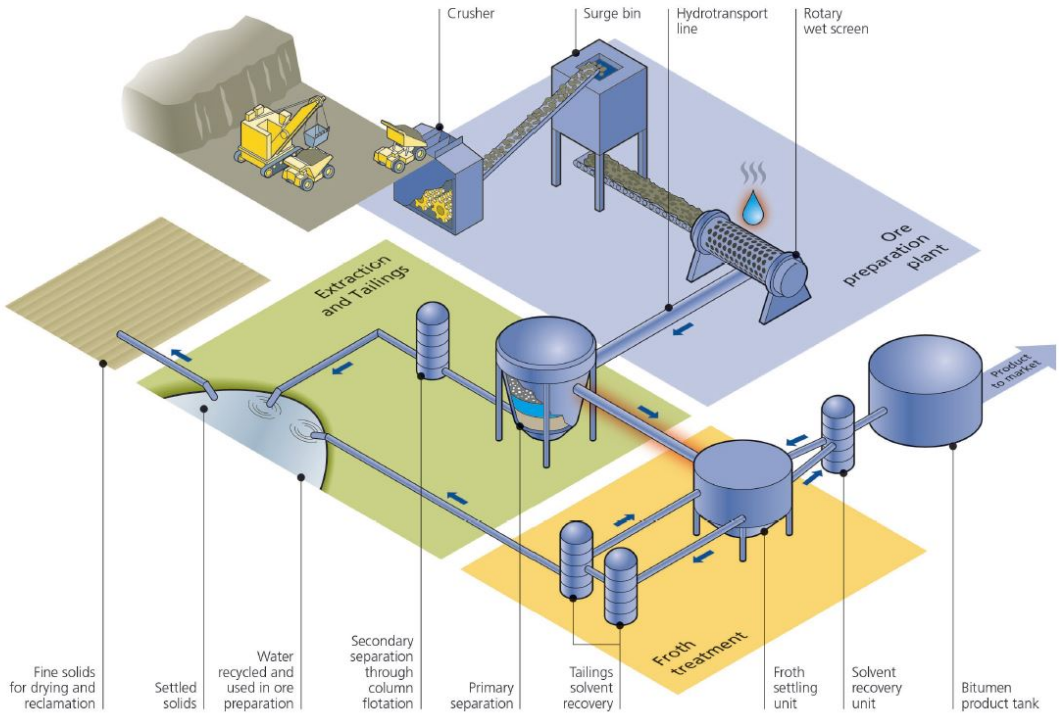

Figure 2.1: Fort Hills oil sands extraction process. Reproduced from Suncor [15].

solids. This quality is not a good enough to be fed to upgrading or refining operations as the water and solids concentration are too high. As such, froth treatment is employed to remove additional water and solids from bitumen froth.

Froth treatment is a process by which water and solids are separated from bitumen through the addition of a chemical solvent. Two types of froth treatment exist: naphthenic froth treatment (NFT) and paraffinic froth treatment (PFT). NFT uses a heavier less expensive solvent known as naphtha whereas PFT uses lighter, more costly paraffinic solvents (such as n-pentane or n-heptane). The different advantages and disadvantages of each are shown in Table 2.1. This study focuses on paraffinic froth treatment as it produces a product that is cleaner and easier to transport than NFT as a result of asphaltene precipitation, and solvent recovery is less energy intensive as paraffinic solvent has a lower boiling point than naphtha. Additionally, the settling properties of PFT-precipitated asphaltene aggregates are more readily observable than NFT. For clarity, PFT is defined as the process in which a paraffinic solvent (such as n-pentane or n-heptane) is added to bitumen froth in order to promote the separation of water and solids from bitumen. Paraffinic solvent refers to solvents made up of paraffin hydrocarbons also known as alkanes. Naphthenic solvents are solvents that contain a mix of paraffins, naphthenes, and aromatic hydrocarbons.

Table 2.1: Advantages and disadvantages of NFT vs PFT [4].

Napthenic Froth Treatment	Paraffinic Froth Treatment
• Uses heavier napthenic solvent referred to as naphtha (cheaper)	• Uses lighter paraffinic solvent (costly)
• Asphaltenes do not precipitate out, leading to higher yield but lower-quality product	• Asphaltenes precipitate out, producing very high-quality product
• Product quality: 98 wt% bitumen, 2 wt% water + solids	• Product quality: 99.9 wt% bitumen, < 0.1 wt% water + solids
• Stable bitumen/water emulsions form that are difficult to deal with	• Precipitated asphaltenes can cause fouling, plugging, and foaming issues in vessels

Asphaltenes by nature do not readily mix with low-molecular weight paraffin hydrocarbons and readily mix with to aromatic hydrocarbons and resins [16]. As such, the addition of a paraffinic solvent destabilizes asphaltene molecules and causes precipitation and flocculation of asphaltenes. Consequently, these asphaltenes combine with dispersed solids and water droplets to form asphaltene aggregates which settle out of bitumen froth. In doing so this process of asphaltene precipitation leads to the removal of water and solids and significantly lowers the bitumen viscosity. Typical asphaltene aggregates are depicted in Figure 2.2.

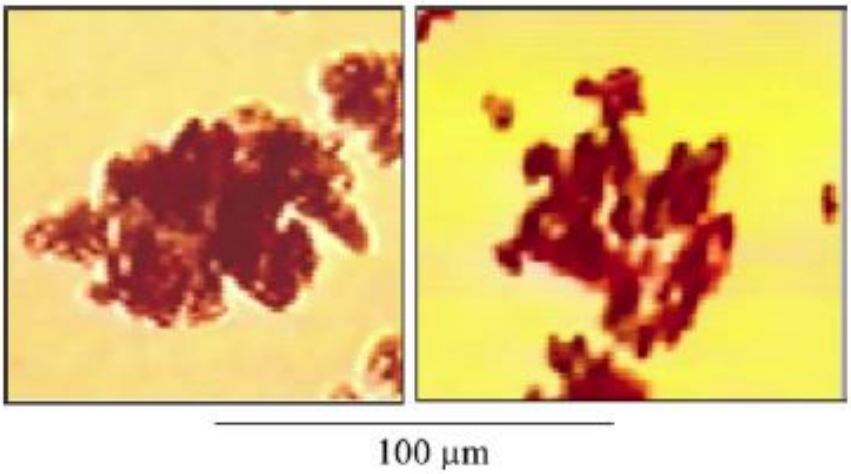

Figure 2.2: Asphaltene aggregates precipitated using n-heptane. Reproduced from Long et al. [11].

In paraffinic froth treatment, mixing facilitates the contact between bitumen froth and solvent leading to the precipitation of asphaltene aggregates in solution. During this process, the energy dissipation from mixing impacts the size and structure of forming aggregates which ultimately changes their settling rates. These changes in settling properties determine the sizing of settlers and energy required by downstream pumps to keep aggregates suspended when transferring the underflow. Thus, one of the objectives of the current study is to determine how mixing conditions affect the settling properties of asphaltene aggregates. Some previous work by others on these mixing condition effects are discussed in greater detail in Section 2.7.

2.2.2 Solvent Deasphalting (SDA)

Since as far back as the 1940s, solvent deasphalting has been used in oil refineries to produce deasphalted oil (DAO) [7]. Conventional SDA operations combine heavy feedstock vacuum residue with solvent in order to precipitate out a low-value pitch phase leaving a high-quality DAO product. Early SDA units achieved this through the use of mixer-settler combinations as previously shown in Figure 1.1. The settlers used were either horizontal or vertical as long as sufficient residence time was given to allow the pitch phase to settle out [7]. One important characteristic of SDA is production of an asphaltene-rich pitch phase which separates out as liquid droplets that coalesce into an extremely viscous fluid at the temperatures conditions that SDA is typically performed ($>$ 140 °C) [17]. This phase can be difficult to deal with due to its high viscosity and as such temperature must be maintained high enough to keep it in a fluid state to flow [18].

Recently, interest in partial upgrading technologies has led to new research into the implementation of SDA with SAGD bitumen emulsion feedstock [5, 6]. A key difference

that this application presents compared to conventional SDA is the presence of water in the emulsion feed that is not present in the typical vacuum residue. This water exists in the feed trapped as droplets in the emulsion and as free water. Due to this water, the application of SDA to a bitumen emulsion feed can result in three fluid phases: DAO, asphaltene pitch, and water [5]. Ideally, in the interest of removing water and solids from the feed, the available free water in the system acts as a carrier fluid to move the viscous liquid pitch phase out of the settler underflow. However, this three-phase separation poses a problem in that the water and pitch phases do not readily mix as pitch is typically made up of aromatic hydrocarbons and asphaltenes [7]. A predicted major issue with this is the case of continuous operation where overflow and underflow are being constantly drawn out of the settling vessel. In this case, if the middle pitch layer cannot leave with the DAO overflow or water underflow, the phase could grow and eventually block vessel outlets. One potential case for how this pitch growth would look is shown in Figure 2.3.

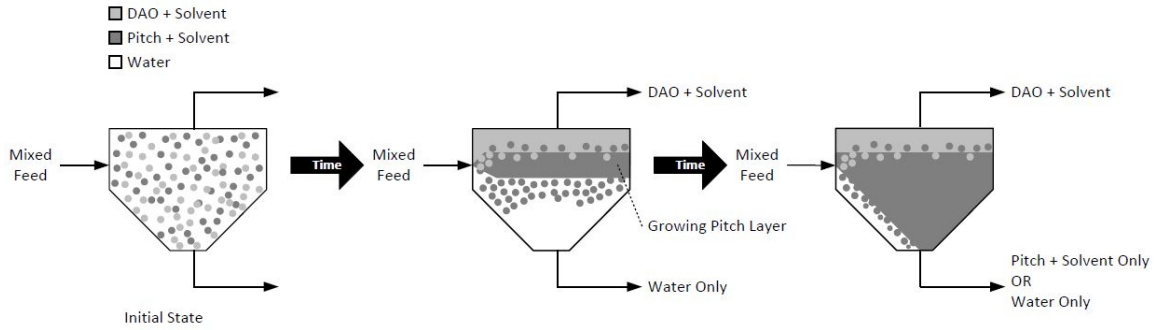

Figure 2.3: Illustration of potential case for a growing pitch layer. Adapted from Breakey and Cheung [19].

To prevent this scenario, the addition of partial mixing aimed at achieving a mixed two-phase underflow with a single-phase overflow has been proposed. By achieving a mixed pitch/solvent + water underflow, the issue of a growing pitch layer and the issue of needing to sacrifice maltenes to flow the pitch can both be solved by implementing partial mixing. This would significantly boost the separation performance and overall viability of the technology. Hence, one of the aims of the current study is to determine the feasibility and conditions necessary to create a homogenous two-phase underflow in a three-phase system without entraining either underflow phase into the overflow. Additionally, successful partial mixing would result in the entrainment of pitch droplets into water to produce a mixed underflow. In this case, the intensity of partial mixing would alter the size of entrained pitch droplets affecting their ability to coalesce and separate from water. The changes to pitch droplet properties caused by partial mixing ultimately determine the energy needed by downstream pumps to keep the pitch and water phase mixed and flow to the rest of the process.

As the use of SDA with a SAGD bitumen emulsion feed is still a new concept, very little is known about the technology. Moreover, testing the actual process at the appropriate temperature and pressure conditions (160 °C and 44 bar based on an SDA partial upgrading process in development) is rather complicated because of the specialized equipment and procedures required to do so as shown in the work by Johnston et al. [17]. Additionally, these tests are not likely to provide good visual information on the formation of the three-phase layer due to the inability to observe the separation of the layers [17]. Thus, the current study employs cold flow analogue fluids in order to analyze a more simplified case as a proof of concept for partial mixing of three phase systems at ambient temperature and pressure conditions. Additional discussion of three-phase separation can be found in Section 5.2.1.

2.2.3 Mixing Challenges in PFT and SDA

Clearly, mixing is a key part of the separation performance of both PFT and SDA processes. In PFT, the formation of asphaltene aggregates is controlled by mixing, which brings bitumen froth and solvent together. As such, the settling properties of formed asphaltene aggregates can be directly changed by mixing conditions. In SDA, mixing can be used as powerful tool to alter settling properties, such as pitch droplet size, so that pitch can become entrained within the underflow water phase causing more effective separation from the DAO overflow. Therefore, it can be said that both in PFT and SDA, mixing conditions determine the settling properties of the heavy products as they separate from the feed. Since these properties determine to the sizing of settlers and energy required to keep aggregates suspended in pipelines, knowledge of how mixing affects these properties can help improve the effectiveness of oil sands extraction overall.

From the above discussion, it can also be seen that PFT and SDA in partial upgrading are different as well. To begin with, PFT and SDA each deal with very different bitumen feeds. PFT feeds are typically bitumen froth with around 10 wt% solids whereas a partial upgrading SDA feed is bitumen emulsion with no solids. This results in the solvent-addition separation in PFT process to result in two phases: a clean diluted bitumen product, and asphaltene aggregates which contain solids and water. In contrast, SDA partial upgrading could result in three phases of products: DAO, pitch, and water. These differences lead to different mixing challenges faced by each solvent addition treatment process. For PFT, mixing is important during the first contact between the bitumen feed and solvent prior to settling as mixing conditions impact asphaltene aggregate formation leading to changes in settling properties. For partial upgrading of bitumen emulsion with SDA, the potential for products to separate into three phases in the settler after initial mixing of solvent and feed presents a different problem. In order to impact separation performance here, additional partial mixing of the three-phase system must be introduced

in the settler. Figure 2.4 illustrates the differences in mixing challenges faced by each technology.

To address these mixing challenges, the current study examines the effects of mixing on PFT and SDA as separate studies. PFT tests focus on varying the mixing conditions used to combine bitumen froth and solvent and analyzing the effects of these mixing conditions on formed asphaltene aggregates. On the other hand, SDA testing focuses on testing mixer configurations that can achieve partial mixing of two underflow phases in a three phase system.

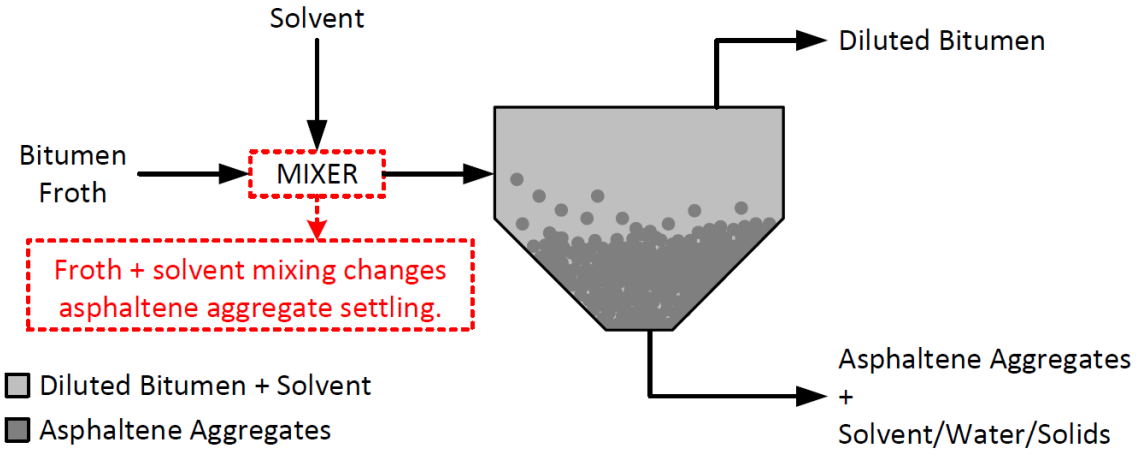

(a) Paraffinic Froth Treatment

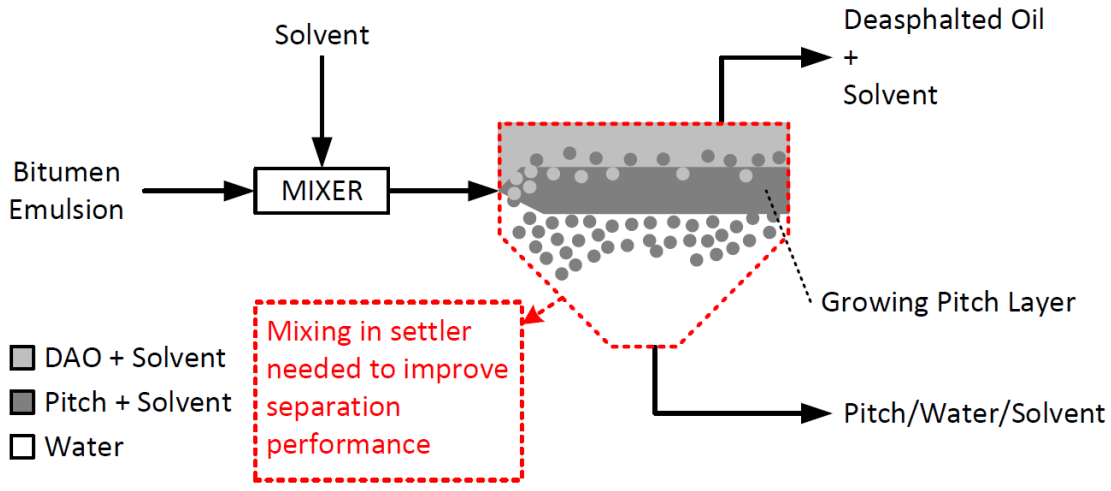

(b) Solvent Deasphalting of Bitumen Emulsion

Figure 2.4: Comparison of PFT and SDA.

2.3 Aims of Mixing

As discussed in Section 2.2, mixing is a crucial step in the separation performance of PFT and SDA. When discussing mixing, it is important to define the goals of mixing in each of these processes. To define these goals, it must first be made clear what is considered "good mixing".

When it comes to mixing, there are many proposed definitions for what is considered "well mixed". The most widely accepted of these definitions comes from Kukukova et al. [20] in which mixing is described by three parameters: the intensity of segregation, the scale of segregation, and the exposure of the dispersed phase. Figure 2.5 illustrates these parameters. Intensity of segregation refers to the uniformity of concentration [20]. The scale of segregation defines the length scale of mixing that is desired in any given application [20]. For example, it can be taken as a measure of droplet size in operations involving flocculation and coalescence. Exposure represents the rate of change of segregation [20]. It is a measure of the physical contact between two or more substances, the strength of interaction between them, and how far from the maximum mixed state a system is [20]. As such, exposure can be considered a driving force for change.

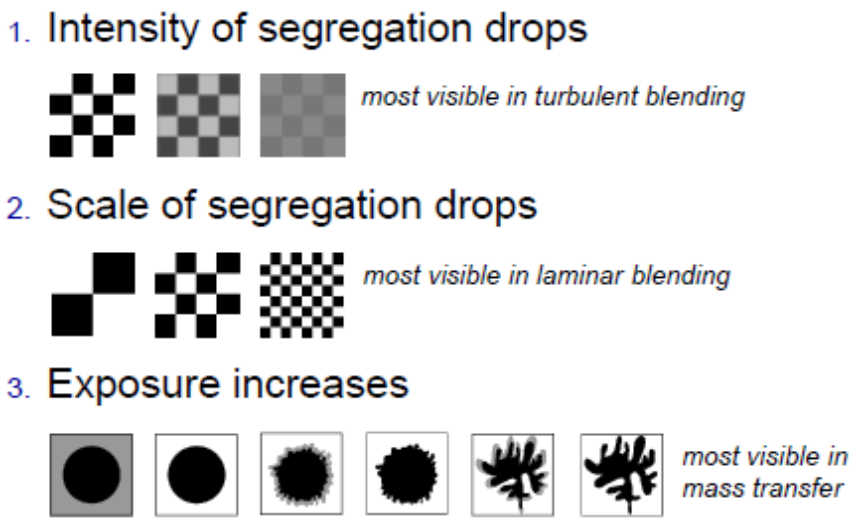

Figure 2.5: Dimensions of segregation. Reproduced from Kresta [21].

When taking these definitions together, good mixing is defined as mixing aimed at achieving a chosen uniformity of concentration or droplet size fast enough to support a desired reaction. Within the context of PFT, mixing aims to adequately combine bitumen froth and solvent uniformly such that precipitation of asphaltene aggregates removes solids and water efficiently from the feed. When applying SDA to partially upgrade bitumen emulsion, in order to overcome the issues of a three-phase product described in Section 2.2.2, mixing in the settler aims to break down pitch droplets into entities small enough to be entrained in the underflow water phase.

2.4 Mixing Equipment

Traditionally, in-line static mixers are the primary mixing technology employed in PFT and SDA operations as they can provide good mixing between fluids in a short amount of time. In many other processes and in lab-scale testing, stirred tanks are the most commonly used mixers as they can cover a wide range of mixing conditions. A brief review of these technologies is provided here.

2.4.1 Static Mixer

In its simplest form a static mixer can be described as a series of stationary mixing elements placed inside a pipe [22]. Figure 2.6 shows some examples of static mixers available in industry today. Static mixers work on the basic principle that these stationary internal elements act as baffles which fold and reorient flow passing through the pipe in order to radially mix the contents [22]. Because of this, static mixers in industry are most often employed in continuous operation where there is a constant flow of feed to be mixed. For PFT and SDA, static mixers provide consistent, high intensity mixing between bitumen feed and solvent in a relatively short amount of time. In terms of lab-scale testing, varying mixing conditions with static mixers can be accomplished through changing the number of elements and flow rate. However, this can be tricky as certain static mixers only work in laminar or turbulent flow. Varying mixing conditions is often much simpler with stirred tanks.

Figure 2.6: Examples of static mixers. From left: vortex mixer (KVM), corrugated plate mixer (SMV), wall-mounted vanes (SMF), cross-bar mixer (SMX), helical twist mixer (KHT), cross-bar mixer (SMXL). Reproduced from Paul et al. [22].

2.4.2 Stirred Tank

Involved in over 50% of the world's chemical production, mechanically stirred tanks are by far one of the most common mixing technologies in use today [22]. Stirred tanks can be used in continuous operation, with a consistent feed and exit stream, or in batch operation, in which feed is combined in the tank and product is withdrawn after mixing for a certain amount of time. Figure 2.7 shows the schematic of a typical stirred tank. Fundamentally, a stirred tank mixes its contents by physically moving material around using impeller blades [22]. The effectiveness of mixing in stirred tanks depends largely on geometry of the vessel and impeller as well. When it comes to lab-scale testing, mixing conditions in stirred tank can be easily varied by changing the impeller speed and duration of mixing. This provides an advantage over static mixers as the purchase of multiple mixing elements is not necessary to test a wide range of mixing conditions. Additionally, batch testing is often preferred for bench-scale mixing experiments as setups are usually simpler. In that regard, stirred tanks are simpler than static mixers in batch operation as testing only requires the stirred tank itself whereas a feed tank, pump, and collection tank are needed for batch testing of a static mixer. As such, the current study focuses on characterizing mixing using batch testing in a stirred tank geometry.

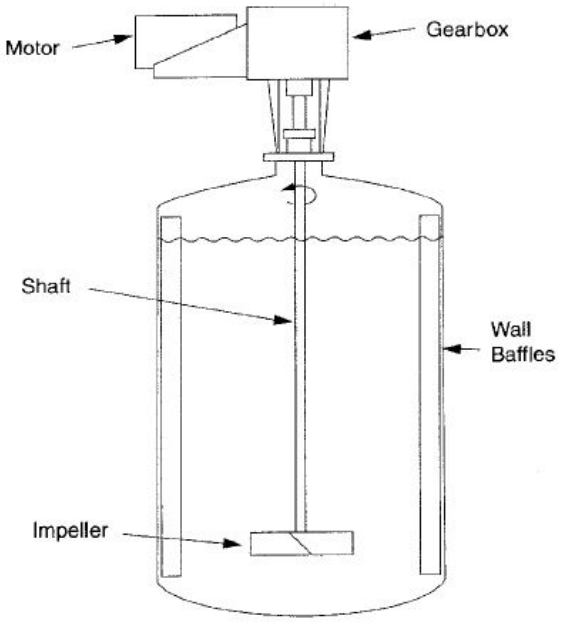

Figure 2.7: Schematic of a conventional stirred tank. Reproduced from Paul et al. [22].

2.4.3 Impellers

One of the focuses of the current study is to test mixer configurations in order to achieve partial mixing of two underflow phases in a three-phase system. Accordingly, some basic knowledge of impeller functionality is provided here. Impeller and tank geometry also have a large impact on how mixing occurs in general. In fact, the impeller blade width, number of blades, blade angle, diameter-to-tank-diameter ratio (D/T), baffle configuration, and impeller clearance all influence the mixing in any given stirred tank application [22]. Impeller geometry also dictates the flow pattern within the vessel. There are two main types of flow patterns produced in a stirred tank depending on the impeller type: axial and radial [22].

Axial flow impellers produce flow patterns that involve pumping fluid in one direction (up or down depending on the orientation of impeller) creating a single circulation loop [22]. Marine impellers and Lightnin A310 hydrofoils are both good examples of commonly used axial flow impellers. Marine impellers resemble propellers typically used on watercraft and provide high pumping of fluid in one direction. Meanwhile, the Lightnin A310 hydrofoil consists of three pitched slightly-curved blades that produce a conical pumping flow similar to a draft tube.

Radial flow impellers push fluid radially to produce two circulation loops, one below and one above the impeller [22]. The Rushton turbine is one of the most commonly used radial flow impeller in industry [22]. Rushton turbines typically consist of a flat disc with six paddles. When mixing, these paddles push flow outward radially towards the vessel walls producing a high shear rate.

The flow patterns of axial and radial impellers are shown in Figure 2.8. A marine, Lightnin A310, and Rushton turbine are shown in Figure 2.9.

Ideally, good partial mixing of the underflow in a three-phase system occurs with an impeller configuration that can draw down and disperse the middle phase into the bottom

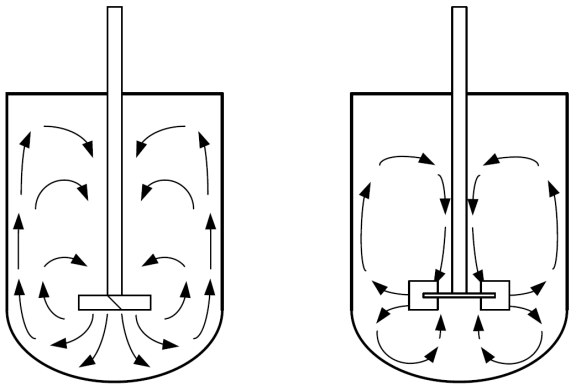

Figure 2.8: Flow patterns for axial (left) and radial (right) impellers. Adapted from Kresta et al. [23].

Figure 2.9: Marine (left), Lightnin A310 hydrofoil (middle), and Rushton (right) impellers.

phase without pulling the top phase as well. This is essentially a liquid-liquid dispersion which is a common mixing problem. For the dispersion of a lighter liquid phase into a heavier liquid phase, the Handbook of Industrial Mixing [22] recommends the use of a multi-impeller system with a top axial impeller with a bottom radial impeller. This combination produces high flow with low power as the axial impeller entrains the lighter phase into the radial impeller for dispersion into the heavier phase [22]. As such, this is a good starting point when considering impeller combinations for partial mixing. More detailed discussion of the considerations that went into the experiment design of SDA partial mixing are given in Section 5.2.

2.5 Mixing Characterization

Since mixing is so important to solvent addition treatment processes, it is just as important to discuss how it is characterized. Mixing is typically quantified by either mixing intensity or energy input. Mixing intensity is defined as the rate of energy dissipation during mixing while mixing energy refers to the total energy input during a set time. In order to more adequately define mixing intensity and mixing energy in more physical terms a discussion about energy dissipation is necessary.

For an impeller, mixing intensity refers to the rate at which energy is transferred from the impeller to the fluid and then ultimately dissipated. As such, energy dissipation is a key measure of mixing intensity. Since mixing energy is dissipated as heat, energy dissipation can also be interpreted as the rate at which kinetic energy is converted heat. The rate at which turbulent kinetic energy dissipates per unit mass is one of the most important measures to characterize mixing [23]. Of course, in typical mixing devices, energy dissipation is not the same at all locations or at all times during mixing. In fact, the

local energy dissipation at the impeller can vary by a factor of up to 10× the average [24]. An average energy dissipation, can be calculated by dividing the total mixing power, P (energy/time), by the total mixture mass, m_{total} [22]:

$$\varepsilon_{mix} = \frac{P}{m_{total}} \tag{2.1}$$

This average energy dissipation is often taken as a measure of mixing intensity [22]. In a stirred tank, the power is given by the equation:

$$P = N_p \rho N^3 D^5 \tag{2.2}$$

where N_p is the power number, ρ is the density of the continuous phase , N is the impeller rotational speed (rotations/second), and D is the impeller diameter. The power number is simply a non-dimensional variable to characterize the power consumed by the impeller and dissipated throughout the fluid. Table 2.2 shows the power numbers for some common impellers relevant to this study. Note that the values given in Table 2.2 are for turbulent mixing where the power number is relatively constant as opposed to laminar or transitional mixing where the power number changes with Reynolds number [22].

Table 2.2: Impeller power numbers for turbulent mixing. Taken from Paul et al. [22]

Impeller Type	N_p
45 ° pitch blade turbine (PBT), 6 blades	1.64
Lightnin A310 hydrofoil	0.3
Rushton turbine	5.5

When scaling up a mixing process from a successful bench-scale test to the pilot scale and ultimately industrial scale, the primary objective is to design a system that achieves the same quality of mixing in the large-scale process as was observed at the bench scale. Both the rate of energy dissipation (mixing intensity) and mixing time are important factors to consider when characterizing mixing for scale up. Mixing intensity , ε_{mix} (power/mass), and mixing time , t (, can be combined to give a single scaling variable: mixing energy, $E = \varepsilon_{mix} \times t$ where E is in units of energy/mass [14]. If a process is found to scale by mixing energy, then testing allows mixing conditions from batch process (mixing intensity × mixing time) to be translated to continuous processes (mixing intensity × residence time) because how that mixing energy is achieved should not matter [14].

The choice to scale by mixing intensity vs. mixing energy could lead to very different equipment choices as shown in Figure 2.10. Based off the definition of mixing energy, it is clear that two extreme approaches can be taken to achieve the same mixing energy value: low mixing intensity with a long mixing time (such as mixing using turbulence in a long

Figure 2.10: Difference in equipment choice based on mixing needs.

pipe flow or a stirred tank at low impeller speeds), or high mixing intensity at a low mixing time (such as mixing through a static mixer or a stirred tank at high impeller speeds). If a process scales with mixing energy, then how that mixing energy is achieved should not matter. However, if the mixing process scales with mixing intensity, then the choice of equipment becomes rather important. For instance, if a solvent addition treatment process were incorrectly scaled by mixing energy when mixing intensity was important, equipment could be chosen that does not provide enough mixing intensity to homogeneously mix solvent and bitumen feed. This could result in uneven precipitation, leaving parts of the feed completely unaffected by solvent by the time the mixture reaches the settler resulting in poor separation performance overall. On the other hand, if a solvent addition process was scaled by mixing intensity when mixing energy was important, inadequate mixing times could lead to smaller aggregate/droplet sizes which would result in slower settling times. Slower settling times would require larger settlers with more residence time to deal with this. As such, both mixing intensity and mixing energy are important variables to be considered when scaling up a mixing process.

Currently, very few studies in PFT mixing distinguish between the effects of mixing intensity and mixing energy on settling. As such, it is unclear which mixing parameter is more important to the PFT process. One study was found that examined the effects of mixing speed and time on asphaltene floc sizes. This study is discussed in more detail in Chapter 3.

2.6 Particle and Droplet Settling Theory

Recall from Section 1.3 that aggregate/droplet settling properties are important to solvent-addition operations as they influence the sizing and specification of the settlers. As such, alongside mixing parameters, variables that define settling should be identified as well.

Generally, the settling of particles or droplets in a fluid medium is discussed in two scenarios: (1) individual particle and droplet settling, or (2) hindered settling of particles and droplets. Individual settling refers to the case of a single particle or droplet settling in a infinite fluid medium with no other particle or droplets around it. Hindered settling refers to the settling of particle or droplets with other particles/droplets around them causing slower settling overall due to interactions between particles/droplets. Both are important to discuss when characterizing settling.

2.6.1 Individual Particle and Droplet Settling

One of the most critical parameters to discuss in aggregate settling is the terminal settling velocity (u_∞). Terminal settling velocity is the constant speed at which a particle falls through a fluid medium when the drag and buoyancy forces from the fluid equal the force of gravity caused by the particle's weight. For a single solid spherical particle settling in an infinite medium of Newtonian fluid, the terminal velocity can be given from the force balance as:

$$u_\infty = \left[\frac{4gd(\rho_s - \rho_L)}{3C_D\rho_L}\right]^{1/2} \tag{2.3}$$

where g is the acceleration due to gravity, d is the particle diameter, ρ_s is the particle density, ρ_L is the fluid density, and C_D is the drag coefficient. The drag coefficient depends upon the particle Reynolds number, Re_p, which is the ratio of inertial to viscous forces of the flow surrounding the particle and can be given by:

$$Re_p = \frac{\rho_L u_\infty d}{\mu_L} \tag{2.4}$$

where μ_L is the fluid viscosity. For spherical particles, the correlations for C_D are written as:

$$C_D = \frac{24}{Re_p} \qquad Re_p \leq 0.3 \tag{2.5a}$$

$$C_D = \frac{24}{Re_p}\left(1 + 0.15Re_p^{0.687}\right) \qquad 0.3 < Re_p \leq 1000 \tag{2.5b}$$

$$C_D \approx 0.445 \qquad 1000 < Re_p \leq 10^5 \tag{2.5c}$$

In general, particles in a PFT settler settle in Stokes' regime ($Re_p \ll 1$). In this case, $C_D = 24/Re_p$ and Equation (2.3) can be rewritten as the well-known Stokes' Law:

$$u_\infty = \frac{d^2 g(\rho_s - \rho_L)}{18\mu_L} \tag{2.6}$$

From Equation (2.6), it can be seen that for a given fluid, an individual particle's size (diameter), density, and settling velocity are the key parameters to characterizing its settling properties.

2.6.2 Settling of Fractal Structures

It is generally accepted in the literature that asphaltene aggregates are fractal structures [11, 25, 26]. Fractal structures are defined as irregularly shaped systems with the same degree of irregularity on all scales [27]. For the settling of porous structures, a general force balance on a spherical porous aggregate settling in an infinite medium is given by [28]:

$$\frac{(\rho_a - \rho_L)}{(\rho_p - \rho_L)} = (1 - \epsilon) = \frac{3\rho_L \Omega C_D}{4g(\rho_p - \rho_L)d_a} u_a^2 \tag{2.7}$$

where ρ_a, ρ_p, and ρ_L are the aggregate, primary particle, and liquid densities (kg/m^3), respectively, ϵ is the aggregate porosity, Ω is the correction factor for drag experienced by a porous aggregate compared to a solid sphere, and u_a and d_a are the measured aggregate settling rate (m/s) and diameter (m), respectively. The difference between the aggregate and liquid density is often defined as the effective density, $\rho_{eff} = \rho_a - \rho_L$, and can be obtained by multiplying Equation (2.7) through by $(\rho_p - \rho_L)$ to get:

$$\rho_{eff} = \frac{3\rho_L \Omega C_D}{4g d_a} u_a^2 \tag{2.8}$$

2.6.3 Hindered Settling of Particles and Droplets

Stokes' Law as given in Equation (2.6) is limited to describing a single spherical particle settling in an infinite medium. In reality, in most settling applications, particles settle with other particles around them. Particle-particle, particle-fluid, particle-wall interactions, and even upward liquid flow all act to reduce the particle settling velocity of individual particles producing what is known as hindered settling. In PFT, many individual asphaltene aggregates precipitate out together upon the addition of solvent [9, 16]. It is not too difficult to imagine that these aggregates would interact with one another, hindering other individual aggregate settling. By far the most famous equation describing hindered settling comes from Richardson and Zaki [29] which relates the hindered settling velocity, u_s (m/s), to the terminal settling velocity:

$$\frac{u_s}{u_\infty} = (1 - C)^n \tag{2.9}$$

where C is the volume concentration of solids, and n is the settling index which depends on the particle Reynolds number. When settling in the Stokes regime ($Re_p \leq 0.3$) the value of n is 4.7 [29].

Overall, the settling properties discussed here are crucial when evaluating the effects of mixing on solvent addition treatment processes as these properties determine the design of settlers and energy requirements to suspend solids during pipeline transport. For instance, lower settling velocities would indicate the need for a larger settler or lower system flow rates in order to provide enough residence time for effective separation of products. As such, the resulting settling properties of asphaltene aggregates and pitch droplets can be a good indicator of how mixing influences the overall separation performance of solvent addition treatment processes.

2.7 Mixing Effects on Settling Properties

Based on the discussions thus far, it is clear that mixing has the potential to impact the settling properties of heavy products in solvent addition treatment processes. In particular, the settling of asphaltene aggregates formed in PFT and pitch droplets formed in SDA are of interest. However, how mixing impacts these settling properties remains largely unknown and is the subject of the current study. While there are very few studies that focus on the aspect of mixing in PFT processes and none that could be found for SDA, one can discuss the likely effects of mixing on solvent addition treatment processes based on the available studies and fundamental knowledge of mixing. For instance, it is expected that higher mixing intensities would lead to smaller aggregate/droplet sizes during mixing as greater shearing forces from the fluid would be present [22]. In turn, smaller aggregate/droplet sizes would result in slower settling based on the relationship seen in Stokes' law (Equation (2.6)). A more detailed discussion of mixing effects on PFT and SDA processes is continued in Sections 2.7.1 and 2.7.2, respectively.

2.7.1 Mixing in Paraffinic Froth Treatment

2.7.1.1 Effects of Laminar Shear

As mentioned in Section 2.2.1, the addition of solvent in PFT results in the precipitation of asphaltenes which undergo aggregation with dispersed solids and water droplets in bitumen froth to form asphaltene aggregates. Aggregation is known to be a dynamic process in which rates of aggregation and fragmentation of colloidal particles initially compete, changing the size distribution based on the dominant process [16]. Eventually, after some amount of time, a steady state is reached when aggregate and fragmentation rates balance, resulting in a stable unchanging floc size distribution [16]. Since the physical act of mixing causes shearing, it is important to examine the effects of shear on aggregate settling properties. Rahmani et al. [16] studied the effects of shear rate, particle concentration, and solvent composition on the evolution of asphaltene aggregate floc sizes

in a model system. This model system consisted of extracted asphaltenes being mixed with toluene-heptane solvent for at 300 rpm for 15 s in an unbaffled beaker then transferred to a Couette cylinder to be sheared under laminar flow conditions.

Figure 2.11 shows the aggregate size findings by Rahmani et al. [16] with regards to shear rate. Based on Figure 2.11, Rahmani et al. [16] described the flocculation process of asphaltene aggregates as follows: In the beginning, aggregation rate dominates the flocculation process. As the floc size reaches a maximum, fragmentation rate becomes significant balancing aggregation rate. From this point, the average floc size decreases from the maximum to a steady state size. This is caused by either large fragile flocs fragmenting or floc structures reorganizing to become more stable. Ultimately, Rahmani et al. [16] concluded that, under laminar flow conditions, higher shear rates resulted in higher initial aggregation rate but led to smaller steady state floc sizes due to higher fragmentation rate. They found that the average steady state floc sizes go from roughly 250 μm at low shear rate (1.2 s^{-1}) to about 100 μm at high shear rate (12.7 s^{-1}).

In another study on the effects of shear on asphaltene aggregates, Rahmani et al. [30] produced aggregates in a stirred tank reactor at various fluid shear rates. Figure 2.12 shows their results of mixing at two different impeller speeds. As shown in Figure 2.12, the correlation between aggregate settling velocity and aggregate size is quite poor. Note that based on Equation (2.1) and Equation (2.2), it is apparent that mixing intensity is proportional to impeller speed cubed (N^3). Thus, Figure 2.12 is also showing a difference in mixing intensity. Based on this, it can be said that there is a 10$\times$ mixing intensity difference seen here between the two cases in Figure 2.12. However, the difference in settling rates between mixing intensities is not very pronounced.

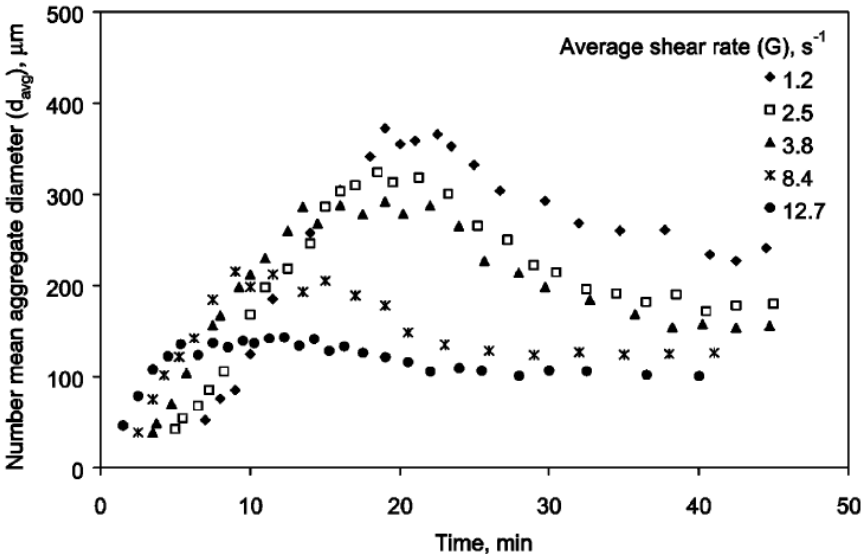

Figure 2.11: Evolution of asphaltene aggregate size as a function of laminar shear rate in a Couette cylinder device. Reproduced from Rahmani et al. [16].

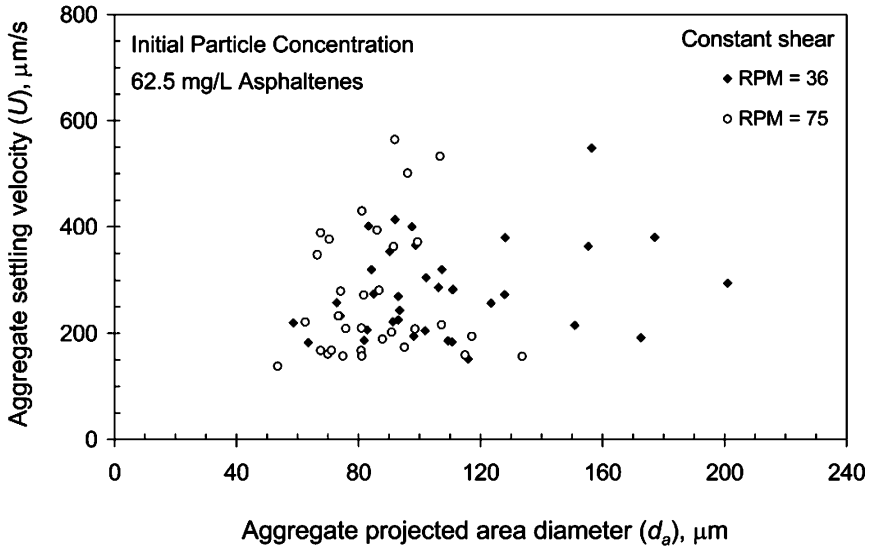

Figure 2.12: Settling velocities of individual aggregates from different shear rates. Reproduced from Rahmani et al. [30].

Rahmani et al. [30] also showed that extracted asphaltene aggregates had higher porosity and lower density with increasing size indicating highly porous structures. This result is shown in Figure 2.13. Furthermore, they found that three-dimensional size-density fractal dimensions ranged from 1.3 to 2.0 [30]. Fractal dimension, a quantitative value between 1 and 3, is often used to describe structure of aggregates [27]. Values closer to 1 indicate a linear structure while values closer to 3 indicate a more compact structure [27, 30, 31]. Thus, Rahmani et al. [30] concluded that the observed fractal dimensions confirmed the more porous structure of extracted asphaltene aggregates. The trend observed in Figure 2.13 could explain the poor correlation between settling rate and aggregate diameter observed in Figure 2.12 as according to Equation (2.7) $u_a \propto \sqrt{\rho_{eff} d_a}$. This proportionality indicates that because larger aggregates have lower effective densities, the overall settling rate would not change that much.

Overall, the studies by Rahmani et al. [16, 30] show that shearing in laminar flow caused by mixing can impact the settling properties of asphaltene aggregates. In particular, their studies indicate that higher shearing produces smaller aggregates and that smaller aggregates are less porous. This combined effect of shearing on aggregate size and porosity results in minimal change to aggregate settling rates between different shear rates caused by mixing. These results imply that changes in mixing intensity in laminar flow conditions have little effect on aggregate settling rate, but huge impacts on aggregate size and structure.

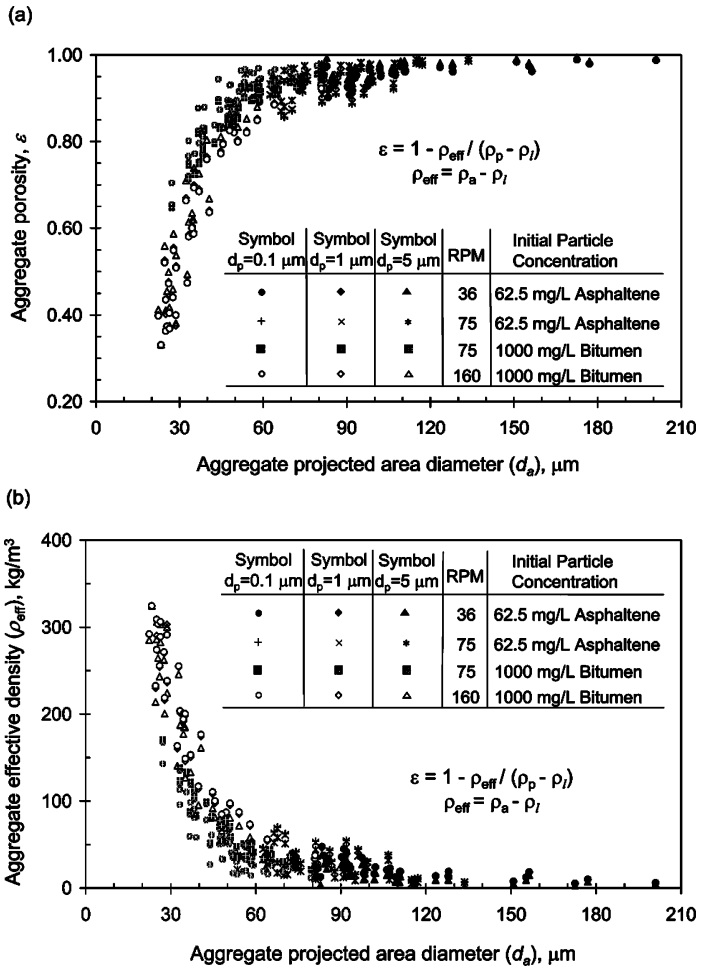

Figure 2.13: Asphaltene aggregate porosity and density as functions of diameter. Reproduced from Rahmani et al. [30].

2.7.1.2 Effects of Mixing Energy

Zawala et al. [9] studied the effect of increasing mixing energy (mixing intensity $\times$ time) on asphaltene aggregates produced from paraffinic froth treatment. In their experiment, n-pentane was mixed with bitumen froth (56% bitumen, 34% water, 10% solids) inside a bench-scale windowed autoclave at various mixing speeds and durations. Their setup consisted of a 62.5 mm diameter cylindrical autoclave vessel that was 187.5 mm in height. Two 6-bladed pitch blade turbines, 31.3 mm in diameter, were set at a clearance of 31.3 mm and used to perform all mixing. Mixing speed and time were varied between 700 – 1500 rpm and 2 – 60 min, respectively.

In terms of individual aggregate settling velocities, Zawala et al. [9] found a clear separation in the settling velocities of aggregates produced from different mixing energies. This result is shown Figure 2.14. Figure 2.14 shows that at a constant mixing energy, increased diameter led to higher settling velocities; however, aggregates produced from

higher mixing energy resulted in overall higher settling rates. Based on Equation (2.1) and Equation (2.2), the mixing power and thereby mixing intensity increases to the cube of the impeller speed (N^3). This results in about a 10× more mixing intensity experienced by the data shown in white dots compared to the black dots in Figure 2.14. This is the same mixing intensity difference seen in Figure 2.12 from Rahmani et al. [30]. However, given that the mixing time was kept constant in Figure 2.12, there is only a 10× mixing energy difference seen in Rahmani et al. [30] study compared to the 100× mixing energy difference presented in Figure 2.14. This difference in mixing energy as a result of mixing time could explain why the data is so distinctly apart in Figure 2.14, but not in Figure 2.12. Clearly, the effect of mixing energy is more complicated and requires further investigation.

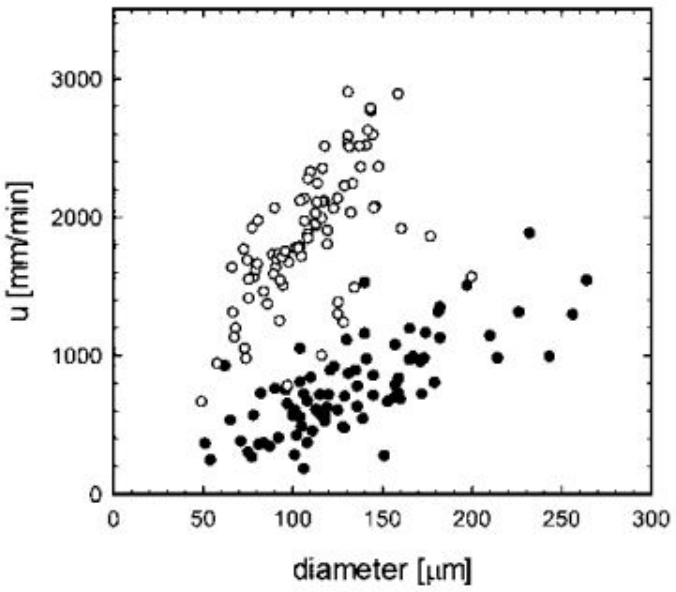

Figure 2.14: Settling velocities of individual aggregates from different mixing conditions: black dots – 700 rpm, 6 min, white dots – 1500 rpm, 60 min. Reproduced from Zawala et al. [9].

Zawala et al. [9] also investigated the hindered settling velocities of asphaltene aggregates as they settled inside the autoclave (in-situ settling). This was done by recording the settling of asphaltene aggregates through the window on the side of their autoclave vessel. They found that these hindered settling velocities were significantly influenced by the mixing energy at which they were produced as can be seen in Figure 2.15. It can be clearly seen from Figure 2.15 that increasing the mixing energy appears to increase the aggregate settling rate. When comparing, the results in Figure 2.15 are consistent with the Zawala et al.'s [9] findings in Figure 2.14. That is, asphaltene aggregates settled faster as individual aggregates and in the hindered settling case when produced at higher mixing energies. From Figure 2.15, it was also noted that Zawala et al. [9] reported all results as a function of mixing energy. Based on the definition of mixing energy discussed in

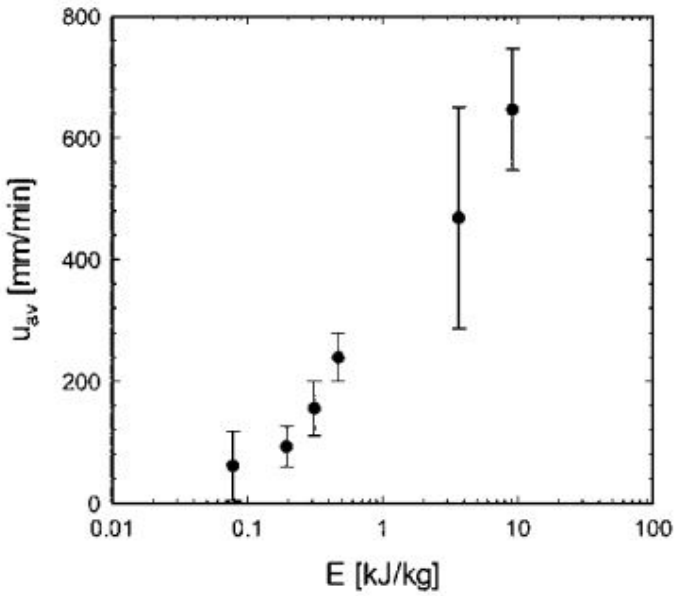

Figure 2.15: Average hindered settling velocities of asphaltene aggregates as a function of mixing energy. Reproduced from Zawala et al. [9].

Section 2.5, it is known that a single mixing energy value can be obtained with various combinations of mixing intensity and time, which means that the exact conditions for each test cannot be retrieved from the data.

Upon investigating the reason that higher mixing energy produced faster settling aggregates, Zawala et al. [9] found that increasing the mixing energy only led to slight change in aggregate size. Figure 2.16 shows their results. Similar to Figure 2.14, there is about 10× more mixing intensity in distribution B than distribution A in Figure 2.16. Additionally, given that mixing energy is the mixing intensity × mixing time, this results in about a 100× more mixing energy input into distribution B compared to A. However, as it can be seen from Figure 2.16, this increase in mixing intensity and energy only results in a slightly more narrow distribution and about a 9% decrease in mean diameter. As such, Zawala et al. [9] concluded that the separation in settling rate shown in Figure 2.14 is not likely a result of changes in aggregate size.

Further investigation into why higher mixing energy produced faster settling aggregates despite the small change in aggregate size revealed that increased mixing energy created aggregates with higher dispersed solids (DS) percentage. From this, Zawala et al. [9] concluded that higher mixing energy produced denser rather than more porous aggregates as a result of increases dispersed solids content. Consequently, as indicated by Equation (2.7), the increased effective density of aggregates led to increased settling velocities, thus explaining the observed relationship between mixing energy and settling rate. Finally, Zawala et al. [9] found that using an n-pentane solvent produced nonporous

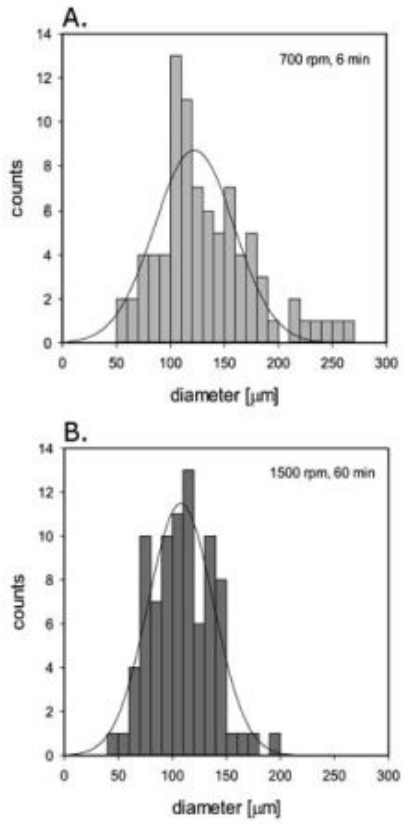

Figure 2.16: Size distribution of aggregates from different mixing conditions: (A) 700 rpm, 6 min, and (B) 1500 rpm, 60 min. Reproduced from Zawala et al. [9].

aggregates made up of only dispersed solids (DS) and precipitated asphaltenes (PA) with no observable water droplets (WD). This is contrary to an earlier studies by Long et al. [11, 32], who found that asphaltene aggregates produced with heptane (C7) or with a pentane/hexane blend (C5C6) were porous and contained water droplets giving WD/DS/PA aggregates. This discrepancy could be due to the fact that Zawala et al. [9] reported an immediate appearance of large water droplets at the bottom of the autoclave upon stopping mixing indicating an unstable water-in-oil emulsion at their test conditions. These water droplets coalesced very quickly as a separate phase which could explain their absence in the aggregates seen by Zawala et al. [9]. Long et al. [11, 32] did not report any case of water coalescence when precipitating asphaltenes with their C7 or C5C6 blend.

In summary, the studies discussed here show that changes in mixing energy can alter the size and density of asphaltene aggregates formed in paraffinic froth treatment which ultimately affects their settling velocity. More specifically, Zawala et al.'s [9] results suggest that increasing mixing energy produces aggregates that are composed of more dispersed solids resulting in greater density leading to faster settling. The implication of these results is that mixing conditions in PFT operations are important as they change the settling

properties of asphaltene aggregates that influence settler design and energy requirements for suspending solids during pipeline transport.

2.7.2 Mixing in Solvent Deasphalting

The application of solvent deasphalting to a bitumen emulsion feed has the potential to result in three liquid phase products: a DAO + solvent phase, a pitch + solvent phase, and a water phase [5]. Because of this, while there were no studies found on mixing in SDA, discussion of the mixing of immiscible liquid–liquid systems can be performed instead. In particular, principles governing droplet breakup and coalescence in mixing can aid in understanding the behavior of pitch droplets subjected to partial mixing.

In the mixing of any given immiscible liquid-liquid system, droplets experience deformation caused by mechanical forces of moving surrounding fluid. Surface and internal forces of the droplet resist this deformation as they attempt to minimize surface tension and return the droplet to a spherical shape [22]. Fluid forces that cause drop deformation are often referred to as shear forces . Droplet breakup occurs either when shear forces overcome these resistance forces or when droplets collide with solid surfaces such as impellers, baffles, and vessel walls. Many studies have been done looking at droplet breakup in dilute systems where coalescence is negligible [22]. Generally, these studies all agree that the mean droplet size is inversely proportional to the maximum energy dissipation in the system. This makes sense as energy dissipation can used to characterize the shear forces that cause droplet breakup. Since, as discussed in Section 2.5, energy dissipation is a direct measure of mixing intensity, it can be said that higher mixing intensities are expected to reduce droplet size.

Coalescence acts as a competing mechanism to droplet breakup and is the process by which two or more droplets combine to form larger drops. This process takes on two major steps in the mixing of immiscible liquid-liquid systems: collision and then film drainage [22]. As droplets approach each other for a collision, a film of continuous phase fluid will keep them apart. This film must be drained in order for coalescence to occur. Successful coalescence only occurs when the interval of time in which drops collide exceeds the time needed for the film to drain between droplets. Contact time and film drainage rate can be affected by hydrodynamic forces. In the case of settling droplets, gravity acts as a constant force over a long duration to encourage coalescence. Additionally, agitation rate can also increase droplet collision frequency promoting coalescence.

Recall from Section 2.2.2 that the application of SDA to a bitumen emulsion feed can result in a three-phase mixing problem in which pitch droplets settle into a growing middle phase which could cause problems in the settler. Based on the knowledge reviewed here, the implications are that pitch droplets tend to coalesce in the middle layer after settling out as gravitational forces bring them together long enough to drain the continuous phase

between them. In fact, a study by Johnston et al. [17] has already shown this to be the case for asphaltene-rich droplets at temperatures above 140 °C, which is already below the operating temperature of typical SDA operations [7]. However, the information reviewed here also indicates that droplet breakup can be induced with mixing. As such, partial mixing of pitch and water phases have the potential to prevent a growing pitch layer problem by preventing pitch coalescence.

2.8 Scope of the Current Study

Based on the review of the literature, the following conclusions can be drawn:

- Solvent addition treatment processes, which involve the mixing of solvent and feed, are important for the separation of heavy materials from bitumen feeds in oil sands extraction.
- Stirred tanks provide a good way to simulate a wide range of mixing intensities and energies by simply varying the impeller speed and mixing duration.
- Mixing is typically quantified using mixing intensity (W/kg) or mixing energy (J/kg) but the importance of each to the downstream settling process has not been well studied.
- The settling properties of aggregates (size, density, and settling rate) formed from PFT are significantly affected by mixing energy input. These properties are important to the settler design and energy requirements to keep solids suspended in pipeline transport.
- The application of SDA to a bitumen emulsion feed is still a new concept and has the potential problem of three-phase separation. As testing at actual SDA temperature and pressure conditions requires complicated and specialized equipment that is unlikely to provide any visual information, investigating partial mixing of a three-phase system is simpler with a cold flow analogue.

Despite being a key step in solvent addition treatment processes, very few studies look at the effects of mixing on aggregate/pitch droplet settling. Of those that do, almost none differentiate between the effects of mixing intensity and mixing energy. This existing knowledge gap presents an opportunity to improve solvent addition treatment processes through improved understanding of how mixing parameters influences aggregate/droplet settling properties. As these properties impact the sizing of settlers and energy requirements to keep solids suspended during pipeline transport, improvements to solvent addition treatment processes can benefit the bitumen recovery operations overall.

Based on guidelines in the Handbook of Industrial Mixing [22] and information from Zawala et al. [9], various mixing intensities, mixing times, and mixer configurations were tested.

2.9 Research Objectives

Based on all of the studies discussed in this chapter, the objectives of this study are to:

- **Establish the importance of differentiating between mixing intensity and mixing energy in PFT**
  - Compare Zawala et al. [9] settling rate and mixing energy results with data from other PFT studies in the literature.
  - Analyze the importance of distinguishing between mixing intensity and mixing energy based on the available literature.
- **Examine the effects of mixing parameters on aggregate settling in PFT**
  - Study mixing intensity and mixing energy effects on aggregate settling properties by changing the impeller speed and mixing time in a stirred tank.
  - Obtain the sizes and settling rates of individual aggregates by visualizing them in a settling column.
  - Obtain the hindered settling rate of precipitated asphaltene aggregates visualizing them in-situ through the use of a windowed autoclave.
- **Determine the mixing configurations needed to produce partial mixing in a three-phase SDA analogue system**
  - Determine the appropriate fluids to create a three-phase system with fluid properties that match a representative SDA stream.
  - Systematically test multiple impeller combinations in a stirred tank setting to determine the most promising combinations to investigate in future pilot-scale tests.
  - Test impeller combinations at various locations within the settler geometry in no-flow and continuous-flow conditions and determine the impeller types, locations, and speeds that produce the best results for two-phase underflow-only mixing in a three-phase system.

Chapter 3

Analysis of Mixing in Froth Treatment Literature

3.1 Introduction

As mentioned in Section 2.1, few studies in froth treatment choose to analyze the effects of mixing on aggregate settling. Most keep mixing energy, mixing intensity, and time constant for their experiments while manipulating other variables such as temperature, solvent-to-bitumen ratio (S/B), etc.. While most studies in froth treatment do not investigate the effects of changes in mixing, many still choose to describe their mixing conditions in terms of stirred tank vessel diameter, mixing speed, mixing duration, and impeller type and diameter [11, 12, 30].

In this chapter, the settling data for several studies on froth treatment are examined with respect to the mixing conditions they were performed at. The data are investigated to determine the validity of observations by Zawala et al. [9] compared to other studies and the importance of considering both mixing intensity and mixing energy separately. Though these data have been reported previously, this analysis is new because it synthesizes the results in a different way to compare and visualize the different effects of mixing intensity and mixing energy on settling in froth treatment. The available data include:

- Hindered settling data from two studies with similar temperature, solvent-to-bitumen ratio (S/B), and solvent choices were compared to results by Zawala et al. [9] to analyze the validity of trends observed in Figure 2.15.
- Data of asphaltene flocs sizes as a function of mixing speed and time were obtained from Rastegari et al. [33] and plotted as a function of a representative mixing energy variable for analysis.

3.2 Comparison of Mixing Effects on Settling Rate

Studies by Kosior et al. [12] and Long et al. [11] were found to have similar temperature, solvent-to-bitumen ratio (S/B), and solvent test conditions compared to the work by Zawala et al. [9]. Table 3.1 shows the conditions tested in each study. Additionally, Kosior et al. [12] performed mixing of bitumen froth and solvent in the same windowed autoclave used by Zawala et al. [9]. Kosior et al. [12] mixed at a mixing speed of 1200 RPM for 30 minutes. Long et al. [11] performed mixing tests using a windowless autoclave with two Rushton turbines running at a speed of 600 RPM for 15 minutes. Using this information, the mixing energy for each study was calculated and compared to Zawala et al. [9] as shown in Figure 3.1. It is immediately apparent from Figure 3.1 that the hindered settling rates of asphaltene aggregates from these studies are all comparable when plotted as a function of mixing energy. Additionally, differences in the trend could be attributed to the slight differences in test conditions of each study shown in Table 3.1. This result is important for two major reasons: (1) it shows that mixing conditions can impact the settling properties of asphaltene aggregates, and (2) that the effect of mixing is not limited to just the one

Table 3.1: Test conditions of various PFT studies

Study	Solvent	S/B	Temperature (°C)	Pressure (MPa)
Zawala et al. [9]	n-pentane	1.8	80	0.6
Long et al. [11]	n-pentane + n-hexane mix	2.0	75	1.0
Kosior et al. [12]	n-pentane	1.6	70	0.8

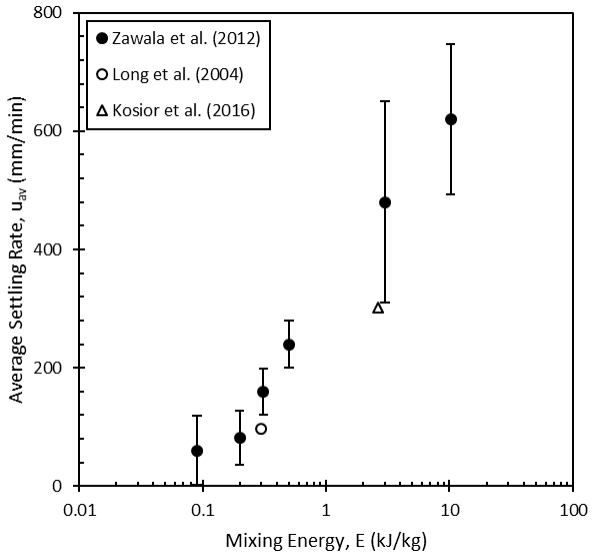

Figure 3.1: Comparison of hindered settling rates in literature. Data from Zawala et al. [9], Long et al. [11], Kosior et al. [12].

study by Zawala et al. [9]. Since these properties impact the settler sizing and deposition velocity in pipelines downstream of any mixing/settling equipment, this indicates that mixing can influence the overall separation performance of bitumen recovery.

3.3 Mixing Intensity vs Mixing Energy

Although the results in Figure 3.1 show the importance of considering mixing in solvent addition treatment processes, a distinction between the effects of mixing intensity and mixing energy is missing from the data. In fact, Zawala et al. [9] only reported a range of mixing intensities and mixing times tested along with the specific mixing conditions of the first and last energy points shown in Figure 3.1. They reported that their lowest and highest mixing energy conditions tested were produced from mixing at 700 RPM for 6 min and 1500 RPM for 60 min, respectively. Based on these two mixing conditions, an attempt was made to back-calculate the likely mixing conditions Zawala et al. [9] used to achieve the mixing energies in between these extremes. This was done by trying various combinations of the known mixing intensities (700 RPM and 1500 RPM) with the mixing times (6 min and 60 min) in order to determine mixing energies and comparing them to the values in Figure 3.1. However, this back-calculation proved unsuccessful leaving the exact conditions that Zawala et al. [9] used to reach each mixing energy unknown. Additionally, no efforts to determine whether mixing energy is the appropriate variable to characterize mixing for solvent addition treatment processes were made by Zawala et al. [9]. This can be an issue, as discussed in Section 2.5, because the choice to scale by mixing intensity or mixing energy can result in very different equipment choices.

While no PFT-related studies were found that distinguished between mixing intensity and mixing energy effects on aggregate settling rate, a study by Rastegari et al. [33] on asphaltene flocculation did examine the effect of varying mixing speed and time on asphaltene floc sizes. Rastegari et al. [33] analyzed the flocculation kinetics of asphaltene flocs using a model system. Asphaltenes were precipitated out from coker feed bitumen, subsequently dissolved in toluene to remove solids, and dried. Solids-free asphaltenes were then dissolved in toluene. At time zero, n-heptane was added to the toluene-asphaltene solution and mixed inside a glass cuvette using a magnetic bar for stirring. This resulted in asphaltenes precipitating out of toluene and then flocculating. Rastegari et al. [33] took asphaltene floc size measurements using a particle-size analyzer at several times during mixing. Figure 3.2 shows the result of varying mixing speed and time on the mean diameter of resulting asphaltene floc populations. From Figure 3.2, Rastegari et al. [33] concluded that increased shear caused from mixing at higher speeds decreased flocculation resulting in smaller asphaltene flocs.

Recall from Section 2.5 that $E \propto N_p \rho N^3 D^5 t$. Since the results shown in Figure 3.2 only

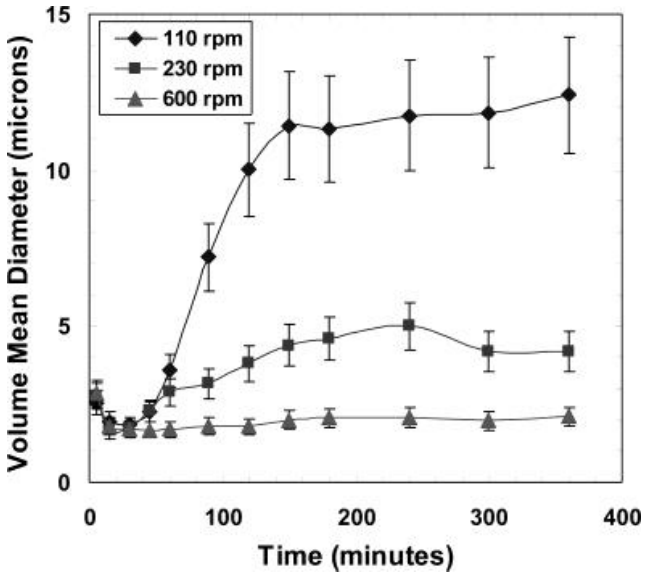

Figure 3.2: Effect of mixing speed and time for a 60/40 n-heptane + toluene mixture. Reproduced from Rastegari et al. [33].

varied the mixing speed and mixing time, combining the mixing speed and mixing time would give a characteristic parameter that represents the mixing energy of the system for those conditions. Based on the definition of mixing energy in provided Section 2.5, this can be done by multiplying N^3 with the mixing time (t) and re-plotting the data as shown in Figure 3.3. This analysis assumes that the magnetic bar used for mixing is equivalent to an impeller, which Rastegari et al. [33] also assumed as part of their analysis.

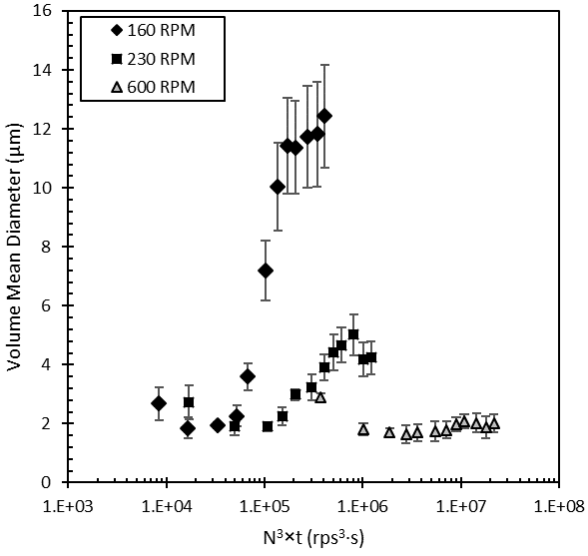

Figure 3.3: Effect of mixing energy on asphaltene aggregate size. Data from Rastegari et al. [33].

If the asphaltene floc size is dependent on mixing energy and not mixing intensity, then combining the mixing conditions into a single parameter (mixing energy) should result in the data collapsing into a single trend. However, as can be seen from Figure 3.3, the data does not collapse into a single trend when plotted as a function of a representative mixing energy variable and instead stays separated based on mixing intensity (stirrer speed). Furthermore, when mixing intensity is kept constant, changes to floc size still occur with time. This indicates that both mixing intensity and mixing energy are important in determining the size of asphaltene aggregates. Additionally, this result is critical since Stokes' law (Equation (2.6)) states that $u_\infty \propto d^2$, meaning that changes in aggregate size due to mixing conditions would significantly affect the aggregate settling rate. Thus, both mixing intensity and mixing energy should be considered when discussing the effects of mixing conditions on settling properties in solvent addition/treatment processes.

3.4 Conclusion

Based on the analysis of settling rate studies in PFT, it is clear that the trend of increasing mixing energy resulting in faster settling is not limited only to the results of Zawala et al. [9]. This is important as it provides strong evidence that mixing conditions impact the settling rate of heavy products in solvent addition/treatment processes. Furthermore, from the analysis of asphaltene floc sizes as they change with mixing conditions conducted by Rastegari et al. [33], it can be concluded that mixing intensity and mixing energy both impact asphaltene aggregate size. Since aggregate size is a key property in settling, it can also be concluded that considering only mixing energy in solvent addition processes is insufficient to fully characterize the effects of mixing on aggregate settling. As such, further investigation of mixing effects on the settling properties of solvent addition treatment processes while distinguishing between mixing intensity and mixing energy is necessary.

Chapter 4

Effects of Mixing on Aggregate Settling in Paraffinic Froth Treatment

4.1 Introduction

Paraffinic froth treatment (PFT) is the process in which a paraffinic solvent (such as n-pentane or n-heptane) is added to bitumen froth in order to induce asphaltene precipitation. Furthermore, from the discussion and analysis provided in Chapters 2 and 3, it is evident that mixing conditions can strongly influence the settling properties of asphaltene aggregates [9, 11, 12]. This chapter describes the investigation of the effect of mixing conditions on the size, settling velocity, and density of asphaltene aggregates produced from paraffinic froth treatment. Bitumen froth and n-pentane were mixed in a windowed autoclave vessel at varying impeller speeds and mixing times. Upon reaching the desired mixing conditions, a sample of the autoclave contents was extracted and mixing was stopped to allow the remaining contents to settle. Extracted samples were diluted and transferred to a clear settling column to obtain both the size and settling rates of individual aggregates. Hindered settling velocities of aggregates were obtained by recording the settling of the remaining unsampled contents through the autoclave vessel window. The results were analyzed and trends based on changing mixing intensity and mixing time were interpreted. These are discussed in detail in Section 4.4.

4.2 Experiment Design

The primary objective of this study is to determine the effects of mixing intensity and mixing energy on the settling properties of asphaltene aggregates in PFT. As such, it is necessary to control both mixing intensity and mixing energy in the experiments. Based on the information provided in Sections 2.4.2 and 2.5, this can be accomplished in a stirred tank by manipulating the mixing/impeller speed and mixing time.

4.2.1 Mixing Equipment and Test Conditions

In the interest of generating results comparable to other PFT studies, the mixing speed and mixing time chosen for this study were selected based on the ranges studied by Zawala et al. [9]. Additionally, all PFT testing was performed at CanmetENERGY's facilities located in Devon, Alberta, Canada using their autoclave equipment. The autoclave vessel used for testing was the same one used by Zawala et al. [9]. In their earlier study using this equipment, Zawala et al. [9] tested mixing speeds ranging from 700 - 1500 RPM (rotations per minute) and mixing times of 2 - 60 minutes. This resulted in mixing energies from approximately 0.09 kJ/kg up to 20 kJ/kg. Recall from Section 2.5 that the mixing intensity and mixing energy depend upon the geometry of the stirred tank, particularly the impeller type and diameter. Since mixing in this study was performed using the same vessel as Zawala et al. [9], the mixing speed and time ranges can be taken directly to generate the same range of mixing energies as their study. Thus, three mixing speeds and times were chosen to be tested in this study: two mixing speeds and times at the low and high extremes of Zawala et al.'s [9] ranges and one mixing speed and time in the middle of that range. Table 4.1 shows the experimental test matrix for PFT tests in the current study. Each test took one full day to complete. Note that only one run was performed at 1500 RPM. Since the equipment belonged to CanmetENERGY, other experiments were performed on the apparatus by CanmetENERGY staff in between days scheduled for the PFT tests. During these other experiments, CanmetENERGY staff encountered a safety problem such that autoclave operation above 1200 RPM would risk equipment failure. A CanmetENERGY safety audit indicated that operation above this RPM was no longer safe. As the 2 minute and 60 minute test points at 1500 RPM were scheduled after this safety issue arose, data could not be obtained for these test conditions. By matching the range examined by Zawala et al. [9], it is clear that the proposed test matrix can generate comparable results to other PFT studies in literature.

Table 4.1: Experimental test matrix for mixing measurements.

Mixing Speed, N (RPM)	Mixing Time, t (min)
700	2
	30
	60
1000	2
	30
	60
1500	30

4.2.2 Settling Column Tests

When studying the settling properties of individual aggregates, Zawala et al. [9] recorded extracted sample aggregates settling in a column filled with a clear medium as opposed to dark diluted bitumen. The fact that PFT is a precipitation reaction indicates that precipitation depends on the solubility of asphaltenes in the surrounding medium solution. Thus, in order to perform these settling column tests a medium that does not further dissolve aggregates or allow entrapped diluted bitumen to further precipitate must be created. To do so, one must match the solubility characteristics of the medium the aggregates would originally be settling in. Following the procedure by Zawala et al. [9], the Hildebrand solubility parameter, δ, provides a convenient way to characterize the solubility of a mixture of fluids.

The original concept of the solubility parameter of a liquid was proposed by Hildebrand [34] which stated the δ of a mixture can be calculated as:

$$\delta_{mix} = \sum_{i=1}^{n} \phi_i \delta_i \tag{4.1}$$

where ϕ_i is the volume fraction of a mixture component and δ_i is their solubility parameter. Each component δ_i can be calculated by:

$$\delta_i = \sqrt{\frac{\Delta H_i - RT}{V_i}} \tag{4.2}$$

where ΔH_i is the enthalpy of vaporization, V_i is the molar volume, R is the universal gas constant, and T is the temperature.

In replicating the procedure by Zawala et al. [9], the current study used this knowledge of the solubility parameter to create a clear diluent medium to visualize individual aggregate settling by matching the δ of the diluted bitumen sample to the δ of the diluent mixture. It should be noted that the Hildebrand solubility parameter is the simplest solubility value and cannot fully describe the solubility of something as complex as bitumen. However, for the purposes of this work, the use of more accurate non-ideal solution theory [35] was not required because of the desire to replicate the procedure by Zawala et al. [9] as closely as possible. Section 4.3.4 discusses this procedure in more detail.

4.3 Experimental Method

Recall from Sections 2.4.2 and 2.5 that, in a stirred tank geometry, mixing intensity and energy can be varied by changing impeller speed and mixing time. Further, from Section 2.6,

the settling properties of aggregates can be described by two methods: individual aggregate settling, and hindered settling. Based on this, the general procedure for experiments was divided into a single mixing phase with two types of settling experiments: individual aggregate settling and hindered settling. This section covers the materials and experiment procedures used to obtain these results.

4.3.1 Materials

A batch of typical sample of bitumen froth consisting of 66 wt% bitumen, 21 wt% water, and 13 wt% solids from the Athabasca oil sands was used in all bench-scale PFT testing. Froth composition was measured by CanmetENERGY using Dean-Stark distillation. In all experiments, the feed, solvent, temperature, pressure, and S/B ratio were kept constant. Reagent-grade n-pentane (EMD Chemicals Inc.) was used as the primary solvent to precipitate asphaltenes from the froth. The temperature and pressure of all experiments were kept at 80 ºC and 0.6 MPa, respectively. The choice of solvent, temperature, and pressure were chosen to replicate the conditions studied by Zawala et al. [9] making the results obtained in this study directly comparable to theirs. Additionally, these conditions match conditions typically seen in industrial operations and various studies on PFT [4, 9, 11, 12, 32]. Reagent-grade toluene and n-heptane (Fisher Scientific) were combined as diluent and used as the medium for aggregate settling tests, which were conducted using a square glass column. The procedure to prepare the diluent is described in Section 4.3.5.

4.3.2 Apparatus and Mixing Procedure

A schematic diagram of the experimental setup is shown in Figure 4.1. The autoclave cell has an inner diameter of 63 mm with a height of 203 mm and a single oblong glass window on one side. Two 35 mm diameter pitch blade turbine impellers with 6 blades along with four standard baffles inside the autoclave used for all mixing in the experiment. The impellers were spaced 63 mm apart and the lower impeller had 7 mm of clearance from the autoclave bottom. A Parr 4848 controller was used to control the motor speed and monitor the pressure and temperature inside the autoclave. Valves V1 to V5 were used collect sample from the autoclave at the appropriate time while valves V6 and V7 were used to introduce and release nitrogen from the system respectively.

The complete assembly is shown in Figure 4.2. To begin the experiment, the main sample of bitumen froth (4 L paint can) stored at room temperature was mixed vigorously for 5 minutes using a large impeller running at 90 RPM in an attempt to ensure the similarity of each froth sample used for testing. A 168 g froth subsample was then collected and combined with 171.8 g n-pentane in the 650 mL stainless steel autoclave cell (Parr Instrument Company). While each froth sample used was not individually tested

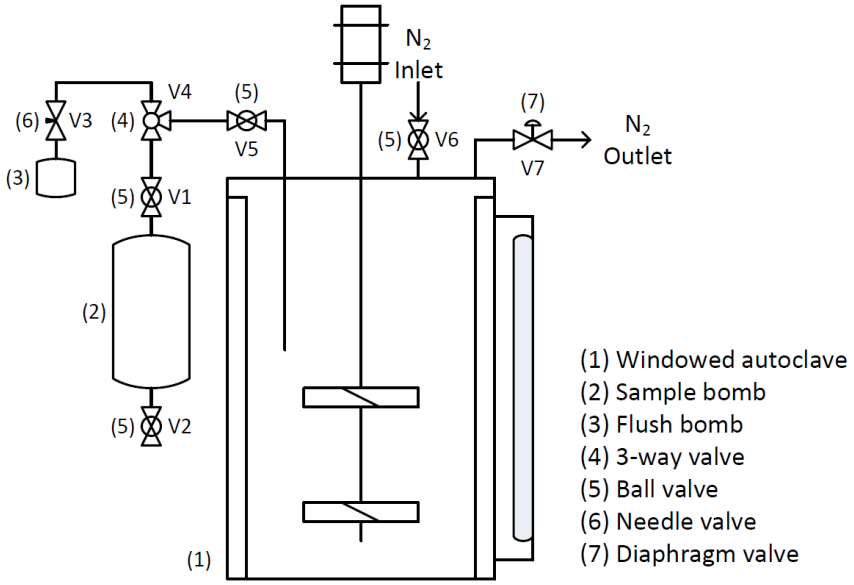

Figure 4.1: Schematic diagram of experimental setup.

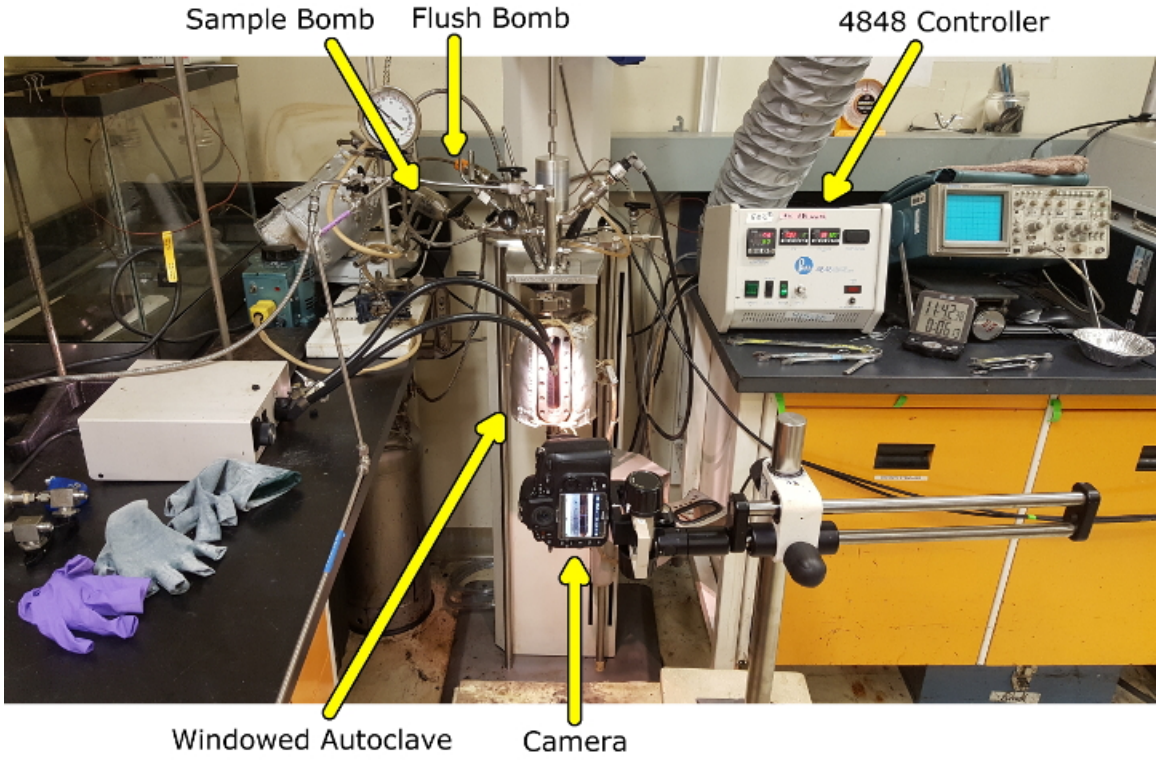

Figure 4.2: Windowed autoclave assembly with camera setup.

to ensure identical properties, it was assumed the samples were representative after the mixing procedure due to the consistent pre-mixing and subsampling procedure that was followed. The autoclave was then sealed and heated slowly to 80 °C. During heating, the contents were gently mixed at 200 rpm. Once the froth and n-pentane mixture reached 80 °C, valve V6 was opened to apply a constant 0.6 MPa pressure to the system. After the pressure was applied, the mixing speed was increased to the desired level (700, 1000, or 1500 rpm) and kept constant for the specified mixing time (2, 30, or 60 min). As soon as the desired mixing conditions for a run were reached, valve V3 was fully opened and valve V4 was turned to direct flow towards the 10 mL flush bomb. Afterwards, valve V5 was opened and any unmixed bitumen froth/solvent stuck in the dip tube was allowed to enter the flush bomb for about 30 seconds. Once the dip tube was flushed, valve V1 was opened and valve V4 was turned to direct sample from the autoclave towards the 150 mL sample bomb. The mixer was kept on during sampling. After sampling was completed, valves V1, V3, and V5 were closed and valve V4 was turned towards the flush bomb. The sample bomb was carefully removed once the rest of the system was shut down.

4.3.3 Hindered Settling Tests

During each experimental run, a Nikon D800E equipped with a macro lens (AF-S VR Micro-NIKKOR 105 mm f/2.8F ED) was set up in front of the autoclave and aimed at the glass window along with some fiber optic lighting. After the sample was taken into the sample bomb, valve V5 was closed and the stirrer was immediately shut off. The settling of all remaining asphaltene aggregates, which were not extracted into the sample bomb, was recorded through the autoclave glass window. A clear ruler was attached onto the glass window in order to track aggregate position. An example of this setup is shown in Figure 4.3.

Figure 4.4 shows the typical settling curve observed by tracking interface heights during PFT. Three distinct zones and two interfaces are typically described in the literature and labeled in the figure [11, 32]. The zones consist of the upper clean oil zone (COZ), the middle hindered settling zone (HSZ), and bottom consolidation zone (CZ). Between the COZ and HSZ exists the upper interface (UI) and between the HSZ and CZ is the lower interface (LI). Where the UI and LI merge, the HSZ disappears and consolidation starts. This point is a local maximum which is known as the consolidation point (CP). Knowing the CP and the initial mixture height (H_0), the hindered settling rate can be calculated by:

$$u_s = \frac{|H_c - H_0|}{t_c} \tag{4.3}$$

Where H_c and t_c are the interface height and time at CP, respectively. The footage obtained and images shown in Figure 4.3 shows settling starting from CP onwards. The upper

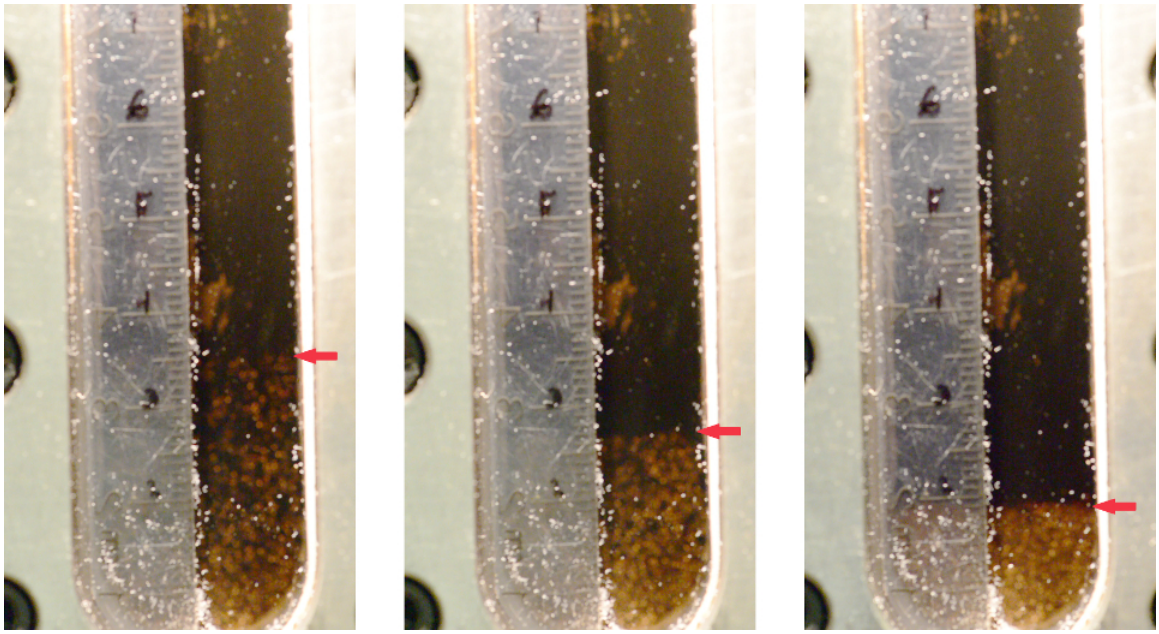

Figure 4.3: Hindered settling test example. Images taken after mixing at 1000 RPM for 30 min. Red arrows indicate interface between the clean oil zone and consolidation zone.

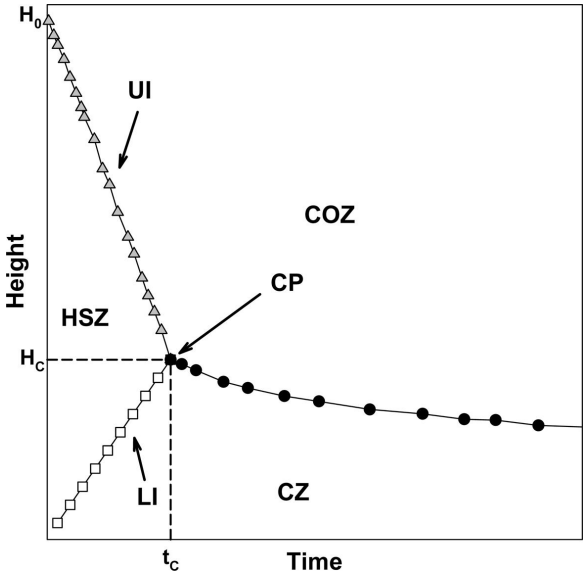

Figure 4.4: Typical diluted bitumen froth settling curve. Reproduced from Kosior et al. [12].

interface was not visible in any of the recordings taken. Additionally, the lower interface was not tracked as it was extremely difficult to see the distinction between the CZ and HSZ through the autoclave window. The liquid level height observed through the window after sampling was taken as the initial interface height, H_0. Following this, the videos were reviewed manually by repeatedly pausing and rewinding the footage to see where the interface height was. Settling mostly occurred within the first 60 seconds of footage and so more interface heights were recorded during this period. Figure 4.5 shows the typical result that was obtained from the videos. The first instance in which no aggregates were observed falling and a complete interface was formed was taken as the CP and Equation (4.3) was used to calculate the hindered settling rate.

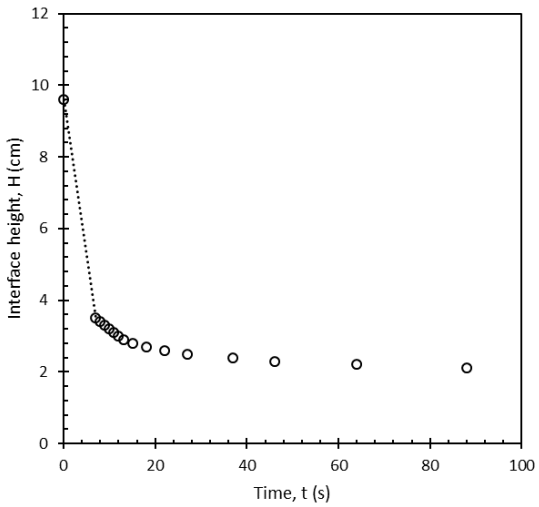

Figure 4.5: Observed asphaltene interface height over time after mixing at 1000 RPM for 30 min.

4.3.4 Diluent Preparation

Samples collected in the sample bomb during mixing were transferred to a clear sample jar and kept in a refrigerator overnight. These samples were always completely opaque suspensions of asphaltene aggregates in diluted bitumen. In order to visualize the settling velocities of individual aggregates, a sample dilution procedure was applied. To prevent further dissolving the asphaltenes, the original n-pentane solvent could not be used as the diluent. As such, diluent was prepared using a mixture of aromatic and paraffinic solvent made from toluene and n-heptane. The proportions of this mixture was determined by matching its solubility parameter, δ, to that of the original diluted bitumen. In doing so, the aggregate structure is preserved in the diluent medium [9]. A sample of diluted bitumen from mixing at 1000 RPM for 30 minutes was analyzed to determine its composition. This composition was assumed to be consistent for all other runs. Additionally, the solubility parameters for the components were obtained from literature [36–38]. The results are summarized in Table 4.2.

Table 4.2: Composition and solubility parameters of diluted bitumen.

Component	Weight fraction, x_i (wt%)	Volume fraction, ϕ_i (vol%)	δ_i
Water	0.01	0.01	48
Asphaltenes	4.28	3.47	21
Maltenes	43.06	34.91	19.1
Solvent (n-pentane)	52.65	61.62	14.3

Based on these values, Equation (4.1) was used to calculate the diluted bitumen solubility parameter to be δ_{dilbit} = 16.2 $(MPa)^{1/2}$. By reapplying Equation (4.1) to the diluent mixture, the volume fractions for toluene and n-heptane in order to match δ_{dilbit} were determined to be 0.31 and 0.69, respectively.

To prepare a sample for glass column settling tests, a beaker was filled with approximately 200 mL of freshly prepared diluent. Aggregates were then extracted from the original sample jar via a small clear plastic pipette. As the contents of the jar had settled out by the time of extraction, the tip of the pipette was placed at the very bottom of the sample jar before drawing in fluid. The pipette was then held vertically with the tip pointing down for a few seconds to allow aggregates to settle to the pipette tip before being released gently into the beaker of fresh diluent.

4.3.5 Square Glass Column Settling Tests at Ambient Conditions

Settling velocities of individual asphaltene aggregates were measured in a square glass column at ambient conditions. Figure 4.6 shows the setup used to record the settling of micro-scale aggregates.

A square glass column, 40 × 40 mm in cross section and 130 mm in height, was set up in front of some fiber optic illumination and a CCD camera (Microcast HD Studio 3CCD HD 1080P) attached to a large zoom lens. The camera was positioned such that video footage of aggregates was taken 20 mm from the bottom of the column. The column was then filled with prepared diluent and covered on top with aluminum foil to prevent solvent evaporation. Aggregates were taken from the diluted sample beaker using a small plastic pipette. The pipette was then held vertically for a few seconds before releasing aggregates into the centre of the diluent-filled column through a small hole in the aluminum foil cap. Care was taken release only one or two aggregates at a time.

Video footage of aggregate settling was converted to images and analyzed by a MATLAB program created by Dr. David Breakey. Settling aggregates were tracked and the number of frames in which the aggregate are visible in the field of view was determined. The settling time of any given aggregate was then calculated based on the number frames

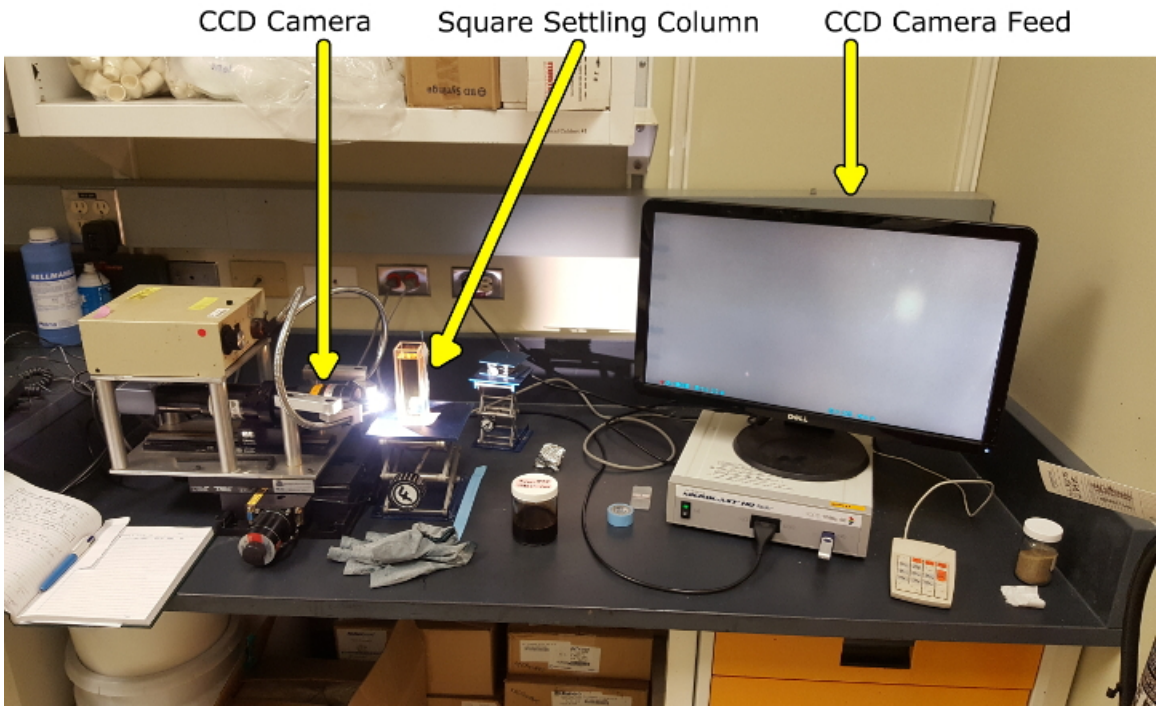

Figure 4.6: Individual aggregate settling test setup.

it takes to settle through the field of view and the recording speed of the camera. In the current study, the camera recorded at 30 frames per second. The size of aggregates was calculated as:

$$d_{eq} = \sqrt{\frac{4A}{\pi}} \tag{4.4}$$

where d_{eq} is the area equivalent diameter defined as the diameter of a sphere with the same area, and A is the average area of the falling aggregate from image analysis. Individual aggregate settling velocities, u, were calculated in MATLAB as:

$$u = \frac{\sqrt{\Delta x^2 + \Delta y^2}}{\Delta t} \tag{4.5}$$

where Δx and Δy are the change in coordinates of the aggregate over the time interval Δt. The change in the horizontal (Δx) component of aggregate settling was included in the settling velocity calculation to account for differences in drag force affecting an irregularly shaped aggregate compared to a spherical particle. Based on the results from the MATLAB program, less than 30% of the aggregates had an x-component to their settling motion. While this technique was largely successful in determining aggregate settling trends, several challenges arose that made drawing more quantitative conclusions from the data difficult. Appendix A provides a detailed discussion with sample images of the successes and challenges of this detection technique.

4.4 Results and Discussion

4.4.1 Reliability of Individual Aggregate Settling Results

Several challenges were encountered involving the measurements taken for the settling of individual aggregates. These challenges were primarily related to the techniques used to obtain measurements. To begin with, while much care was taken to release only one aggregate at a time, this was not always possible resulting in many aggregates appearing over several images. These images were difficult to process because several aggregates were either out of focus or very small making them hard to detect. Figure 4.7 shows an example of this. This led to another challenge of the biased detection of aggregates.

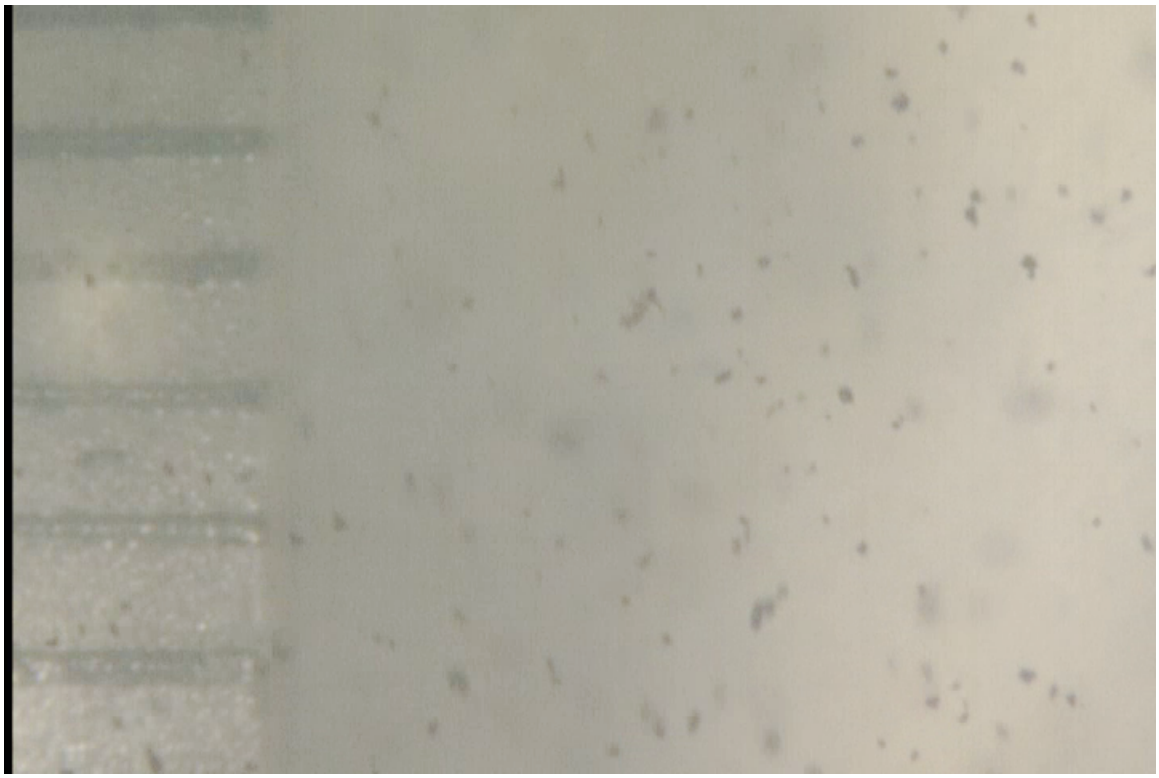

Figure 4.7: Sample image of aggregates produced from mixing at 1000 RPM for 2 min before processing.

Depending on the parameters set, the program became more sensitive to different parts of the particle size distribution (PSD). In other words, certain settings resulted in the detection of larger aggregates while excluding smaller ones and vice versa. This is clearly shown in Figure 4.8 where a clear aggregate size cutoff is noticed at $d = 100\mu m$. However, the PSD results from running the program at different settings could not be combined because of overlap in the data and the inability to determine which measurements were duplicates for so many aggregates. Appendix A provides more detail on challenges associated with the image processing technique.

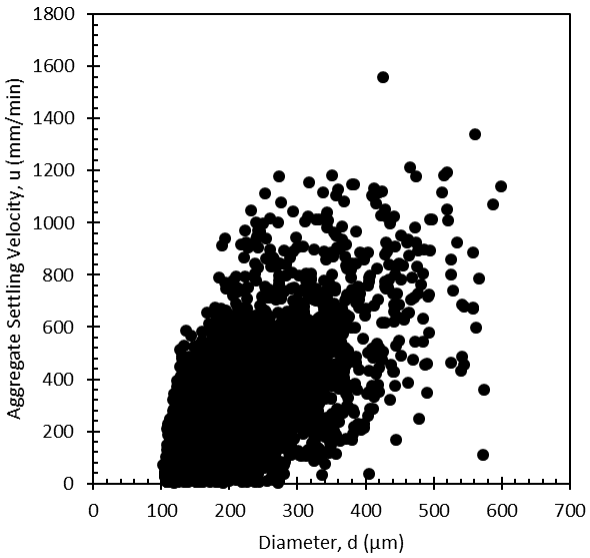

Figure 4.8: Individual aggregate settling velocities and sizes for aggregates produced from mixing at 700 RPM for 2 minutes.

Among the greater challenges identified was the movement of diluent fluid in some test cases. This was observed in some videos where small settling aggregates floated upward indicating that the act of dispensing sample into the column resulted in some fluid movement. Naturally, this is an issue as fluid movement would affect observed aggregate settling rates. In addition to this, another major issue identified was the effect of sampling on aggregate sizes. As previously described in Section 4.3.2, aggregates were sampled using a pressure gradient between the autoclave and the sampling bomb. This method of sampling presents two potential problems: (1) aggregates larger than the diameter of the sampling tube are either not sampled or broken up resulting in a biased sample, and (2) the shear from traveling through the sample tube could alter aggregate structures. Both cases can result in samples that are not representative of the ones formed inside the autoclave.

With these challenges in mind, it is important to evaluate the reliability of the data in the context of the objectives of this study. Overall, the technique performed well for the majority of images obtained in which only one or two aggregates are settling in the field of view. The program was able to detect and distinguish between aggregates and changes in the background, such as dark waves produced from leftover dilbit in the sample. This was true even when there were 5–10 medium-sized aggregates within the same image. The technique does not perform well when there are many difficult-to-see small aggregates settling at once. However, this issue primarily occurred in data sets where aggregates were produced from mixing for only 2 minutes. Figure 4.9 shows a comparison between the average diameter as a function of mixing energy for individual aggregate results

produced from an old version of the MATLAB program and the updated version used for final data extraction. The updated version contains different detection parameters to exclude some false positives created by changes to the background caused by dark waves produced by leftover dilbit in the samples. It is clear from Figure 4.9, that while the values observed changed, the trends that appear do not. This is important as the objective of this study is to determine the effects of mixing intensity and mixing energy on settling properties. Since the observed trends do not change despite the changes in the detection parameters, qualitative conclusions about mixing intensity and mixing energy effects can still be made from the data while quantitative ones cannot. Additionally, the challenge of bias caused by sampling reinforces that quantitative conclusions should not be assessed from the data. Generally, it can be concluded that the data is reliable enough to comment on trends produced by mixing parameters, but not on quantitative changes to aggregate settling properties. Thus, the objective of the study can still be met despite the challenges encountered.

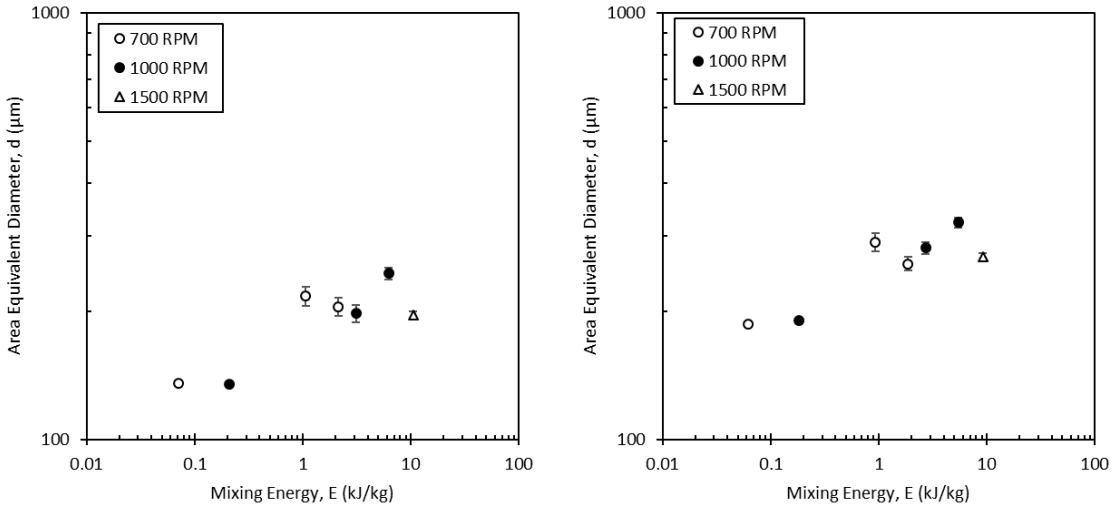

(a) Old

(b) Updated

Figure 4.9: Effect of mixing conditions on the average size of individual aggregates.

4.4.2 Effects of Mixing on Individual Aggregate Settling

Figure 4.10 shows the measured settling velocities of individual asphaltene aggregates produced from the lowest (700 RPM, 2 min) and highest (1500 RPM, 30 min) mixing energy conditions as a function of diameter. Two things are immediately apparent from Figure 4.10: (1) larger individual aggregates had higher settling rates, and (2) there is almost no distinguishable difference between mixing energy inputs. Based on Equations (2.1) and (2.2), the mixing energies of the 700 RPM/2 min and 1500 RPM/30 min case

were determined to be 0.07 kJ/kg and 10.5 kJ/kg, respectively. This works out to be about a 150× mixing energy difference. Given the vast difference in mixing energy, it appears that the settling velocity of individual aggregates is not substantially affected by mixing conditions. However, there is significant scatter shown in the data. Because of this, a clear trend is not apparent. A better idea of the effects of mixing on individual aggregate settling can be obtained by plotting the average settling rate of all the tested mixing conditions.

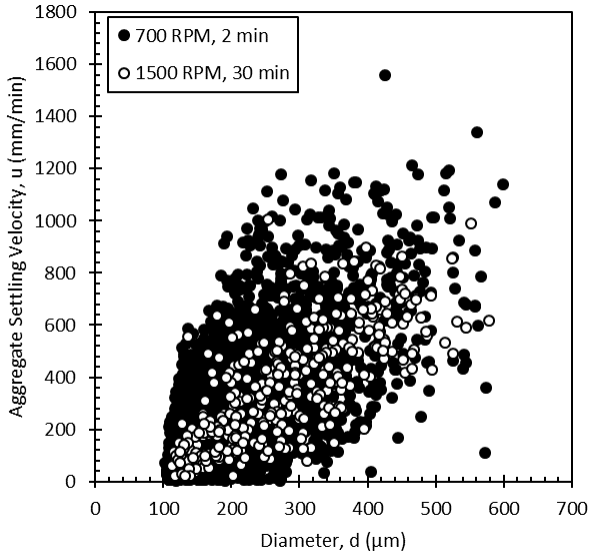

Figure 4.10: Comparison of individual aggregate settling velocities for different mixing conditions.

Figure 4.11 shows the experimental average settling rate of individual aggregates as a function of the mixing energy input. Error bars shown are the standard error of measurements and were obtained by:

$$\sigma_m = \frac{\sigma}{\sqrt{n_{meas.}}} \tag{4.6}$$

where σ_m is the standard error, σ is the standard deviation, and $n_{meas.}$ is the number of measurements. Generally, the trend observed in Figure 4.11 indicates that increasing mixing energy leads to faster settling individual aggregates. This result is important as it is a clear indicator that mixing conditions can change the settling properties of asphaltene aggregates formed in PFT. Additionally, Figure 4.11 shows differences in the change in settling velocity with increasing mixing energy depending on the mixing speed at which aggregates were formed. Aggregates formed from mixing at 700 RPM appear to have settling velocities that increase with increasing mixing energy at a different rate than those formed from mixing at 1000 RPM. Assuming that mixing is fully turbulent (N_p is constant) and a constant diluted bitumen density (ρ), it can be seen from Equations (2.1)

and (2.2) that the mixing speed (N) can be taken as a direct measure of changes in mixing intensity. Therefore, mixing intensity also affected aggregate settling properties. Note that the assumptions of constant N_p and ρ were made for all figures in this study such that differences in mixing intensity were shown by different mixing speeds.

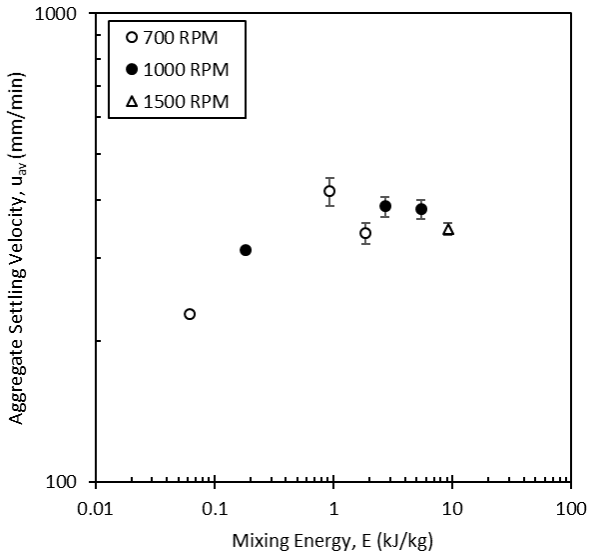

Figure 4.11: Effect of mixing conditions on the average settling rate of individual aggregates.

Based on Stokes' law (Equation (2.6)), the settling velocity of an individual aggregate is mainly affected by the properties of the fluid and the aggregate itself. Since the fluid medium in which aggregates settled was the same throughout all tests, the changes in settling velocity as a function of mixing energy are due to changes in the aggregate size and density. Figure 4.12 shows the size distributions of asphaltene aggregates produced from mixing at 700, 1000, and 1500 RPM, respectively. All diameters are taken as area equivalent diameter and calculated from measured aggregate projected areas according to Equation (4.4). The normal distribution curves have also been plotted after calculating the average and standard deviation for each data set.

From Figure 4.12, it can be seen that for the same mixing impeller speed, increasing mixing time slightly shifts the curves to the right. This indicates an increase in aggregate diameter with increasing mixing time. Since mixing speed is directly related to mixing intensity, it can be said that for a given mixing intensity, increasing mixing time appears to increase the average aggregate diameter. This indicates that the system has not yet reached the steady state aggregate size over the shorter tested periods. As the impeller speeds remained constant, this increase in aggregate size indicates aggregate growth over time.

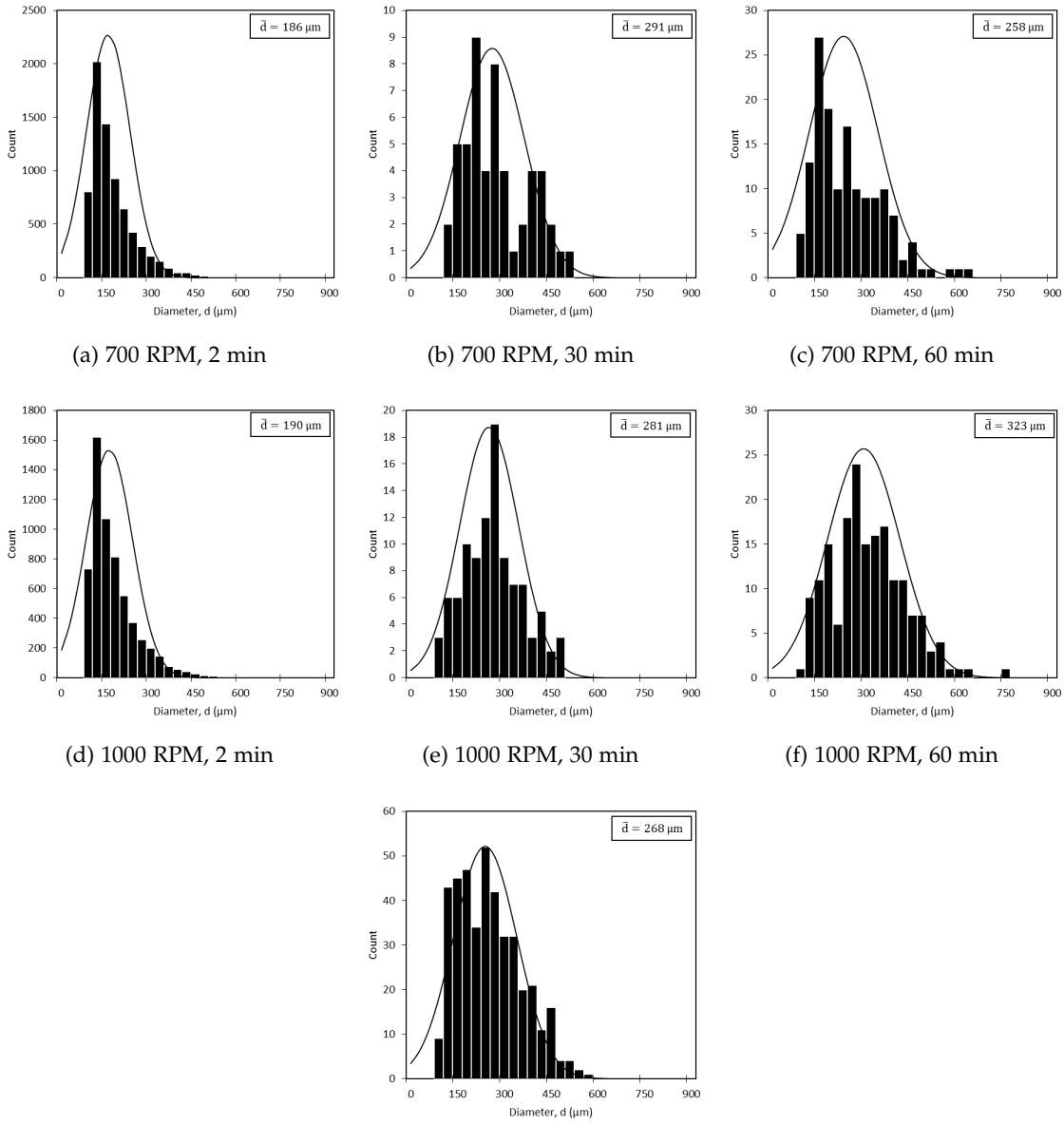

(a) 700 RPM, 2 min (b) 700 RPM, 30 min (c) 700 RPM, 60 min

(d) 1000 RPM, 2 min (e) 1000 RPM, 30 min (f) 1000 RPM, 60 min

(g) 1500 RPM, 30 min

Figure 4.12: Size distributions of individual aggregates formed from different mixing conditions.

In order to obtain a clearer picture of the effects of mixing on asphaltene aggregate size, the average area equivalent diameters along with the standard errors were plotted as a function of mixing energy as shown in Figure 4.13. It can be seen that increasing mixing energy produces larger aggregates overall. This trend holds true even when mixing intensity is fixed. As such, it can be concluded that longer mixing times enable aggregates time to grow leading to the results seen in Figure 4.13. Additionally, there appears to be a slight separation in the trend depending on the mixing intensity at which aggregates were produced. Mixing at 700 RPM leads to larger aggregates produced at lower mixing intensities than 1000 RPM or 1500 RPM does. This could be a result of lower shearing of formed aggregates from impeller blades at lower speeds causing less breakup. Overall, this implies that the largest aggregates are produced by higher mixing energies achieved through low mixing intensities with long mixing times.

Based on Figure 4.13, it was concluded that increases in mixing energy led to the formation of larger aggregates. From Stokes' law (Equation (2.6)), the settling velocity is directly proportional to d^2 and as such larger aggregates produced by higher mixing energies are expected to settle more rapidly. Comparing the settling velocities in Figure 4.11 and area equivalent diameters in Figure 4.13, it can be seen that there is a consistency in the results in that there is separation of the data depending on mixing intensity that is apparent. In both figures, lower mixing intensity results in larger aggregates that settle more rapidly. However, while the settling velocities in Figure 4.11 do increase with mixing energy, it does not increase to the square of diameter. This discrepancy indicates that other parameters, such as aggregate density and structure, may also be affected by mixing energy given that the fluid medium remains the same in all tests.

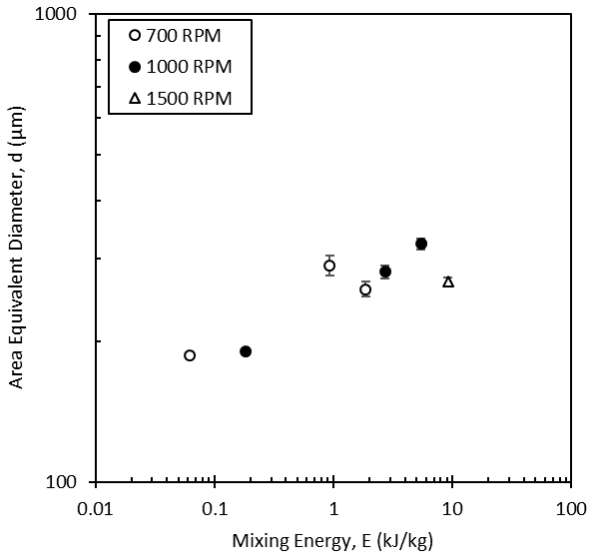

Figure 4.13: Effect of mixing conditions on average aggregate size.

From the results seen here on individual aggregate settling velocities, it can be concluded that increasing mixing energy led to generally higher settling velocity. Figure 4.14 shows the experimental effective densities of individual asphaltene aggregates produced from mixing at 700, 1000, and 1500 RPM, respectively as a function of diameter. Recall from Section 2.6.2 that effective density is defined as the difference between the aggregate and fluid densities not the actual aggregate density itself. All aggregate effective densities were calculated using Equation (2.8). Due to a lack of information about the aggregate permeability, it was assumed that $\Omega = 1$ (i.e. that the particles are impermeable spheres). Additionally, it was found that the observed aggregates settled with a particle Reynolds number range of $0.0004 \leq Re_p \leq 11.9$ with the majority of them having $Re_p > 0.3$. As such, the drag coefficient, C_D, was calculated using the correlations in Equation (2.5). From Figure 4.14, it can be seen that larger aggregates were found to have lower effective densities in all cases. This trend matches well with the settling of porous aggregates observed by Rahmani et al. [30] which was previously shown in Figure 2.13. Rahmani et al. [30] found that aggregate porosity generally increased with increasing projected area diameter. Consequently, the increase in aggregate porosity meant a decrease in aggregate effective density just as observed in the present study.

There is also significant scatter observed in Figure 4.14. This could be caused by a number of factors. To begin with, not all aggregates are created exactly the same; some spend more time near the impeller where shear forces are high while others spend more time further from the impeller where shear forces are lower. The amount of shear force experienced by an aggregate would alter its size with higher shearing breaking up larger aggregates into smaller ones. Another reason is that the observed aggregates were irregularly shaped and not spherical. The shape and orientation of an aggregate affects the drag force acting on it which ultimately affects the settling velocity. These phenomena help explain the large scatter seen in Figure 4.14. Additionally, as discussed in Section 4.4.1, the sharp limits on aggregate sizes seen in Figure 4.14 are a result of the MATLAB program not detecting aggregates smaller than 100 μm due to the detection parameters set.

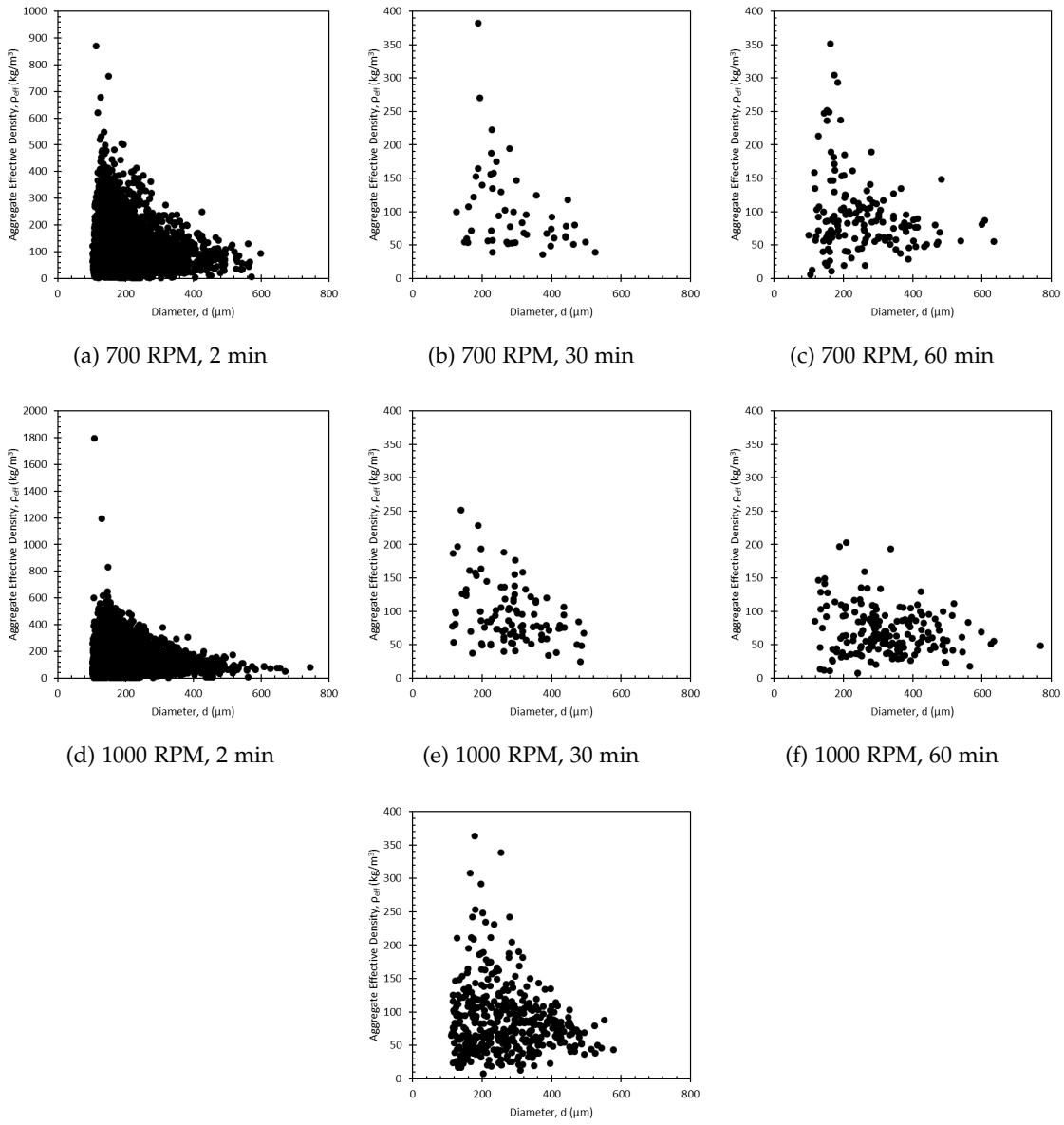

(a) 700 RPM, 2 min

(b) 700 RPM, 30 min

(c) 700 RPM, 60 min

(d) 1000 RPM, 2 min

(e) 1000 RPM, 30 min

(f) 1000 RPM, 60 min

(g) 1500 RPM, 30 min

Figure 4.14: Effective density of individual aggregates.

Figure 4.15 shows the average aggregate effective densities as a function of the mixing energy. It is clear from Figure 4.15 that the aggregate effective density generally decreases with increasing mixing energy. Recall from Figures 4.13 and 4.11 that increasing mixing energy led to larger aggregates and higher settling rates. Based on these observations, and the similarity to the results of Rahmani et al. [30] it can be concluded that the aggregates in this study are most likely porous in structure. This result is significant as it shows that mixing conditions can influence the settling properties of asphaltene aggregates in PFT through changing their structure as well as size.

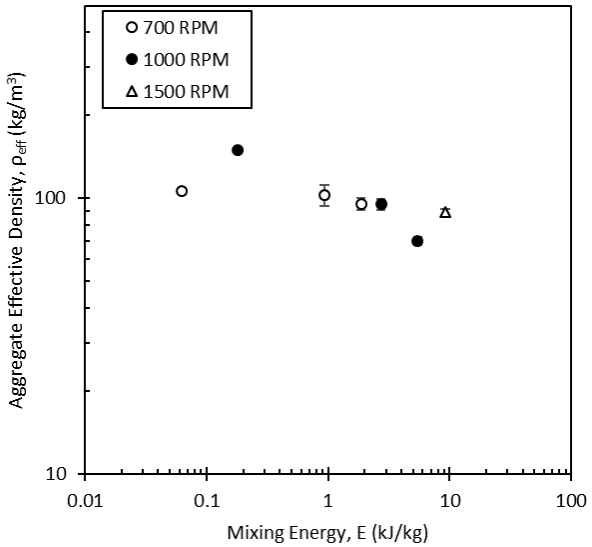

Figure 4.15: Effect of mixing conditions on aggregate effective densities.

The settling velocity of an individual aggregate is known to be a function of aggregate size and density. Generally, larger and more dense aggregates will lead to higher settling velocities. However, according to Figures 4.13 and 4.15, increasing mixing energies formed larger but less dense aggregates. Based on Stokes' law, these changes to aggregate size and effective density would have opposite effects on settling rate since $u \propto \rho_{eff} d^2$. As such, further analysis was performed to determine which variable had a greater influence on settling velocity in the current study.

Figure 4.16 shows the average settling velocities of individual aggregates as a function of the mixing energy along with the best fit line of a log-log function of the data. Additionally, the expected slopes of the best fit line are shown based on cases where the settling velocity is solely dependent on either aggregate size or effective density. These expected trends were obtained by fitting the data in Figures 4.13 and 4.15, then multiplying each slope by the exponent of the respective variable in Stokes' law (Equation (2.6)). It is clear from Figure 4.16 that the slope of the best fit line of the settling rate data is closer to the slope produced from assuming dependence on aggregate size rather than effective density. This

indicates that higher mixing energy increased aggregate settling rates despite the lowered density. Thus, it can be concluded that aggregate size had a greater influence than effective density on the aggregate settling velocities observed in this study.

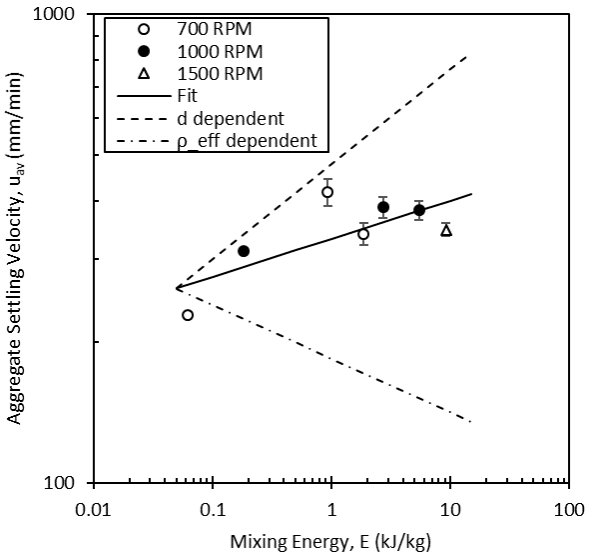

Figure 4.16: Comparison of aggregate size and effective density influences on settling velocity.

4.4.3 Effects of Mixing on Hindered Settling

When analyzing aggregate settling properties, the discussion cannot be limited to the settling of individual aggregates. Since, in most applications, particles settle with other particles, it is important to also examine how aggregates settle with other aggregates. Figure 4.17 shows the measured hindered settling rates of asphaltene aggregates as a function of the mixing energy for each mixing speed. It can be seen from Figure 4.17 that for a given mixing speed (and thus intensity) increasing the mixing energy generally increases the in-situ settling rate of aggregates. However, it can also be seen that higher mixing energy does not necessarily lead to higher settling rate as the points do not follow a single line. Instead, Figure 4.17 shows that lower mixing intensity leads to higher overall in-situ settling rates of asphaltene aggregates. The evidence presented here agrees with what has been presented in the literature in the sense that increasing mixing energy leads to higher settling rates. However, the data also suggests that the mixing intensity at which asphaltene aggregates are produced also play a role in their settling properties.

When comparing the hindered settling velocities in Figure 4.17 to the individual settling velocities in Figure 4.11, one major discrepancy noted is the fact that the hindered settling rates are larger than the individual settling rates for the 700 RPM cases. Theoretically this does not make sense as according to Equation (2.9) the hindered settling velocity should be lower than the individual aggregate settling velocity due to particle-particle interactions

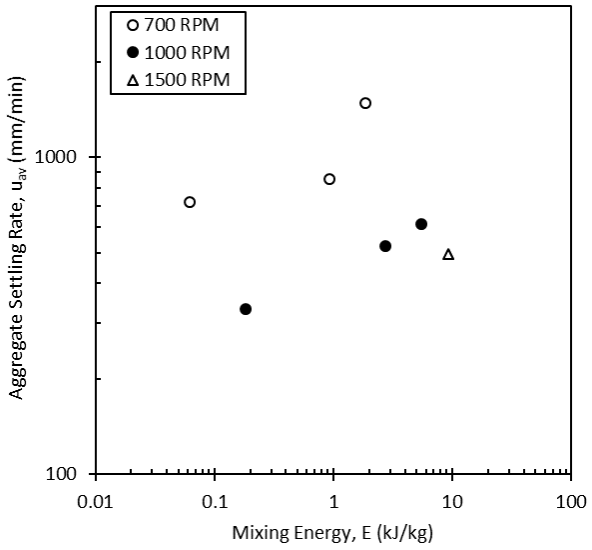

Figure 4.17: Effect of mixing conditions on in-situ aggregate hindered settling rate.

reducing the overall settling. The 1000 RPM and 1500 RPM cases do not suffer from this discrepancy. One possible explanation for this could be due to biased sampling in which the method of sampling itself favored smaller aggregates. Since low impeller speed would produce lower shearing, precipitated asphaltene aggregates would be able to grow. It is possible that aggregates in the 700 RPM case grew to be larger than what was extracted for individual aggregate settling tests and that the sampling procedure itself broke up these larger aggregates along the way. Thus, the in-situ hindered settling rate was observed to be higher than individual settling. The implication of this is that samples used for individual aggregate settling tests may not be entirely representative of formed asphaltene aggregates due to the biased sampling. As this bias would be applied to all samples taken, this would further imply that any quantitative conclusions drawn from individual aggregate settling tests would be invalid, but conclusions made about general trends would still be okay.

The results in Figure 4.17 also agree with the conclusions reached from individual aggregate settling tests. Generally, for a fixed mixing intensity, increasing mixing energy led to higher settling rates. This is consistent with the trend in Figure 4.11. Furthermore, Figure 4.17 supports the previous conclusion that aggregate size has a bigger impact on settling rate. This is because when compared to the size and effective density trends seen in Figures 4.13 and 4.15, respectively, it can be seen that lower mixing intensity produced larger, less dense aggregates, which here still led to much higher hindered settling rates as a result of the greater influence of aggregate size. This could be due to low shearing occurring at lower impeller speeds and high mixing times allowing aggregates to grow. Overall, this indicates that asphaltene aggregates with the highest hindered settling rate can be produced from mixing at low intensities for long mixing times.

4.4.4 Comparison of Results with Literature

In order to further analyze the data, results shown in Sections 4.4.2 and 4.4.3 are compared to the literature. In particular, since the procedure and conditions of this study were based on the work by Zawala et al. [9], differences between the results will be discussed at length.

To begin with, the trend observed for the settling velocities of individual aggregates in this study differ vastly from the findings of Zawala et al. [9]. This is apparent when comparing this current study's results to theirs as shown in Figure 4.18. The results of both studies show a clear positive trend between individual aggregate diameters and settling velocities. However, they observed distinctly higher settling velocity data for aggregates produced at 100× the mixing energy whereas this separation is not as apparent in the current study where a 150× mixing energy difference exists between the higher and lower cases shown. In fact, this lack of separation is more comparable to Figure 2.12 from Rahmani et al. [30] in which porous aggregates produced from mixing energies approximately 10× apart showed no distinct difference in settling velocities. This result suggests that aggregates formed in the current study differ in settling properties from the ones seen by Zawala et al. [9].

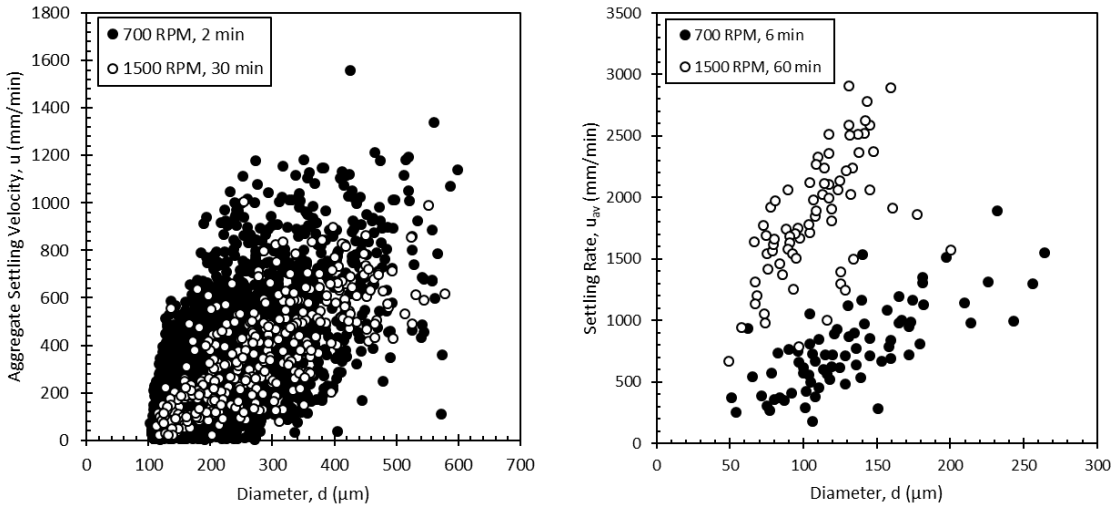

(a) This study (Appeared originally as Figure 4.10) (b) Zawala et al. [9] (Appeared originally as Figure 2.14)

Figure 4.18: Comparison of individual settling velocity results.

This difference in settling properties can affect the overall settling rate of aggregates, which is most clearly seen when comparing the hindered settling velocities as seen in Figure 4.19. Generally, both figures show that higher mixing energies led to higher settling rates. However, Zawala et al. [9] found that all hindered settling rate data fell into one trend line when plotted against mixing energy (Figure 4.19(b)). In other words, mixing intensity did not matter when considering aggregate settling rate. This obviously differs

from what was found in the current study in which different mixing intensities appear to produce different settling rate curves which do not all fall into a single trend line. This observed difference when taking mixing intensity into account indicates that mixing in PFT processes should not be characterized using only mixing energy.

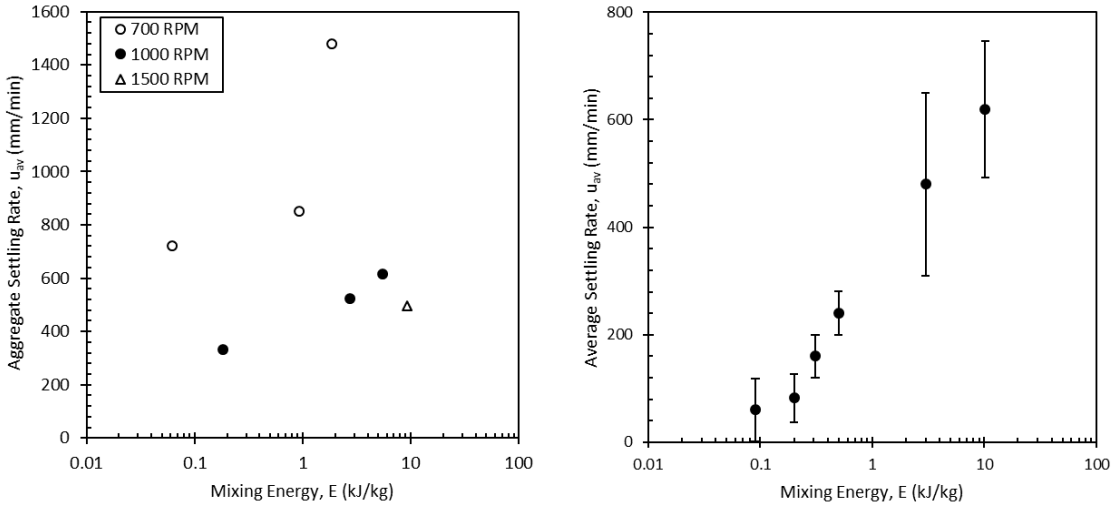

(a) This study (Appeared originally as Figure 4.17) (b) Zawala et al. [9] (Appeared originally as Figure 2.15)

Figure 4.19: Comparison of hindered settling velocity results.

The most likely explanation for the differences seen in the individual and hindered settling velocity results is that the aggregates observed in the current study are structurally different compared to the aggregates observed by Zawala et al. [9]. Recall from Section 2.7.1.2 that Zawala et al. [9] found aggregates that were very compact without a porous structure as no water droplets were trapped inside their aggregates. They also noted that during their experiments large water droplets appeared and coalesced immediately at the bottom of their vessel upon stopping mixing. This indicated an unstable emulsion and the rapid separation of water was concluded to be the reason that aggregates contained no water droplets in their structure. In contrast, the separation and coalescence of water following the stoppage of mixing was not observed in any experiment performed in the current study. Because of this difference in observation, it is believed that the water in the current study likely became part of the precipitated asphaltene aggregates leading to different aggregates than Zawala et al. [9] observed.

Evidence of the difference in aggregate structure observed by Zawala et al. [9] and the current study can be investigated further by comparing aggregate size and density results. Figure 4.20 shows a comparison of the lowest and highest mixing energy point size distributions of the current study with that of Zawala et al. [9]. It is clear from Figure 4.20, that the current study saw a clear increase in aggregate size with mixing energy whereas

Zawala et al. [9] only found a 9% change in aggregate size between their lowest and highest mixing energies. This shows that mixing conditions had an effect on aggregate size in this study whereas the size of compact aggregates observed by Zawala et al. [9] remained mostly unchanged due to mixing. The discrepancy of aggregate size change with mixing conditions is evidence that aggregates in the current study differed from those seen by Zawala et al. [9].

In terms of aggregate density, Zawala et al. [9] concluded that increasing mixing energies formed more dense aggregates as the composition of aggregates changed to include more dispersed solids. The current study finds the exact opposite where increasing mixing energy created less dense aggregates. Moreover, this study observed that the effective densities of individual aggregates decreased with increasing aggregate size. This

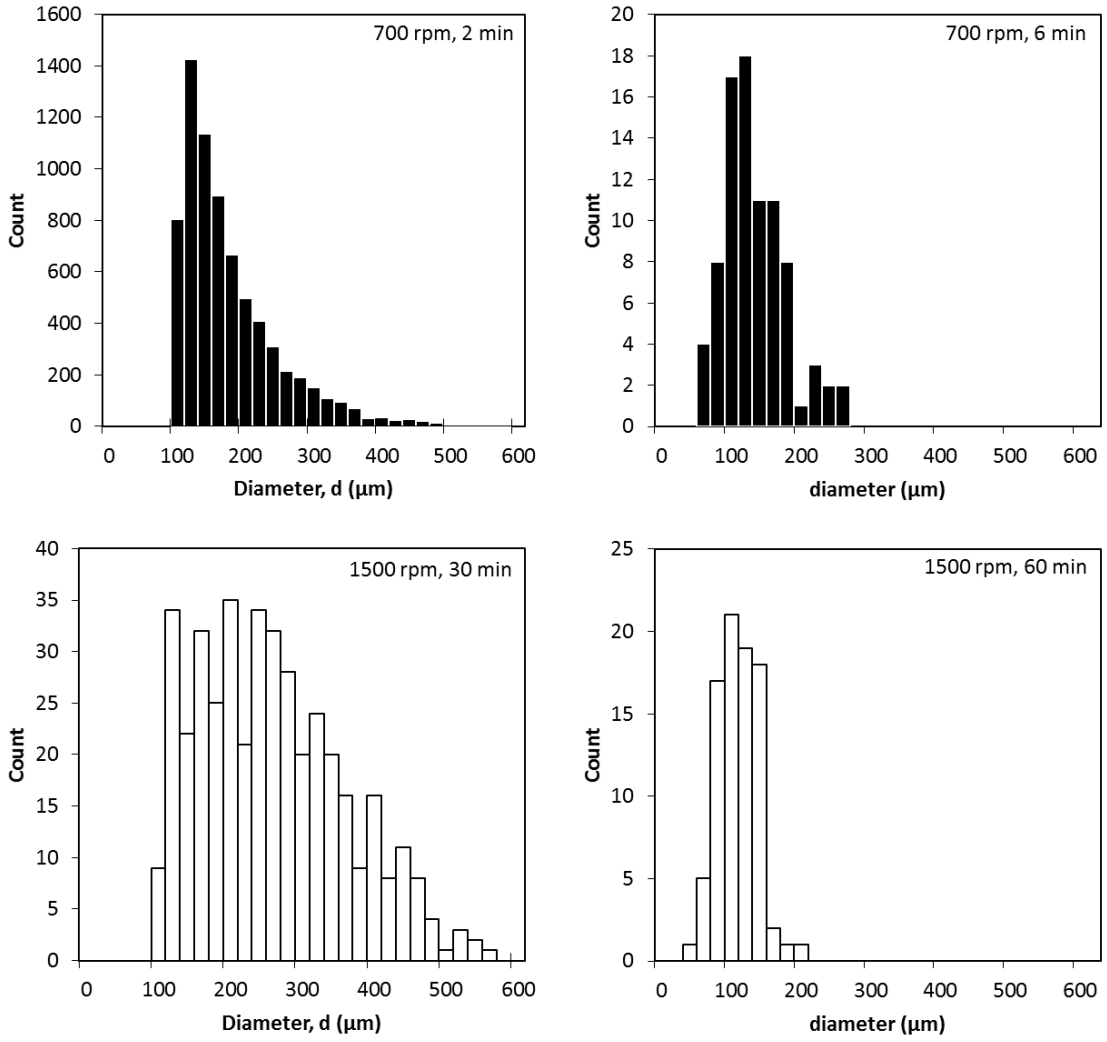

(a) This study

(b) Zawala et al. [9] (Appeared originally as Figure 2.16)

Figure 4.20: Comparison of size distribution results.

trend matched well with observations by Rahmani et al. [30] which observed the settling of porous asphaltene aggregates. As such, there is a likelihood that the aggregates in the current study are also porous. This clearly differs from Zawala et al. [9] who observed extracted asphaltene aggregates under a microscope to be compact structures consisting of only precipitated asphaltenes (PA) and dispersed solids (DS) with no water droplets (WD). This is contrary to earlier studies [11, 32] which observe porous WD/DS/PA aggregates.

Considering these differences in the aggregate size and density changes as a function of mixing conditions, it is clear that the aggregates of the current study differ vastly from those studied by Zawala et al. [9] despite duplicating their procedures and test conditions. Whereas Zawala et al. [9] found that increasing mixing energy produced denser aggregates without much change in size, the current study finds that increases to mixing energy yields larger and less dense aggregates. Furthermore, the current study finds that differences in mixing intensity also appear to have effects on aggregate size, density, and ultimately settling rate. These differences have already been discussed in Sections 4.4.2 and 4.4.3. The reason for such a large difference in the formed aggregate properties can be explained by comparing the feed stocks used in the current study and by Zawala et al. [9]. The current study used froth consisting of 66 wt% bitumen, 21 wt% water, and 13 wt% solids whereas Zawala et al. [9] used froth with 56 wt% bitumen, 34 wt% water, and 10 wt% solids. It is immediately apparent that the froth in the current study contained less water and more bitumen and solids than that of Zawala et al. [9]. Having less water may have helped to create more stable conditions during mixing and prevented the separation and coalescence of water as its own phase upon the stoppage of mixing that Zawala et al. [9] observed. Additionally, since the froth-to-solvent ratio was kept constant between this study and Zawala et al. [9], the difference in froth compositions results in a different solvent-to-bitumen (S/B) ratio as well. In the current study, the S/B works out to 1.5 compared to an S/B ratio of 1.8 in Zawala et al. [9]. The S/B ratio used in the current study is closer to that of Kosior et al. [12] which utilized an S/B ratio of 1.6. Recall from Chapter 3 that settling rate results by Kosior et al. [12] had the largest deviation from Zawala et al. [9] when plotted as a function of mixing energy. These results suggest that the froth composition plays a key role how mixing effects the settling properties of asphaltene aggregates in PFT operations. Further, the differences in aggregate settling results compared to Zawala et al. [9] are likely due to these discrepancies in the composition of froth used in the current study.

4.5 Conclusions

It is clear from the results shown in this chapter that the mixing intensity and energy when mixing paraffinic solvent and bitumen froth have a significant impact on the settling properties of formed asphaltene aggregates. Overall, it was found that increasing mixing energy produces aggregates with higher settling velocities. Additionally, higher mixing energies produced larger aggregates that were less dense. Since the aggregate settling velocity increased with higher mixing energies despite the fact that aggregates were less dense, it was concluded that the aggregate size was more influential to the settling than density. This is consistent with Stokes' law settling in which $u_\infty \propto \rho_{eff} d^2$. When plotted as a function of mixing energy, results were separated depending on the mixing intensity used for testing. Lower mixing intensities were found to produced faster settling rates. It was concluded that this was due to weaker shear forces at lower mixing intensities, enabling larger aggregates to form and remain unbroken during mixing. For constant mixing intensity, increasing the mixing time, and thus total mixing energy, still increased aggregate settling rates. As such, the fastest settling aggregates were found to form under low mixing intensity and high mixing time conditions.

The results of this study were compared to the findings by Zawala et al. [9] as the procedures and test conditions of the current study were based on their work. Both studies showed that increasing mixing energy resulted in asphaltene aggregates with higher settling rates. However, while Zawala et al. [9] found that increasing mixing energy resulted in increased aggregate densities but had no effect on aggregate sizes. The current study showed that increasing mixing energy decreased aggregate densities and increased aggregate sizes. Furthermore, aggregates in the current study were found to have decreasing effective density with increasing aggregate size matching that of past studies by Rahmani et al. [30]. This trend is associated with porous aggregates indicating the aggregates in the current study were porous. As only two phases were observed after mixing was completed, it was concluded that these porous aggregates were likely made up of precipitated asphaltenes, dispersed solids, and water droplets. In contrast, Zawala et al. [9] observed aggregates to be compact structures without the presence of water droplets. This difference in structure of aggregates was attributed to the fact the froth composition in the current study was 66 wt% bitumen, 21 wt% water, and 13 wt% solids compared to the 56 wt% bitumen, 34 wt% water, 10 wt% solids froth used by Zawala et al. [9]. Thus, the difference in aggregate structure due to differences in froth composition was deemed the primary cause of the discrepancy of results between the current study and the work of Zawala et al. [9].

Chapter 5

Partial Mixing of a Three-Phase Solvent Deasphalting Analogue

5.1 Introduction

The partial upgrading of a bitumen-water emulsion via high temperature and pressure solvent deasphalting (SDA) has the potential to produce three liquid phases when allowed to settle: a light deasphalted oil (DAO) phase, an asphaltene pitch phase, and a water phase [5]. Solvent is distributed to the DAO and pitch phases. Ideally, DAO + solvent (henceforth just referred to as DAO) is extracted as the overflow product while pitch + solvent and water phases make up the underflow. This relies on the water phase acting as a carrier fluid to move the pitch phase out of the settler. However, since the pitch + solvent (henceforth referred to just as pitch) and water phases do not move together, it is necessary to introduce partial mixing of these two phases to remedy this. As the use of SDA with a bitumen emulsion feed is relatively new and testing at operating temperature and pressure conditions is complicated, a three-phase analogue was employed to simplify the study of controlling a three-phase system such that partial mixing produced a homogeneous two-phase underflow without entrainment into the overflow.

This chapter describes the development and use of an analogue alcohol–hydrocarbon–brine system to investigate the feasibility of partial mixing in SDA processes. The choice of alcohol, hydrocarbon, and brine fluids were based on matching the density ratios of a known SDA process being developed for partial upgrading. Fluids were placed into a clear vessel with geometry matching that of a future planned bench-scale SDA test vessel. Impeller speeds were increased to the point of the fluids being fully mixed then decreased until only partial mixing of the bottom two phases. The most promising impeller combinations were then tested in a clear horizontal settler geometry, similar to future planned pilot-scale settlers, under no-flow conditions. The best performing impellers were

finally tested in a continuous flow loop setup with the clear horizontal settler geometry. Results were obtained by visual observation where pictures and video of the experiment were taken. The focus was on determining the impeller configurations and speeds that resulted in successful partial mixing of the analogue fluids.

5.2 Experiment Design

The main objective of this study is to identify mixing configurations and conditions that produce partial mixing of two underflow phases in a three-phase system without entrainment into the overflow phase. Thus, it is necessary to consider a wide range of impellers and impeller configurations to achieve this goal. However, while there are numerous impeller types available, the current study focused on single and two-impeller configurations with three impeller types previously described in Section 2.4.3: a Lightnin A310 hydrofoil, a Rushton turbine, and a marine propeller. Figure 5.1 shows the impellers used in the current study. These impellers were chosen as they are all commonly used and provide a good range of impeller flow pattern effects on partial mixing quality. The

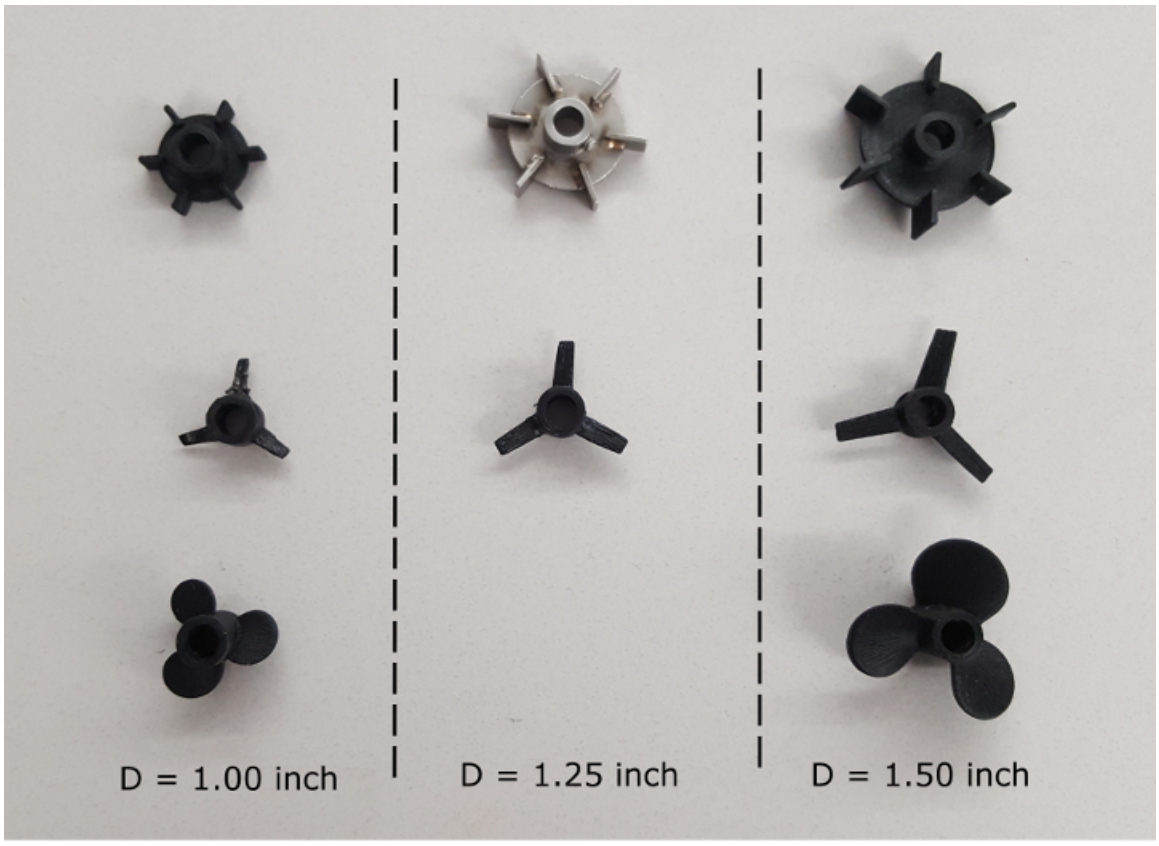

Figure 5.1: Rushton (top row), hydrofoil (middle row), and marine (bottom row) impellers used in the current study.

marine impeller provides a large amount of down pumping motion with little radial mixing. Conversely, the Rushton turbine mixes entirely through radial movement with no down pumping circulation [22]. For single-impeller tests, each impeller was tested at two locations: at the interface of the bottom two phases, and completely submerged in the bottom phase at approximately half the height of the combined underflow (U/F) phases. The test matrix for single-impeller tests is shown in Table 5.1.

Table 5.1: Experimental test matrix for single-impeller partial mixing tests.

Impeller Location	Impeller Type and Size	Impeller Speed
At interface of U/F phases	Rushton, D = 1.00"	0 to 600 RPM
	Rushton, D = 1.50"	
	Lightnin A310, D = 1.25"	
	Lightnin A310, D = 1.50"	
	Marine, D = 1.00"	
	Marine, D = 1.50"	
Submerged in bottom U/F phase at middle of combined U/F height	Rushton, D = 1.00"	
	Rushton, D = 1.50"	
	Lightnin A310, D = 1.25"	
	Lightnin A310, D = 1.50"	
	Marine, D = 1.00"	
	Marine, D = 1.50"	

Note from Table 5.1 all axial impellers tested were placed in a down-pumping orientation. Additionally, the 1.25" diameter Rushton and 1.00" diameter Lightnin A310 impellers were not included in testing. This was because they were unavailable at the time and the tests listed in Table 5.1 were sufficient to draw strong conclusions about partial mixing with single impellers.

For the dispersion of a less dense phase into a denser phase (e.g. oil into water) with two impellers, the Handbook of Industrial Mixing [39] recommends using a top down-pumping axial impeller with a lower radial impeller. This combination uses low power to produce high flow [39]. As such, based on this recommendation and to narrow down the number of configurations tested, all two-impeller combinations were performed with a top axial impeller and bottom radial impeller. As with the single-impeller tests, axial impellers were always placed in a down pumping orientation. The general idea with this configuration is to draw down the middle phase using the pumping of the axial impeller into the radial impeller to disperse it into the bottom phase. Table 5.2 shows the test matrix for two-impeller tests.

Table 5.2: Experimental test matrix for two-impeller partial mixing tests.

Top Impeller	Bottom Impeller	Impeller Speed
Lightnin A310, D = 1.25"	Rushton, D = 1.00"	0 to 600 RPM
Lightnin A310, D = 1.50"		
Marine, D = 1.00"		
Marine, D = 1.50"		
Lightnin A310, D = 1.25"	Rushton, D = 1.50"	
Lightnin A310, D = 1.50"		
Marine, D = 1.00"		

5.2.1 Three-Phase Separation

Since the use of SDA on bitumen emulsion needs to be performed at high temperatures (> 130 °C) a vessel that could withstand such conditions would be required. While such vessels do exist, testing in one would be extremely time consuming (1 day per test) due to the equipment preparation and cleaning procedures required when working with bitumen. As the number of impeller configurations tested was numerous, a cold flow analogue was needed.

Density data for the DAO, pitch, and water phases of a high temperature and pressure SDA process in development for partial upgrading was taken as the basis of design for this study. This was done, instead of using viscosity data, as density is important to the settling characteristics of the system as shown in Equation (2.3). While viscosity affects the drag force term, C_D, it is clear from Equation (2.3) that, when settling occurs outside of Stokes regime, preserving the density ratio when developing an analogue is more important in order to match the settling characteristics of the SDA process. Within Stokes regime, density and viscosity are both equally important as it can be seen from Equation (2.6). Since the the density ratio is important over all settling regimes, it was used to develop the analogue. Thus, using the data, the density ratios of the DAO-to-water phase and pitch-to-water phase were calculated to be 0.60 and 0.75, respectively.

From this, there is the challenge of finding a three-fluid system that matches the calculated density ratios, because three-phase systems often end up with phases that are a mixture of all the initial components while being rich in one phase [40–42]. This phenomenon makes it difficult to guarantee the density ratio of the final phases match the original process without extensive phase diagram data. Knickerbocker et al. [40] found that benzyl alcohol always ended in three pure phases when mixed with any alkane hydrocarbon and brine. Because of this, benzyl alcohol was chosen as the pitch phase analogue due to its immiscibility with the other two phases meaning that it will not form phases that are rich in one substance or another. This makes it so the density of each phase

does not depend on the amount of each initial phase in the mixture making it easier to calculate density ratios of the analogues. Given the density of benzyl alcohol (1040 kg/m^3) at room temperature and the calculated density ratios, the density of the hydrocarbon and brine phases were calculated and fluids matching those densities were found. The details of the chosen hydrocarbon and brine phases are given in Section 5.3.1.

5.3 Experimental Method

Experiments performed in the current study were broken into three parts. In the first part, testing was done in a glass beaker stirred tank geometry. In the second and third parts, conditions for partial mixing were executed in a clear scaled-down model of a horizontal settler based on a future planned pilot scale settling vessel. Part I of the experiments tested numerous single-impeller and two-impeller size and general location combinations in order to narrow down the options for the second part of experiments.

Part II of testing looked at fewer impeller combinations in the horizontal settler geometry under no-flow conditions. During this part, a distinction was also made between vertical entry and horizontal entry mixing configurations. Vertical entry configurations made up the majority of tests and referred to cases where the impeller shaft enters settler the perpendicular to the ground. Horizontal entry tests utilized an L-shaped mixer to have the impeller shaft parallel to the ground. Additionally, for vertical entry tests, the general horizontal location (i.e. closest to the inlet, middle of vessel, closest to the outlet) of impellers along the vessel were also tested.

From part II tests, one single-impeller and one two-impeller vertical entry combination was chosen for part III testing in which in a continuous flow loop through the horizontal settler was used. Horizontal entry impeller configurations were not tested in continuous flow cases because of reasons outlined later in Section 5.4.3.

Ultimately, this progression of experiments led to the identification of promising mixing conditions that enabled partial mixing of two underflow phases in a three-phase system which coincides with our objective. Figure 5.2 shows a schematic of the progression of experimental tests.

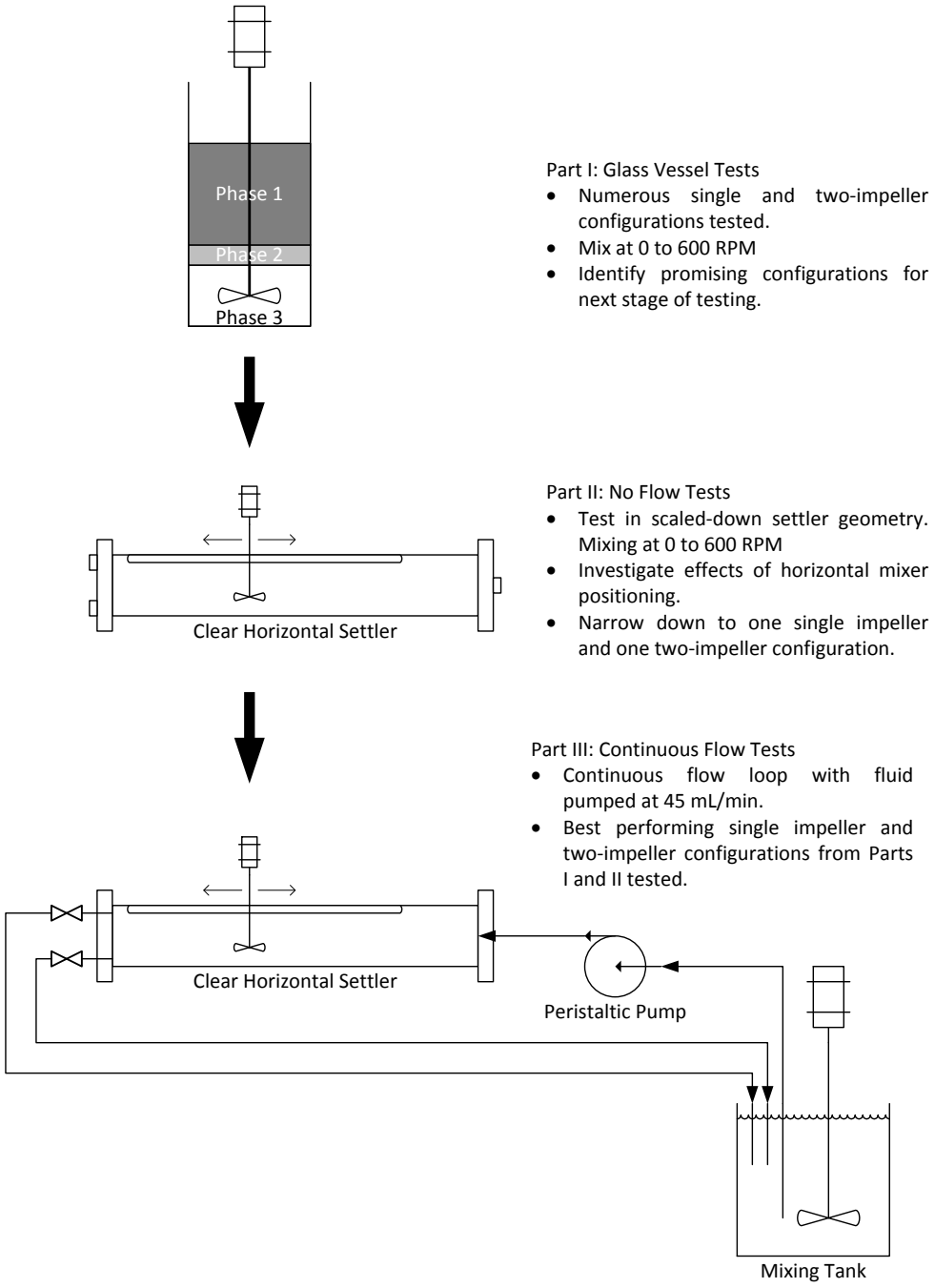

Figure 5.2: Schematic of the progression of experimental test procedures.

5.3.1 Materials

Based on the density ratios mentioned in Section 5.2.1, mineral oil (light, Sigma-Aldrich) and heptane ($\geq$ 99%, Sigma-Aldrich) were chosen as the hydrocarbon phases in the analogue mixtures. Reagent-grade benzyl alcohol ($\geq$ 99%, Sigma-Aldrich) acted as the alcohol phase in all cases. For the brine phase, water was mixed with reagent-grade calcium chloride ($\geq$ 99%, Sigma-Aldrich) to create 40 wt% and 28.9 wt% concentration brines for Stage 1 and Stage 2, respectively.

Fluids were added to the vessel such that the volume percentages of each fluid matched the predicted volume percentages of the planned SDA process. Since the planned SDA process contains two stages, an analogue mixture for each stage was created as follows:

- Stage 1: 58 vol% mineral oil, 9 vol% benzyl alcohol, and 33 vol% water + 40 wt% CaCl2 brine.
- Stage 2: 57 vol% heptane, 5 vol% benzyl alcohol, and 38 vol% of water + 28.9 wt% CaCl2 brine.

Table 5.3: Properties of analogue mixtures.

	Stage 1			Stage 2		
	Phase 1	Phase 2	Phase 3	Phase 1	Phase 2	Phase 3
Component	Mineral Oil	Benzyl Alcohol	Water + 40 wt% $CaCl_2$	Heptane	Benzyl Alcohol	Water + 29 wt% $CaCl_2$
Density @ 20 °C (kg/m^3)	833	1040	1396	684	1040	1270
Viscosity @ 25 °C (cP)	0.95	5.47	-	0.39	5.47	-
Volume (mL)	478	74	272	469	41	313
Density Ratios:						
Phase 1/Phase 3		0.60			0.54	
Phase 2/Phase 3		0.75			0.82	

5.3.2 Equipment Setup and Procedures

As part of the procedure, a simple visual criteria was established to differentiate between successful and unsuccessful cases of partial mixing observed in all testing. Partial mixing with a given impeller configuration was considered a success if:

1. the bottom two phases were thoroughly mixed such that one could not easily determine which phase was which with the naked eye,
2. the top phase was not entrained into the bottom phases during mixing,

3. the height of the interface between the top phase and U/F phases during mixing was comparable to the height of the interface between the top and middle phase under no mixing conditions, and

4. in the case of horizontal settler tests, partial mixing must be observed to reach the U/F outlet of the vessel.

For the second criteria, entrainment of the top phase was checked by observing the interface between the top phase and mixed U/F phases. If this interface was it was relatively flat and steady during mixing, then successful partial mixing was considered achieved. Further, the third criteria was checked by reviewing video recordings and comparing the combined U/F phases heights in no-mixing and mixed conditions.

5.3.2.1 Glass Vessel Tests

A 101.6 mm diameter (T) clear cylindrical tank was used to mix the analogue fluids. The liquid height was set to H/T = 1.0. For glass beaker tests, only a stage 1 mixture of fluid was utilized in all tests. Impeller diameters ranging between 1.0 – 1.5 inches were tested for the three impeller types shown in Section 5.2. A schematic of the experimental setup and procedure is shown in Figure 5.3.

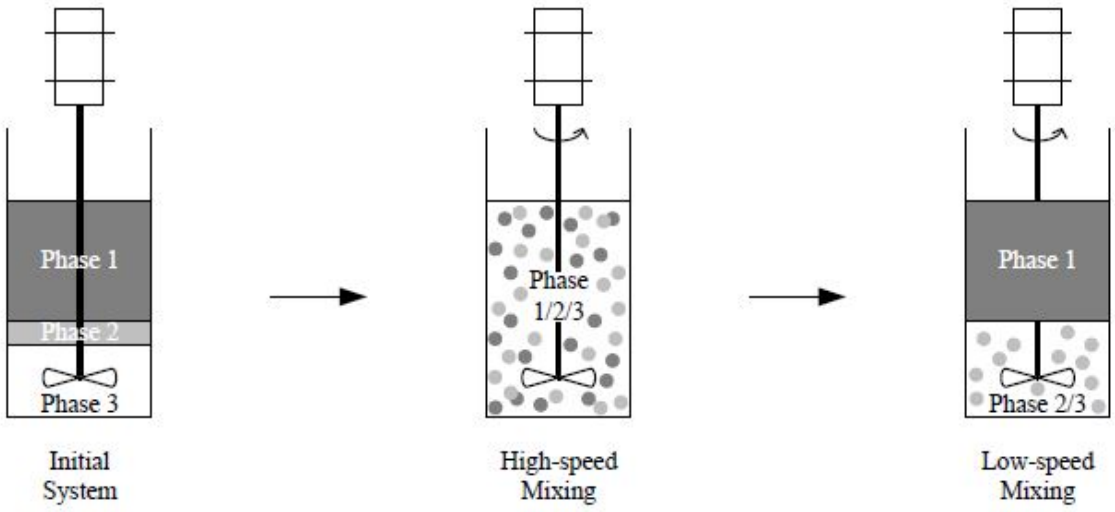

Figure 5.3: Schematic of the experimental setup and general procedure. In this case case phase 1 = mineral oil, phase 2 = benzyl alcohol, and phase 3 = water + 40 wt% $CaCl_2$. Adapted from Breakey [43].

Tables 5.1 and 5.2 previously shown give all of the impeller configurations tested in the glass vessel geometry. As the impeller speeds required to achieve full and partial mixing were unknown, the motor was started on the lowest speed setting and incrementally increased until full mixing was observed, then decreased until steady mixing of only the

bottom two phases was seen. The general procedure for partial mixing tests in the glass vessel was as follows:

1. Pour the appropriate amounts of hydrocarbon, alcohol, and brine analogue phases into the glass vessel.
2. Place and clamp the glass vessel in place under the mixer motor.
3. Setup the test impeller configuration, lighting, and camera.
4. Start recording when no mixing is occurring.
5. Turn on the motor at the lowest mixing speed.
6. Increase the motor mixing speed incrementally until complete mixing of all three phases is observed.
7. Decrease the motor mixing speed incrementally until mixing of only the bottom two phases is observed.
8. Turn off the motor and record the speed of successful partial mixing if it was observed.

5.3.2.2 Horizontal Settler Tests

A clear cylindrical acrylic tube with a slot along the top of the tube was used for the majority of partial mixing tests. The tube was 2 inches in diameter and 10 inches long and designed by Dr. David Breakey to match the geometry of a pilot scale horizontal settler. This horizonal settler was used for no-flow and continuous-flow tests. The procedure followed was identical to that which was stated for glass vessel tests.

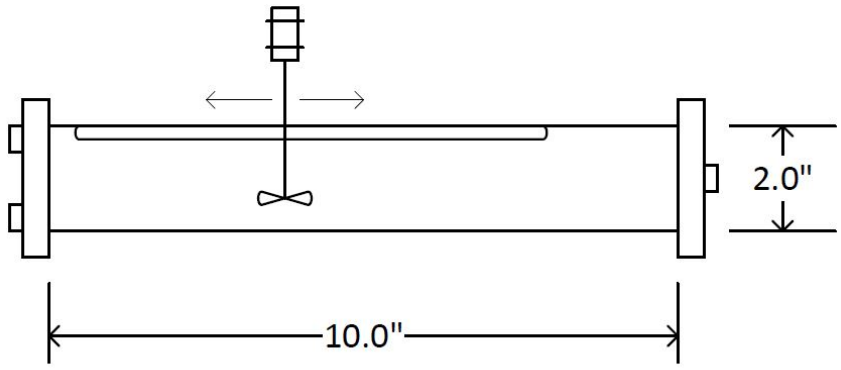

Figure 5.4: Horizontal settler dimensions

Good partial mixing in this horizontal settler geometry was evaluated as described before with the additional condition that mixing dispersed droplets far enough to reach the settler lower outlet. During no-flow testing, vertical entry single-impeller and two-impeller combinations were tested at different horizontal locations along the vessel: closest to the inlet, middle of the slot, and closest to the outlet. Due to limited room in the vessel, two-impeller tests were performed such that the two impellers had the smallest possible separation distance between them. Similar to the glass beaker tests, the impeller speed was started at the lowest setting and incrementally increased to the maximum and then decreased again until two-phase underflow mixing was observed. Video footage of the mixing process as impeller speeds were changed was taken and successful partial mixing speeds were recorded. Some horizontal entry impeller configurations were tested as well using a right-angle shaft attachment.

For continuous flow tests, a flow loop was setup as shown in Figure 5.5. Upon startup, all fluid began in the mixing tank and was thoroughly mixed. Fluids were then pumped into the clear horizontal settler until it was full with outlet valves completely closed. Once full, the inlet flow rate was set to 45 mL/min and outlet valves were adjusted until the fluid level in the horizonal settler stabilized and a steady state was reached. Partial mixing in the vessel was conducted and recorded in a similar manner as no-flow tests.

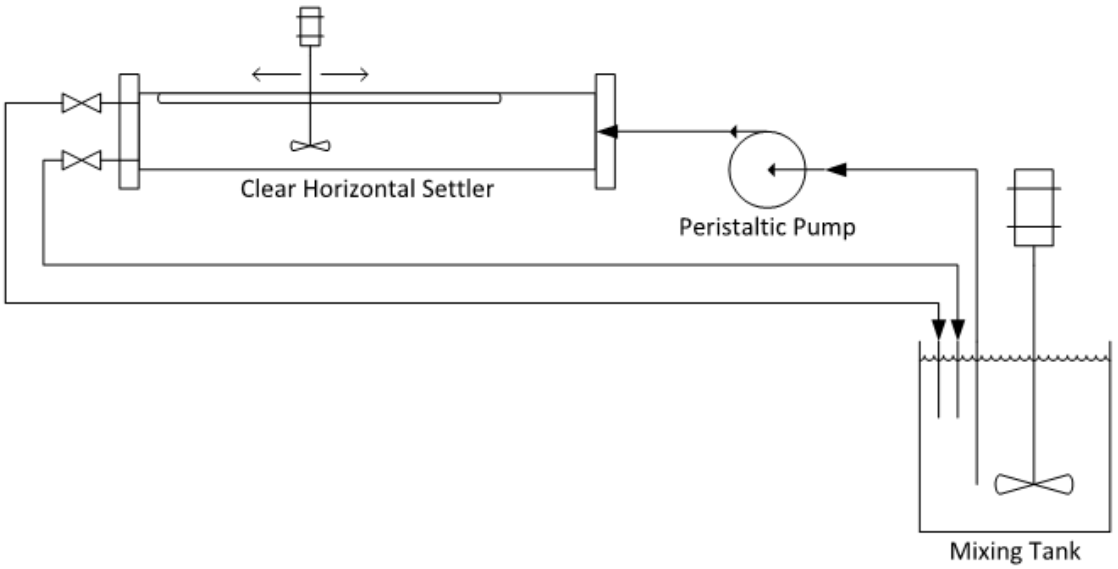

Figure 5.5: Continuous flow setup for partial mixing in a horizontal settler.

5.4 Results and Discussion

5.4.1 Partial Mixing of a Three-Phase System in a Glass Vessel

Figure 5.6 shows the initial system of mineral oil, benzyl alcohol, and brine. As it can be seen from Figure 5.6, the system maintains three distinct phases with the same volume as the inputs. This is unique since, as was discussed in Section 5.2.1, alcohol–hydrocarbon–brine systems typically form phases that are rich in one of the inputs but not pure. Even if the input volumes are all equal, the volume of the final phases depends on the three-phase equilibrium [40–42]. However, as Figure 5.6 shows, it appears that benzyl alcohol is not very miscible in the hydrocarbon or brine phases prior to mixing, making it easy to match the density ratios of the SDA process.

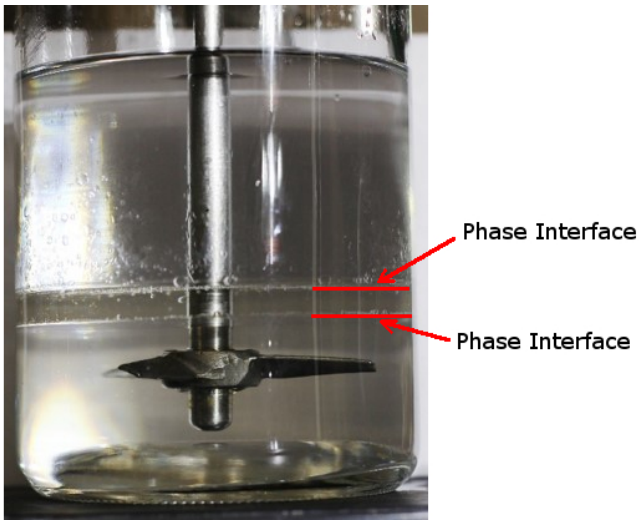

Figure 5.6: Initial system of mineral oil (top), benzyl alcohol (middle), and 40 wt% $CaCl_2$ brine (bottom) phases.

Figure 5.7 shows the partial mixing result for a 1.5-inch hydrofoil impeller when placed at the interface of the U/F phases and when completely submerged in the bottom phase. The impeller speeds shown in Figure 5.7 were chosen based on the points at which partial mixing was the absolute clearest. As it can be seen from Figure 5.7, placing the impeller at the interface of the two phases resulted in partial mixing of the top two phases instead of the desired bottom two phases. Further, having the impeller submerged entirely in the bottom phase resulted in the desired partial mixing result. In fact, what is shown in Figure 5.7 was found to be true for all single-impeller tests in the glass vessel in that placing the impeller at the interface resulted in the undesired partial mixing effect. This result was regardless of impeller type or size. As such, all testing following these single-impeller tests had impellers set to be completely submerged in the bottom most phase.

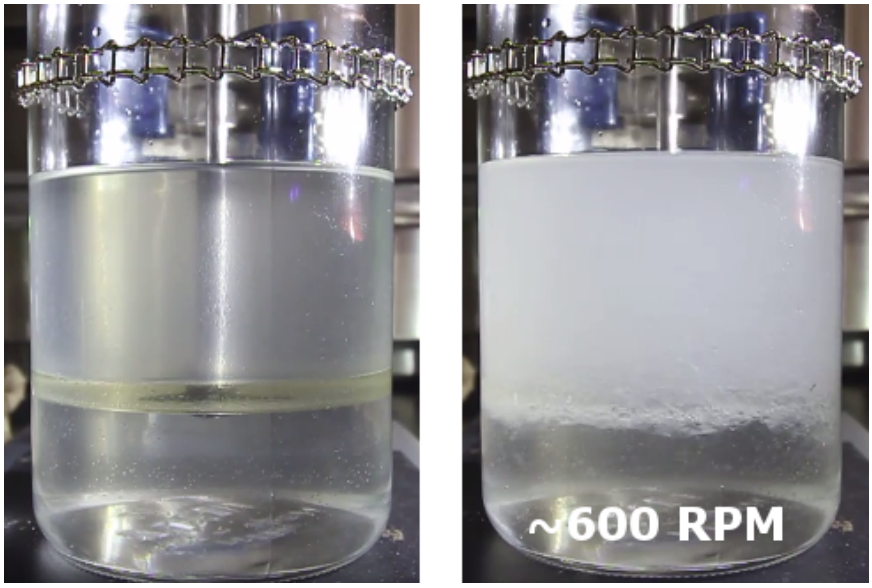

(a) Impeller at interface

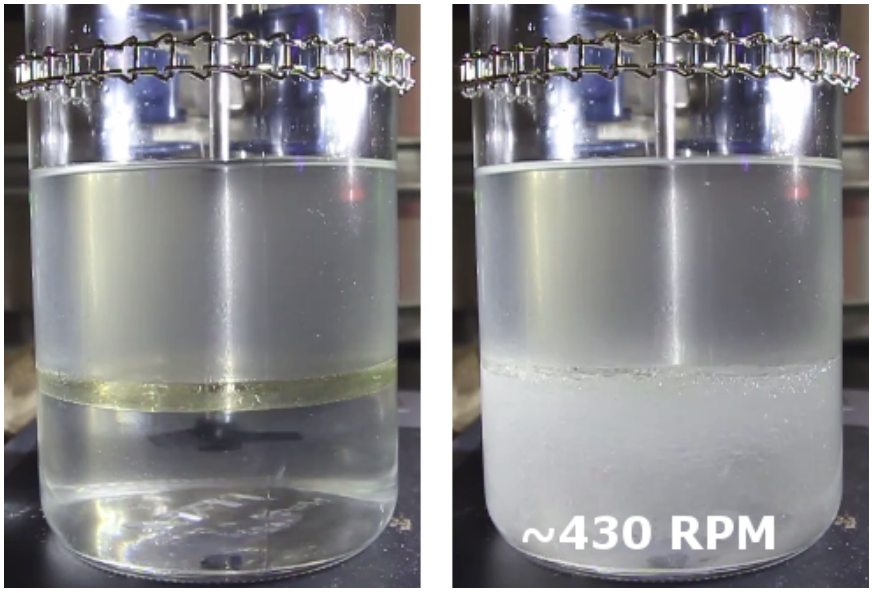

(b) Impeller submerged

Figure 5.7: Partial mixing of three-phase system with single 1.5-inch diameter hydrofoil impeller located at the (a) interface and (b) submerged in the bottom phase.

After mixing was completed and the mixer was turned off, the contents were allowed to fully settle and separate, and then the density of the top phase (originally mineral oil) was checked by extracting 10 mL of sample into a pipette and weighing it. It was discovered that the density remained exactly the same as pure mineral oil. Additionally, after mixing was turned off, the system returned to three distinct phases with the same volumes as initially starting. This is good as it proves the feasibility of mixing the bottom two phases while keeping the top phase unchanged is entirely possible with the analogue system. Further, it shows that the mineral oil/benzyl alcohol/40 wt% $CaCl_2$ brine system could achieve three-phase equilibrium after mixing despite not having equal volumes of each chemical as the input. This extends upon the knowledge of benzyl alcohol–hydrocarbon–brine systems established by Knickerbocker et al. [40, 41], who only showed that mixtures of water with NaCl, benzyl alcohol, and n-alkane hydrocarbons exhibited this three-phase equilibrium behavior when mixed with equal volumes of each phase.

Two-impeller tests performed in the glass vessel were primarily aimed at narrowing down the general impeller combinations that would be most promising for horizontal settler tests. The general results for these tests are shown in Figure 5.8. The impeller speeds shown in Figure 5.8 were chosen based on the point at which the middle phase was observed to mostly disappear and begin mixing with the top or bottom phase. From Figure 5.8, it is clear that partial mixing was only achieved in the case where the top axial impeller was smaller than the bottom radial impeller. Whenever the axial impeller was the same size or larger than the Rushton turbine below it, partial mixing of the top two phases occurred before the bottom phase was mixed. Additionally, since the middle (benzyl alcohol) phase is thin, too much drawdown from the axial impeller would be a

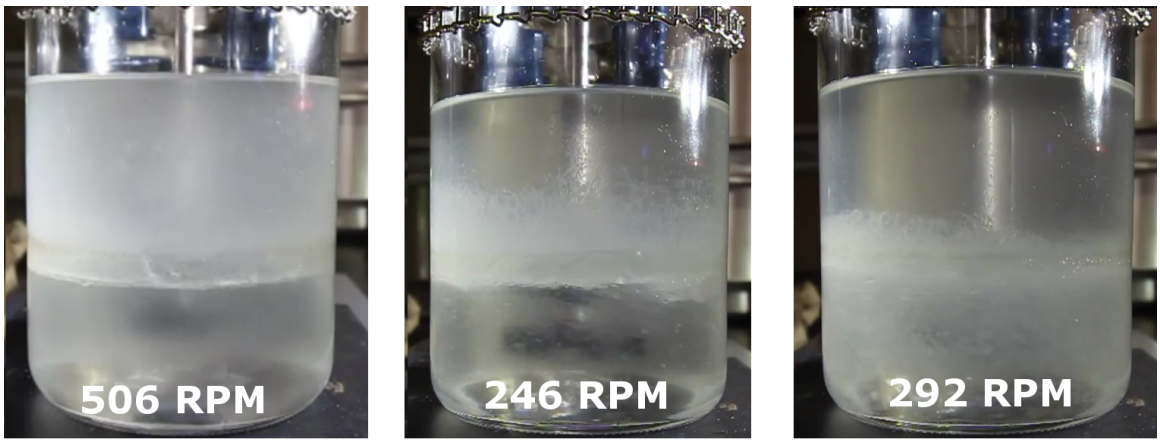

Figure 5.8: Two-impeller glass vessel tests with a Lightnin A310 (top impeller) and Rushton turbine (bottom impeller) combination. Images show mixing for cases where the top impeller is larger (left), the same size (middle), and smaller (right) than the bottom impeller.

problem as it resulted in mixing of all three phases instead of just the bottom two. Recall from Section 5.2 that the idea with the top axial and bottom radial impeller combination was to draw the middle phase down using the axial impeller motion and disperse it with the radial impeller motion. However, if too much drawdown occurs, then the top phase would also be brought down and dispersed into the bottom phase. As the top phase in this model is an analogue for the DAO product in the real process, this ultimately means that partial mixing with too much drawdown actively reduces the yield of the process by losing product to the underflow.

Based on the results and conclusions from the glass vessel tests, no-flow tests in the clear horizontal settler geometry were conducted with two restrictions: (1) impellers should be completely submerged in the bottom phase, and (2) in two-impeller tests, the axial impeller should be smaller than the radial impeller.

5.4.2 Horizontal Settler No-Flow Tests

Due to the results of the glass vessel tests and lack of room in the U/F regions of horizontal settler for impellers larger than 1.25" in diameter, a new test matrix was created for no-flow testing with vertical entry single-impeller configurations. In addition, with the ability to move the impeller horizontally along the settler, the impeller was tested at three general horizontal locations: closest to the outlet, middle of the slot, and closest to the inlet. Table 5.4 shows the newly developed test matrix for single-impeller tests in the horizontal settler geometry. All tests shown in Table 5.4 had the impeller submerged in the bottom phase.

Table 5.4: Experimental test matrix for vertical entry single-impeller partial mixing tests in the horizontal settler geometry under no-flow conditions.

Horizontal Impeller Location	Impeller Type and Size	Impeller Speed
Closest to outlet	Rushton, D = 0.75"	0 to 600 RPM
	Rushton, D = 1.00"	
	Rushton, D = 1.25"	
	Lightnin A310, D = 1.00"	
	Lightnin A310, D = 1.25"	
	Marine, D = 1.00"	
Middle of slot	Rushton, D = 1.00"	
	Rushton, D = 1.00"	
	Rushton, D = 1.25"	
	Lightnin A310, D = 1.00"	
	Lightnin A310, D = 1.25"	
	Marine, D = 1.00"	
Closest to inlet	Rushton, D = 1.00"	
	Rushton, D = 1.00"	
	Rushton, D = 1.25"	
	Lightnin A310, D = 1.00"	
	Lightnin A310, D = 1.25"	
	Marine, D = 1.00"	

Figure 5.9 shows the resulting performance of all three impeller types tested in the single-impeller configuration while being located closest to the outlet of the vessel. Based on the criteria laid out in Section 5.3.2, it was found that successful partial mixing was only seen in cases where the impellers were placed close to the outlet because the mixed U/F phase did not stay mixed all the way to the outlet port otherwise. Additionally, in the single-impeller configuration, both the Rushton and marine impellers failed to achieve successful partial mixing in the horizontal settler geometry. From Figure 5.9, it can be seen that both the Rushton and marine impellers breaks both the top/middle phase and the middle/bottom phase interfaces before good mixing was observed. This indicates that all three phases were being mixed and that partial mixing was not achievable with a single Rushton or marine impeller. Furthermore, it can be seen from Figure 5.9, that the marine impeller had significantly more drawdown and much less radial mixing due to being an axial impeller.

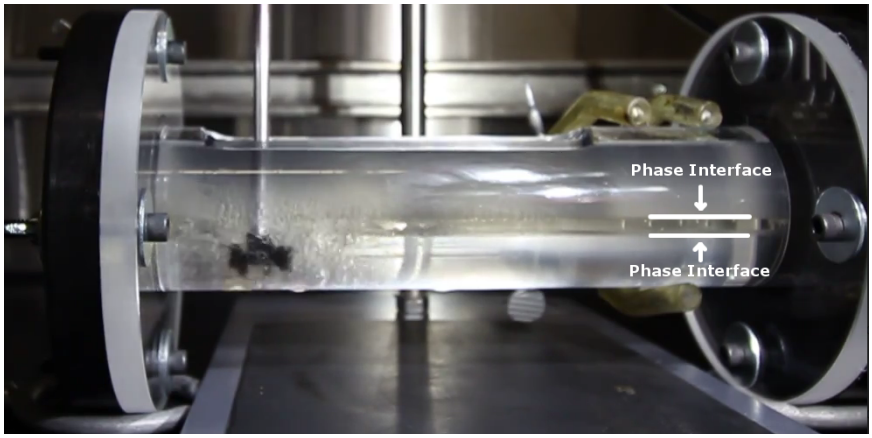

(a) Rushton, D = 1.00"

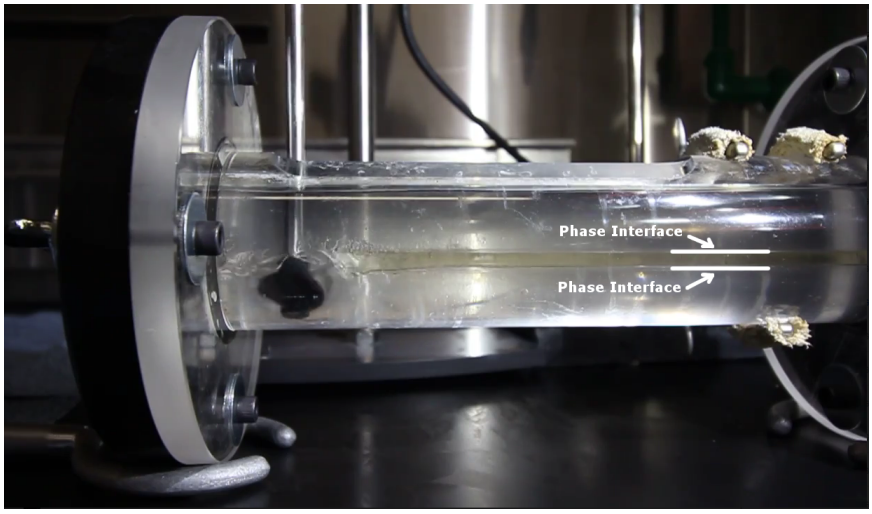

(b) Marine, D = 1.00"

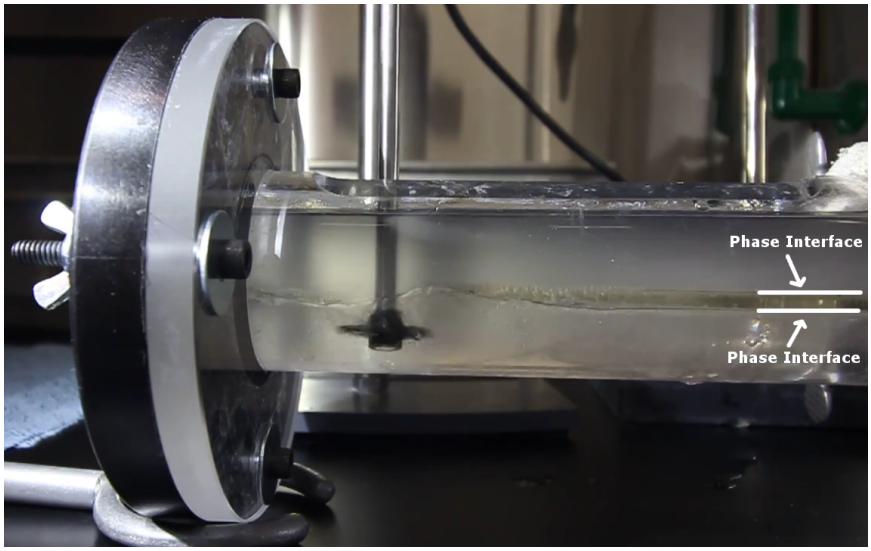

(c) Lightnin A310, D = 1.25"

Figure 5.9: Vertical entry single-impeller partial mixing of three-phase system with a (a) Rushton, (b) Marine, and (c) Lightnin A310 impeller. Vessel outlets are on left side of images.

Of the remaining hydrofoil impellers, the 1.00” diameter Lightnin A310 impeller was unable to draw down the middle phase and mix it with the bottom phase even at the highest motor speed settings. However, in contrast to the performance of the 1.00" diameter Lightnin A310, Rushton, and marine impellers, the 1.25" diameter Lightnin A310 hydrofoil was able to achieve good partial mixing as a single-impeller configuration. This is clearly seen in Figure 5.9 where a distinct line between the middle and top phase was maintained during mixing with the 1.25" Lightnin A310 hydrofoil impeller. This was a good indication that the top phase was not being drawn down or mixed significantly with the U/F phases. Thus, the 1.25” hydrofoil impeller placed closest to the outlet was chosen as the best single-impeller configuration tested for the next stage of testing.

Experiments involving two impellers only looked at two combinations of impellers while varying their horizontal position. Additionally, due to the limited size inside the vessel, impellers were placed as close together as possible in order to submerge them into the bottom phase. The first combination tested involved a 1.00” diameter top hydrofoil impeller paired with a 1.25” diameter Rushton turbine on the bottom set 0.36" apart. The second combination had a 1.00” diameter marine impeller with a bottom 1.25” diameter Rushton impeller separated by 0.50". Similar to the single-impeller tests, three horizontal locations for the impellers was tested for each configuration again. Table 5.5 gives the revised test matrix for two-impeller tests in the horizontal settler under no-flow conditions.

Table 5.5: Experimental test matrix for vertical entry two-impeller partial mixing tests in the horizontal settler geometry under no-flow conditions.

Horizontal Impeller Location	Top Impeller	Bottom Impeller	Impeller Speed
Closest to outlet	Lightnin A310, D = 1.00"	Rushton, D = 1.25"	0 to 600 RPM
	Marine, D = 1.00"	Rushton, D = 1.25"	
Middle of slot	Lightnin A310, D = 1.00"	Rushton, D = 1.25"	
	Marine, D = 1.00"	Rushton, D = 1.25"	
Closest to inlet	Lightnin A310, D = 1.00"	Rushton, D = 1.25"	
	Marine, D = 1.00"	Rushton, D = 1.25"	

Figure 5.10 shows the partial mixing results for both two-impeller combinations tested. Similar to the single-impeller tests, it was observed that good partial mixing that could reach the underflow outlet was only achieved when impeller combinations were placed closest to the outlet. While both two-impeller configurations achieved good partial mixing, it is clear from Figure 5.10 that the two-impeller combination with the marine impeller entrained more into the top phase than the combination containing the Lightnin A310 impeller. This is evident from Figure 5.10 by the more chaotic interface seen when the marine impeller was involved. This result makes sense as the marine impeller has much

more pumping than the Lightnin A310 leading to more drawdown into the bottom Rushton turbine. Too much drawdown is not desired, as entraining the top phase into the U/F phases is essentially mixing that actively reduces DAO yield in the actual process being modeled.

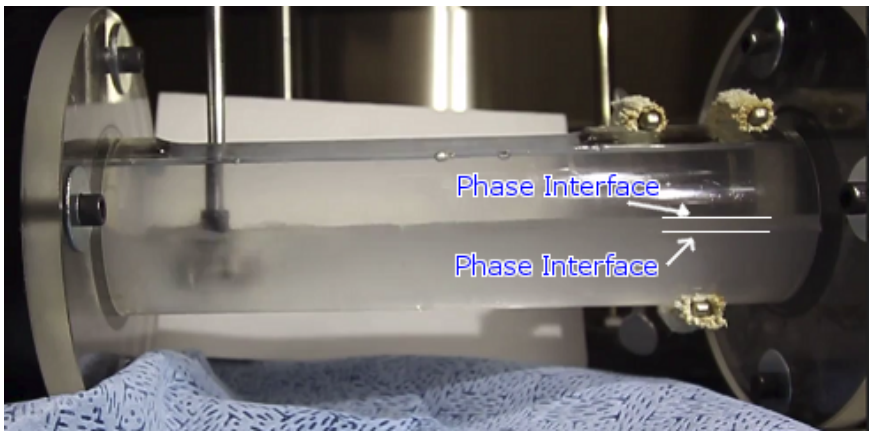

(a) 1.00" Lightnin A310 + 1.25" Rushton

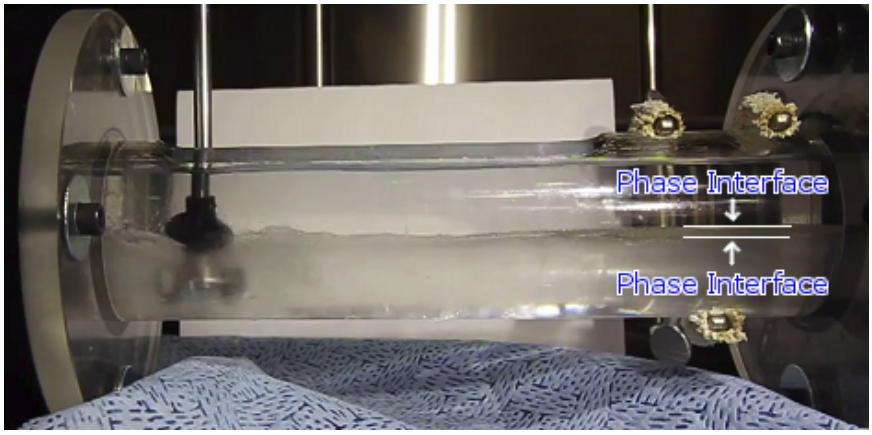

(b) 1.00" Marine + 1.25" Rushton

Figure 5.10: Two-impeller no-flow tests with impellers located closest to the outlet. Vessel outlets are on the left of side of images.

In summary, the single-impeller configuration tests found that only the 1.25" Lightnin A310 impeller produced successful partial mixing based on the criteria laid out in Section 5.3.2. Moreover, two-impeller configuration tests found that while both the combinations considered achieved good partial mixing, it was the 1.00" Lightnin A310 + 1.25" Rushton turbine combination that did so with less entrainment of the top phase. Based on this, the single and two-impeller configurations chosen for continuous flow testing were a 1.25" Lightnin A310 impeller and a 1.00" Lightnin A310 + 1.25" Rushton turbine combination, respectively.

5.4.3 Horizontal-Entry Impeller Tests

As part of the no-flow tests in the horizontal settler, an right-angle shaft mixer was used to simulate partial mixing with a horizontal entry mixer. The mixer assembly consisted of an L-shape angle driver with a drill bit, a connector piece, a support, and the mixing shaft with the impellers. Figure 5.11 shows a schematic of the mixer assembly. The connector and support were used to extend the length of the impeller shaft and provide stability to it during mixing.

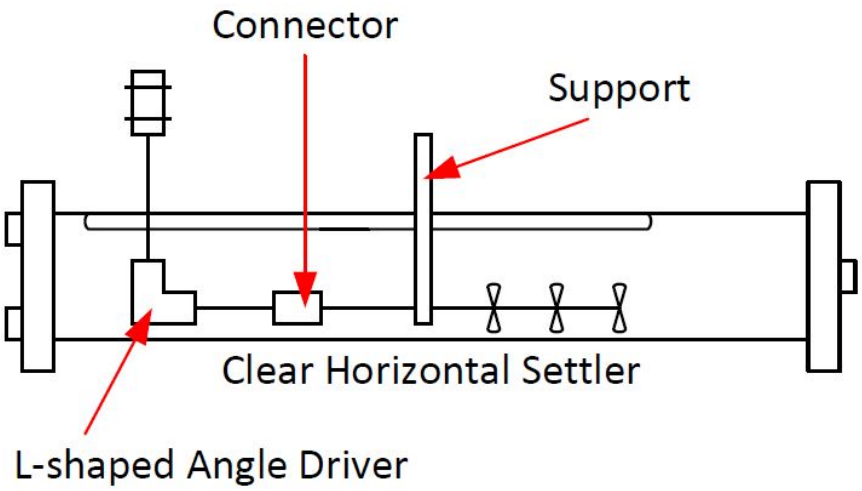

Figure 5.11: Schematic of horizontal entry mixer configuration.

Unlike the rest of the no-flow tests, horizontal entry impeller tests were only performed using a stage 1 mixture. This was because benzyl alcohol dissolved the seal on the L-shaped angle driver drill bit part way through testing which contaminated the analogue fluids with parts of the seal and lubricant that leaked. Tests were performed with smaller 0.75" diameter hydrofoil and marine impellers and the number of impellers along the shaft was varied between 1 to 3 and spaced evenly apart. Table 5.6 shows the test matrix for horizontal entry impeller tests.

Table 5.6: Experimental test matrix for horizontal entry partial mixing tests in the horizontal settler geometry under no-flow conditions.

Impeller Type/Size	Number of Impellers	Impeller Speed
Hydrofoil, D = 0.75"	1	0 to 600 RPM
	2	
	3	
Marine, D = 0.75"	1	
	2	
	3	

Figure 5.12 shows the partial mixing results for all impeller types tested using 3 impellers spaced evenly along the shaft. Horizontal entry mixing with only 1 or 2 impellers along the shaft was largely unsuccessful as regions of the middle phase which were not directly above a given impeller remained unmixed. From Figure 5.12 it is clear that while partial mixing of the underflow phases was achieved with 3 impellers, there was much entrainment of these phases into the top phase. Regardless of the impeller type used, the point at which the middle phase mixed with the bottom phase was only seen with significant entrainment of the U/F fluids into the top phase. This is more evident in the video footage as the mixed zone fluctuates wildly during partial mixing. In the actual SDA process, this entrainment of the U/F phases into the top phase would result in contamination of the DAO product which is clearly undesired.

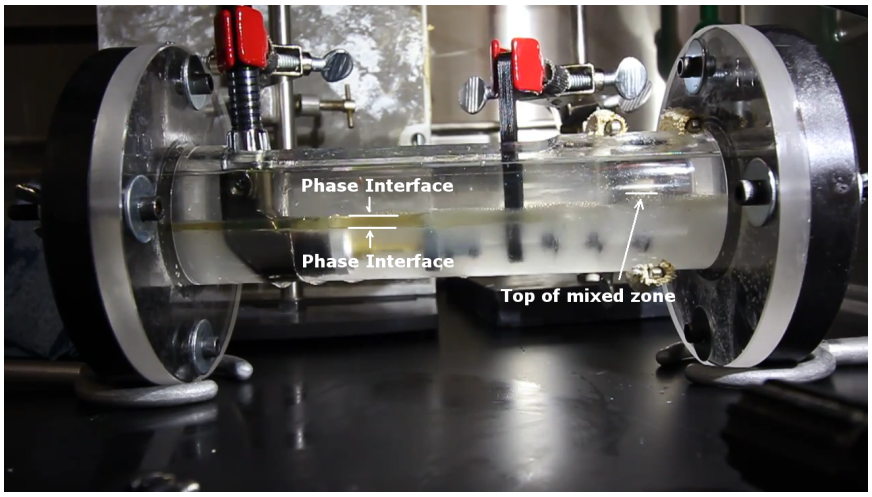

(a) 0.75" Hydrofoil

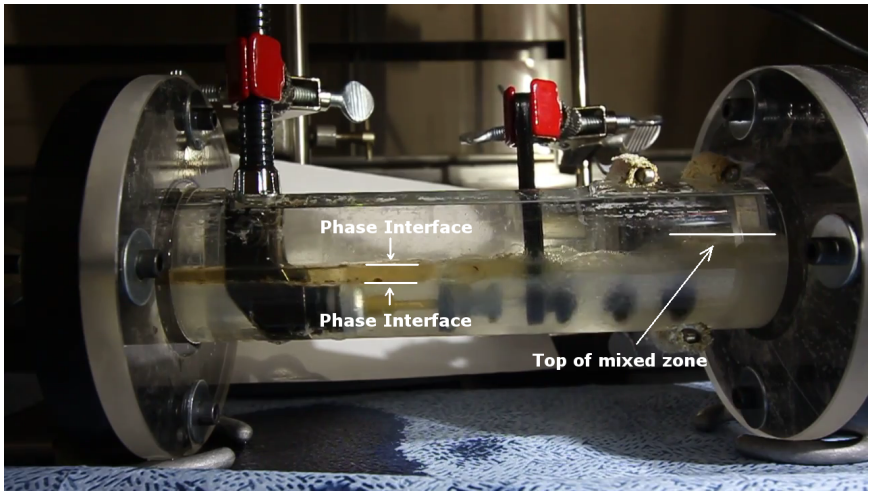

(b) 0.75" Marine

Figure 5.12: Horizontal entry impeller tests with 3 impellers.

Due to the unsuccessful results observed with horizontal entry impeller mixing along with the tendency for benzyl alcohol to dissolve the L-shaped mixer seals and contaminate the analogue fluids, partial mixing with horizontal entry was not pursued any further in this study with continuous flow testing. From the results obtained, it was concluded that horizontal entry impeller mixing does not work to achieve partial mixing according to criteria laid out in Section 5.3.2.

5.4.4 Continuous Flow Tests

From the results of the glass vessel and no-flow horizontal settler tests, a single-impeller configuration using the 1.25" diameter Lightnin A310 impeller and a two-impeller configuration involving a top 1.00" diameter Lightnin A310 with bottom 1.25" diameter Rushton impeller was tested under continuous flow conditions. Each continuous flow test was performed with the stage 1 fluid mix and repeated with the stage 2 fluid mix.

Figures 5.13 and 5.14 show the the partial mixing of stage 1 and stage 2 three-phase systems for the chosen single-impeller and two-impeller configurations, respectively. Overall, both configurations performed well in continuous flow tests with almost no observable entrainment of the top phase. While it is not clear from the photos, it can be seen in the video footage of these tests that there were bubbles of benzyl alcohol in the U/F outlet line. These bubbles indicate successful partial mixing as the middle phase was dispersed into the bottom phase and exited the U/F outlet port accordingly. Furthermore, it was found that successful partial mixing was only achieved when impellers were placed close to the outlet, but not too close. When placed too close to the vessel outlet, mixing would cause significant entrainment of bottom phases into the top phase as impeller motion pushed flow up the vessel outlet walls. After some trial-and-error, it was found that placing the impeller shaft approximately 1.70" away from the vessel exit wall avoided this entrainment entirely.

It can be seen from Figures 5.13 and 5.14 that the impeller speed at which partial mixing was achieved was similar between stage 1 and stage 2 mixtures. Note that one key difference between the stage 1 and stage 2 analogue mixtures is the choice of hydrocarbon in each. Mineral oil in the stage 1 mixture is much more viscous than heptane in the stage 2 mixture. Since benzyl alcohol and calcium chloride brine was used as the U/F phases in both stage 1 and 2 mixtures there is difference in the relative viscosities between the top phase and U/F phases in each mixture. The fact that the performance of partial mixing is so similar despite this difference in stage 1 and 2 mixtures is important as it indicates the results obtained in this study were not limited by the choice to match the density ratio data only. Additionally, this similarity of performance despite relative viscosity differences in stage 1 and 2 mixtures implies that partial mixing is fairly independent of the viscosity difference.

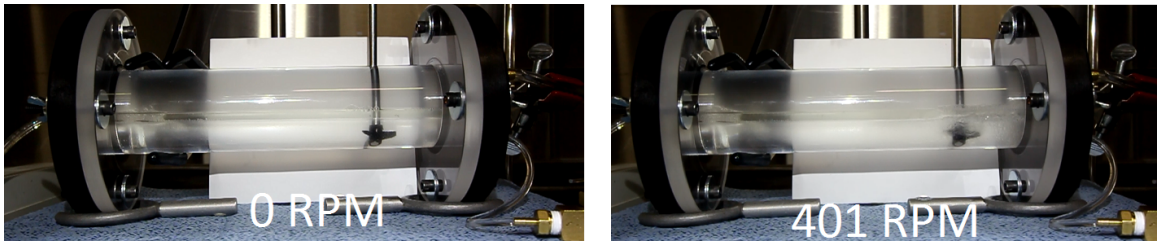

(a) Stage 1

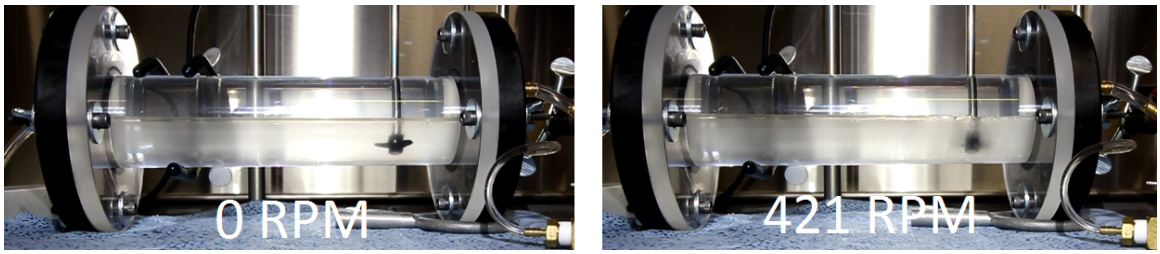

(b) Stage 2

Figure 5.13: Mixing with single 1.25" diameter Lightnin A310 impeller in horizontal settler under continuous flow conditions.

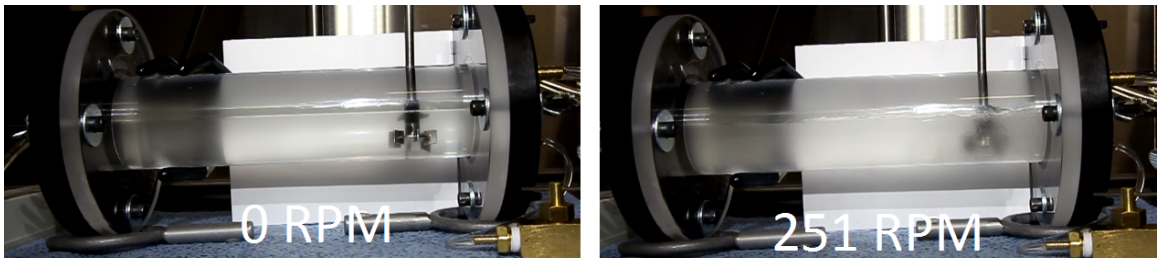

(a) 1.00" Hydrofoil + 1.25" Rushton

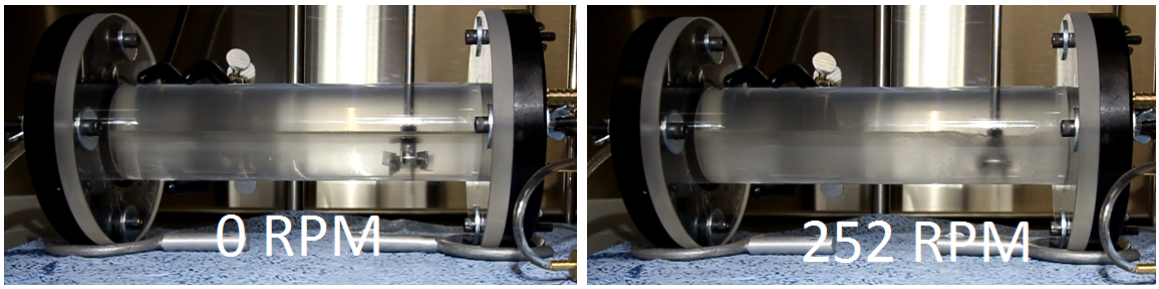

(b) 1.00" Marine + 1.25" Rushton

Figure 5.14: Mixing with 1.00" diameter Lightnin A310 + 1.25" Rushton impeller in horizontal settler under continuous flow conditions.

Despite being in a continuous flow loop, it was also noted that the mixed fluid at the inlet separated out almost immediately. This made it such that the performance of impellers inside the horizontal settler itself was nearly identical to the no-flow test cases. For settler design, this immediate separation of phases indicates that a smaller vessel could be used to achieve the same separation result. However, this quick separation of phases may not necessarily be the same in the actual SDA process because of the differences between the analogue fluids and the SDA phases. In the actual process, the middle pitch phase is expected to be extremely viscous and droplet sizes would likely be very different from the analogue as well [17]. Droplet size is important as larger droplets are more likely to interact and coalesce forming into a separate pitch phase whereas smaller droplets would more readily become mixed into the water phase. Furthermore, based on Equation (2.6), the differences in viscosity and droplet sizes would affect the settling rate of pitch droplets. Here, the fluids used are all relatively low viscosity with benzyl alcohol having the highest at 5.74 cP. As a result of these low viscosities, fluid droplets are able to flow easier and settle faster into three phases when left undisturbed. Additionally, the inlet velocity of the mixture in the pilot and commercial scale processes is many times higher than the 24 mm/s (45 mL/min in 1/8" ID pipe) tested here. At these higher inlet mixture velocities, it is expected that higher horizontal momentum carry the mixture further into the settler creating a larger, distinct mixed region to appear at the inlet which was not observed with the analogue.

Comparing the results of the single-impeller and two-impeller configurations, it was found that the two-impeller 1.00" hydrofoil + 1.25" Rushton combination performed better than the single 1.25" hydrofoil impeller for a couple of reasons. Firstly, the single impeller required a much higher mixing speed before good partial mixing was observed. This would ultimately result in higher energy costs. Secondly, the two-impeller combination produced smaller droplets of benzyl alcohol when mixing the bottom U/F phases. While this difference is clearer in the videos, comparing Figures 5.13 and 5.14 one can see the impellers in the two-impeller configuration are less visible due to more smaller droplets obscuring the view.

Overall, the two-impeller configuration with a top 1.00" diameter Lightnin A310 hydrofoil impeller and bottom 1.25" diameter Rushton turbine was found to perform the best under continuous flow conditions, where the desired partial mixing occurred at lower impeller speeds (and thus energy costs) while producing a finer dispersion of the middle phase into the bottom phase.

5.5 Conclusions

From the above results and discussion, it was observed that:

- Impellers must be submerged in the bottom phase and not any phase interfaces to avoid mixing the top and middle phases together.
- Two-impeller combinations required a smaller top axial impeller with a larger bottom radial impeller to accomplish partial mixing.
- Successful partial mixing in the horizontal settler geometry was achieved with a single 1.25" diameter Lightnin A310 impeller and a two-impeller combination with a top 1.00" Lightnin A310 impeller and 1.25" Rushton turbine on the bottom.
- Horizontal-entry impeller combinations were unsuccessful at achieving partial mixing due to excess entrainment into the top phase.
- Impeller speeds at which partial mixing was achieved were extremely similar for both stage 1 and stage 2 analogue mixtures.

Ultimately, it was concluded that a vertical entry two-impeller system with a top axial impeller smaller than the bottom radial impeller was the best configuration to create a mixed two-phase underflow in a three-phase system through partial mixing. In this study a Lightnin A310 and Rushton turbine were used as the axial and radial impellers, respectively. While it was not varied, it was found that a diameter ratio of 0.8 between the axial and radial impellers placed at about a 0.39" clearance from the bottom of a 2.00" diameter horizontal settler achieved the best partial mixing result. This configuration prevented excessive drawdown of the top phase while dispersing the middle phase into the bottom phase as small droplets. Additionally, by placing the impellers approximately 1.70" away from the horizontal settler outlet port, U/F phases were successfully mixed and drawn from the vessel in a mixed state. This small distance away from the outlet port was important in the settler geometry to prevent entrainment of U/F phases into the top phase during partial mixing. Partial mixing results obtained in this study also showed versatility as all no-flow and continuous-flow tests were performed with both stage 1 and 2 mixtures which resulted in the same performance conclusions. This is important as the hydrocarbon top phase in stage 1 and 2 mixtures differed vastly in viscosity indicating that these results were not limited by the choice to match density ratio data only.

Chapter 6

Conclusions and Recommendations

6.1 Conclusions

Solvent addition in oil sands extraction is typically used to separate heavy materials from a bitumen feed. When mixing solvent and feed, the selected mixing parameters can change the settling properties of heavy products as they separate from the feed. As these properties impact the sizing of settlers and deposition velocity in pipelines, understanding how mixing conditions affect these key properties can improve the overall effectiveness of bitumen recovery operations. In this study, the effects of mixing were studied for a paraffinic froth treatment (PFT) process and an alcohol–hydrocarbon–brine solvent deasphalting (SDA) analogue system. The objectives of this investigation were:

- To analyze the effects of mixing intensity (W/kg) and mixing energy (J/kg) on the size, density, and settling velocity of asphaltene aggregates formed during paraffinic froth treatment, and
- To determine the mixer configurations that achieve partial mixing in a three-liquid phase system developed as an analogue to a solvent deasphalting process.

Paraffinic froth treatment experiments were performed in a stirred tank with a window where mixing intensity and mixing energy were varied by changing the impeller speed and mixing duration. Higher mixing energies created larger aggregates that were less dense but settled more rapidly. It was therefore concluded that aggregate size had a greater impact on settling than density. Additionally, aggregates formed at lower mixing intensities settled more rapidly than ones produced at higher mixing intensities because lower mixing intensities produced lower shearing forces allowing for larger, more fragile aggregates to form and stay together during mixing. Furthermore, at a constant mixing intensity, increasing the mixing time (and thus mixing energy) led to faster settling aggregates. Thus, it was concluded that the fastest-settling aggregates would be formed under low mixing

intensity and high mixing time conditions. This conclusion does not support the use of static mixers even though they are the standard choice in operations, since conventionally used static mixers in froth treatment processes today provide high mixing intensity over a short duration. The implications of the results in this study is that mixing bitumen froth and solvent for longer times at lower mixing intensities would produce faster settling aggregates which ultimately reduce the size of settlers needed to adequately separate diluted bitumen product from froth.

Experiments focused on the partial mixing of an alcohol–hydrocarbon–brine SDA analogue were performed with various mixing configurations. Tests were first performed in a glass beaker and then moved into a cylindrical horizontal settler geometry under no-flow conditions and continuous-flow conditions. At each step, mixer configurations were eliminated until only a few needed to be tested under continuous-flow conditions. After extensive testing, a two-impeller combination with a down-pumping Lightnin A310 impeller placed above a Rushton turbine was found to achieve the best partial mixing. The final impeller configuration had the Lightnin A310 with a diameter of about 0.8$\times$ the Rushton turbine diameter. Partial mixing that prevented drawdown of the top phase while dispersing the middle phase into small droplets in the bottom phase was achieved by placing this impeller configuration with a clearance of 0.39" in a 2.00" diameter vessel. Moreover, the impellers were placed 1.70" away from the settler outlet wall in order to prevent entrainment of the mixed underflow phases into the top phase. This placement also enabled a well mixed underflow to be drawn from the bottom of the horizontal settler in continuous-flow tests. Finally, partial mixing tests in the horizontal settler geometry was performed with two different analogue mixtures representing the first and second stage of a real process. The results obtained in this study showed versatility since the chosen impeller configuration performed similarly in both mixtures. This is important since the hydrocarbon top phase of these mixtures were vastly different viscosities indicating that the results were not limited by choosing to match only the density ratio of fluids with the real process.

6.2 Recommendations for Future Work

The differences seen between the results of the current study and those of Zawala et al. [9] warrant further investigation. For instance, it is unclear why Zawala et al. [9] observed an immediate separation of a distinct water phase upon the stoppage of mixing while the same was not observed in the current study. It is recommended that further testing varying mixing intensity and energy conditions be performed different froth qualities.

Both the current study and Zawala et al. [9] observed increases in aggregate settling rate with increasing mixing energies; however, no upper limit to this increase was seen

within the range of mixing conditions tested. For future work, a wider range of mixing energies should be investigated to determine the limitations of mixing. More specifically, the point at which increasing mixing energy no longer results in faster settling aggregates should be established.

Observation of individual aggregates settling in a square glass column provided a simple method to characterize aggregate size. However, as discussed in Section 4.4.3, the method of sampling may have created a bias in the results. Thus, future studies should consider using non-invasive methods of obtaining aggregate sizes such as Focused Beam Reflectance Measurement (FBRM).

In this study, it has been shown that lower intensity mixing and longer mixing times produce faster settling aggregates. It is important to note that this result was obtained from batch settling tests. As industrial processes are much larger in scale and are typically continuous operations, further work is required to determine the general applicability of these conclusions. It is recommended that future testing of mixing effects on aggregate settling be performed under continuous flow conditions and compared to the results here.

The mixing conditions to achieve complete and partial mixing of the analogue can be used in an autoclave setup of similar geometry to study partial mixing in solvent deasphalting. Using these mixing conditions to design an experiment with actual solvent deasphalting feeds at industrial temperature and pressure conditions is of great interest to test the similarity of the analogue system to the real system.

This work did not analyze the mixing intensity at which partial mixing was achieved. Based on Equation (2.2), $P \propto N^3 D^5$. In the current study, impeller diameter (D) was fixed while impeller speed (N) was adjusted until partial mixing was observed. It is recommended that the partial mixing power input per unit mass (i.e. mixing intensity) be calculated, and experiments performed where the impeller speed is fixed and impeller diameter is adjusted to reach the partial mixing intensity while maintaining turbulent mixing conditions. This would aid in determining the versatility of mixing intensity as a variable for predicting partial mixing conditions.

Finally, while various mixer configurations were tested in the current study, other parameters important to mixing were kept constant or tried under very limited conditions. For instance, variables such as impeller separation distance and submergence distance of the top impeller from the phase interface could not be varied. Additionally, the axial-to-radial impeller size ratio was maintained at 0.8 for all experiments in the horizontal settler. It is recommended that for future testing in a larger scale horizontal settler, the impeller separation distance, submergence distance from the phase interface, and the axial-to-radial impeller size ratio (while maintaining the axial impeller to be smaller than the radial) be investigated to gain more insight into the optimal mixer configuration for partial mixing.

References

[1] J. Dillinger. The World's Largest Oil Reserves By Country. URL https://www.worldatlas.com/articles/the-world-s-largest-oil-reserves-by-country.html, (2018).

[2] Government of Alberta. Old Sands Facts and Statistics. URL https://www.energy.alberta.ca/OS/AOS/Pages/FAS.aspx, (2018).

[3] Alberta Energy Regulator. ST98: 2018 - Alberta's Energy Reserves & Supply/Demand Outlook - Executive Summary. Technical report, (2018).

[4] J. H. Masliyah, J. Czarnecki, and Z. Xu. *Handbook on Theory and Practice of Bitumen Recovery from Athabasca Oil Sands Volume I: Theoretical Basis*. (2011).

[5] B. A. I. Keesom and J. A. I. Gieseman. *Bitumen Partial Upgrading 2018 Whitepaper - AM0401A*. Number March. (2018).

[6] A. Zachariah and A. De Klerk. Partial Upgrading of Bitumen: Impact of Solvent Deasphalting and Visbreaking Sequence. *Energy and Fuels*, 31(9):9374–9380, (2017). doi:10.1021/acs.energyfuels.7b02004.

[7] R. A. Meyers. *Handbook of Petroleum Refining Processes*. (1997). ISBN 0070417962. doi:10.1016/S1351-4180(04)00661-0.

[8] G. P. Laplante. On Mixing and Demulsifier Performance in Oil Sands Froth Treatment. *Department of Chemical and Materials Engineering*, Master of:30–31, (2011).

[9] J. Zawala, T. Dabros, and H. A. Hamza. Settling properties of aggregates in paraffinic froth treatment. *Energy and Fuels*, 26(9):5775–5781, (2012). doi:10.1021/ef300885t.

[10] J. Y. Chong. *Mixing Effects on Chemical Demulsifier Performance in Diluted Bitumen and Froth*. PhD thesis, (2013).

[11] Y. Long, T. Dabros, and H. Hamza. Structure of water/solids/asphaltenes aggregates and effect of mixing temperature on settling rate in solvent-diluted bitumen. *Fuel*, 83 (7-8):823–832, (2004). doi:10.1016/j.fuel.2003.10.026.

[12] D. Kosior, E. Ngo, and T. Dabros. Determination of the Settling Rate of Aggregates Using the Ultrasound Method during Paraffinic Froth Treatment. *Energy & Fuels*, 30 (10):8192–8199, (2016). doi:10.1021/acs.energyfuels.6b01714.

[13] P. Laplante, M. B. Machado, S. Bhattacharya, S. Ng, and S. M. Kresta. Demulsifier performance in froth treatment: Untangling the effects of mixing, bulk concentration and injection concentration using a standardized mixing test cell (CIST). *Fuel Processing Technology*, 138:361–367, (2015). doi:10.1016/j.fuproc.2015.05.028.

[14] J. Y. Chong, M. B. Machado, N. Arora, S. Bhattacharya, S. Ng, and S. M. Kresta. Demulsifier Performance in Diluted Bitumen Dewatering: Effects of Mixing and Demulsifier Dosage. *Energy and Fuels*, 30(11):9962–9974, (2016). doi:10.1021/acs.energyfuels.6b01996.

[15] Suncor. Fort Hills Mining and Extraction Process. URL `http://www.suncor.com/about-us/fort-hills`, (2018).

[16] N. H. Rahmani, T. Dabros, and J. H. Masliyah. Evolution of asphaltene floc size distribution in organic solvents under shear. *Chemical Engineering Science*, 59(3): 685–697, (2004). doi:10.1016/j.ces.2003.10.017.

[17] K. A. Johnston, F. F. Schoeggl, M. A. Satyro, S. D. Taylor, and H. W. Yarranton. Phase behavior of bitumen and n-pentane. *Fluid Phase Equilibria*, 442:1–19, (2017). doi:10.1016/j.fluid.2017.03.001.

[18] J. G. Speight. Solvent Processes. In *Heavy and Extra-heavy Oil Upgrading Technologies*, pages 129–147. (2013). ISBN 9780124045705. doi:10.1016/B978-0-12-404570-5.00006-5.

[19] D. Breakey and A. Cheung. Redesign Concept for Nexen–University of Alberta Solvent Deasphalting Experiments. Technical report, (2018).

[20] A. Kukukova, J. Aubin, and S. M. Kresta. A new definition of mixing and segregation: Three dimensions of a key process variable. *Chemical Engineering Research and Design*, 87(4):633–647, (2009). doi:10.1016/j.cherd.2009.01.001.

[21] S. M. Kresta. Mixing in the Process Industry, CH E 620. University of Alberta, Edmonton, Alberta, Canada, (2017).

[22] E. L. Paul, V. A. Atiemo-Obeng, and S. M. Kresta. *Handbook of Industrial Mixing*. John Wiley & Sons, Inc., Hoboken, New Jersey, (2004).

[23] S. M. Kresta, A. W. Etchells III, D. S. Dickey, and V. A. Atiemo-Obeng. *Advances in Industrial Mixing*. (2016).

[24] G. Zhou and S. M. Kresta. Impact of Tank Geometry on the Maximum Turbulence Energy Dissipation Rate for Impellers. 42(9), (1996).

[25] N. H. G. Rahmani, T. Dabros, and J. H. Masliyah. Fractal structure of asphaltene aggregates. *Journal of Colloid and Interface Science*, 285(2):599–608, (2005). doi:10.1016/j.jcis.2004.11.068.

[26] L. Gmachowski. Aggregate structure and hydrodynamics of aggregated systems. *Colloids and Surfaces A: Physicochemical and Engineering Aspects*, 255(1-3):105–110, (2005). doi:10.1016/j.colsurfa.2004.12.028.

[27] J. Gregory. The Density of Particle Aggregates. *Elsevier Science Ltd.*, 36(4):1–13, (1997).

[28] C. P. Johnson, X. Li, and B. E. Logan. Settling velocities of fractal aggregates. *Environmental Science and Technology*, 30(6):1911–1918, (1996). doi:10.1021/es950604g.

[29] J. Richardson and W. Zaki. Sedimentation and fluidisation: Part I. *Chemical Engineering Research and Design*, 75(3):S82–S100, (1997). doi:10.1016/S0263-8762(97)80006-8.

[30] N. H. Rahmani, T. Dabros, and J. H. Masliyah. Settling properties of asphaltene aggregates. *Energy and Fuels*, 19(3):1099–1108, (2005). doi:10.1021/ef0496707.

[31] F. G. Vaezi. *Effect of Laminar Shear on the Aggregate Structure of Flocculant-dosed Kaolinite Slurries*. PhD thesis, (2013).

[32] Y. Long, T. Dabros, and H. Hamza. Stability and settling characteristics of solvent-diluted bitumen emulsions. *Fuel*, 81(15):1945–1952, (2002). doi:10.1016/S0016-2361(02)00132-1.

[33] K. Rastegari, W. Y. Svrcek, and H. W. Yarranton. Kinetics of Asphaltene Flocculation. *Industrial & Engineering Chemistry Research*, 43(21):6861–6870, (2004). doi:10.1021/ie049594v.

[34] J. Burke. Solubility Parameters: Theory and Application. *The Book and Paper Group of the American Institute for Conservation*, 3:13–58, (1984).

[35] T. Wang and Y. Zhang. Methods for Determining the Solubility Parameter of Bitumen. 38(4):383–389, (2010).

[36] D. M. Koenhen. The Determination of Solubility Parameters of Solvents and Polymers by. 19:1163–1179, (1975).

[37] K. D. Mannistu, H. W. Yarranton, and J. H. Masliyah. Solubility Modeling of Asphaltenes in Organic Solvents. *Energy & Fuels*, 11(3):615–622, (1997). doi:10.1021/ef9601879.

[38] Y. Aray, R. Hernandez-Bravo, J. G. Parra, J. Rodriguez, and D. S. Coll. Exploring the structure-solubility relationship of asphaltene models in toluene, heptane, and amphiphiles using a molecular dynamic atomistic methodology. *Journal of Physical Chemistry A*, 115(42):11495–11507, (2011). doi:10.1021/jp204319n.

[39] D. E. Leng and R. V. Calabrese. Immiscible Liquid-Liquid Systems. In *Handbook of Industrial Mixing*, chapter 12, pages 639–753. (2004).

[40] B. M. Knickerbocker, C. V. Pesheck, L. E. Scriven, and H. T. Davies. Phase behavior of alcohol-hydrocarbon-brine mixtures. *Journal of Physical Chemistry*, 83(15):1984–1990, (1979). doi:10.1021/j100478a012.

[41] B. M. Knickerbocker, C. V. Pesheck, H. T. Davis, and L. E. Scriven. Patterns of three-liquid-phase behavior illustrated by alcohol-hydrocarbon-water-salt mixtures. *Journal of Physical Chemistry*, 86(3):393–400, (1982). doi:10.1021/j100392a022.

[42] S. Negahban, G. P. Willhite, S. M. Walas, and M. J. Michnick. Three-Liquid-Phase Equilibria of Ternary and Quatenary Mixtures, Water/n-Decane/2-Butyloxyethanol and Water/n-Octane/1-Propanol/Sodium Chloride - Experimental Measurements and Their Correlation with the UNIQUAC Model. *Fluid Phase Equilibria*, 32:49–61, (1986).

[43] D. Breakey. Experiment concept for three-phase mixing visualization. Technical report, (2018).

Appendix A

PFT Video Analysis

This appendix discusses the major successes and challenges encountered with the technique used to detect settling aggregates in the videos recorded.

As mentioned in Section 4.3.5, the settling of individual aggregates in a clear diluent-filled square glass column was recorded and the footage analyzed to determine aggregate sizes and settling velocities. These recordings were reviewed and timestamps in which aggregates were seen settling were written down. Footage from these timestamps were then converted into a series of images based on the frame rate of the CCD camera. In the current study, the camera recorded at 30 frames per second resulting in 30 images per 1 second of video converted. Images were processed and analyzed using a MATLAB program created by Dr. David Breakey.

Figure A.1 shows the extracted image of a settling aggregate before and after processing and detection with the MATLAB program was applied. From Figure A.1, the white dashed outline and the cross represent the identified border and centroid of the aggregate, respectively; the colored circle represents the equivalent diameter calculated based on the area identified inside the aggregate border. It is clear from Figure A.1 that the technique implemented by the program was able to successfully detect and determine the equivalent diameter fairly well. Furthermore, even though the aggregate was not entirely within the focal plane of the camera (indicated by it being blurry in the before image) the program was still able to successfully detect it. This was consistent for the majority of data sets in which only one or two aggregates appeared in the field of view at a given time.

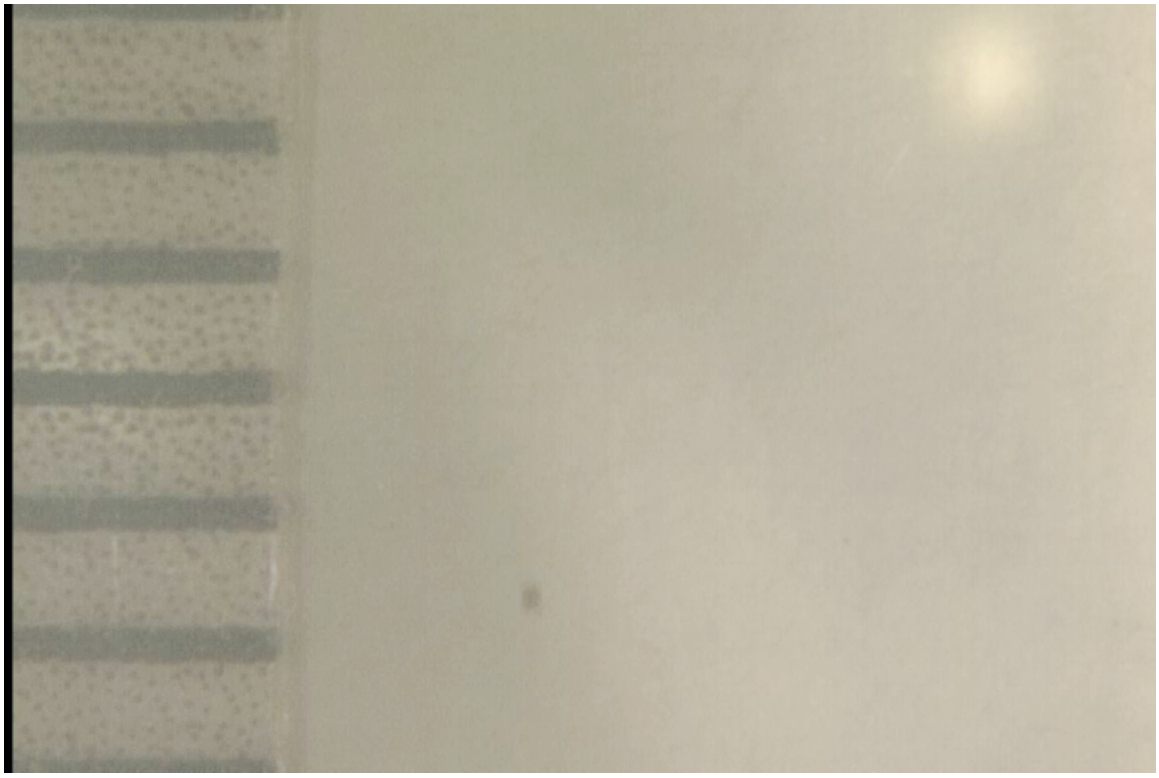

(a) Before processing

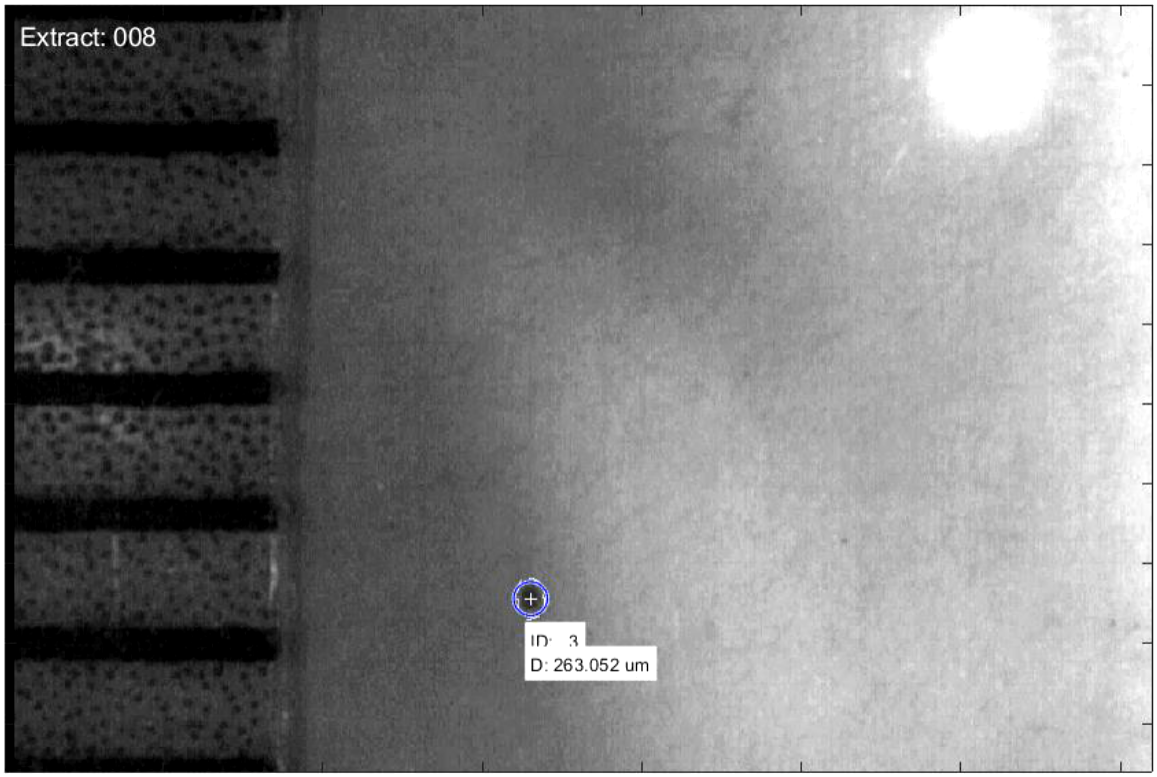

(b) After processing and detection

Figure A.1: Aggregate processing and detection for an aggregate produced at 1000 RPM and 30 min of mixing.

Although great care was taken to release only one aggregate at a time into the glass column, this was not possible for some samples due to the large number of solids formed. In particular, samples taken from tests where mixing was only performed for 2 minutes contained such a large number of aggregates that pipetting only a few at a time was extremely difficult. As such, video of aggregate settling from these samples contained several aggregates in any given frame. Figure A.2 shows an example of this for aggregates produced from mixing at 1000 RPM for 2 min. As it can be seen in Figure A.2, this can be a challenging image to process due to having many very small aggregates that are difficult to see. In fact, one of the major challenges encountered when processing the videos was detecting these small aggregates. This is apparent in Figure A.3 which shows the processed image using the MATLAB code. From Figure A.3, it is clear that while multiple aggregates are detected, many others were not accounted for. Generally, aggregates smaller than 200 μm were not included in the particle size distribution (PSD) because of this. Adjustments were made to filtering values during processing that was able to bring the minimum size detected down to 90 μm, but the issue of small aggregates being very difficult to see remained. Additionally, these smaller aggregates had a tendency to be counted multiple times as new aggregates when processing images.

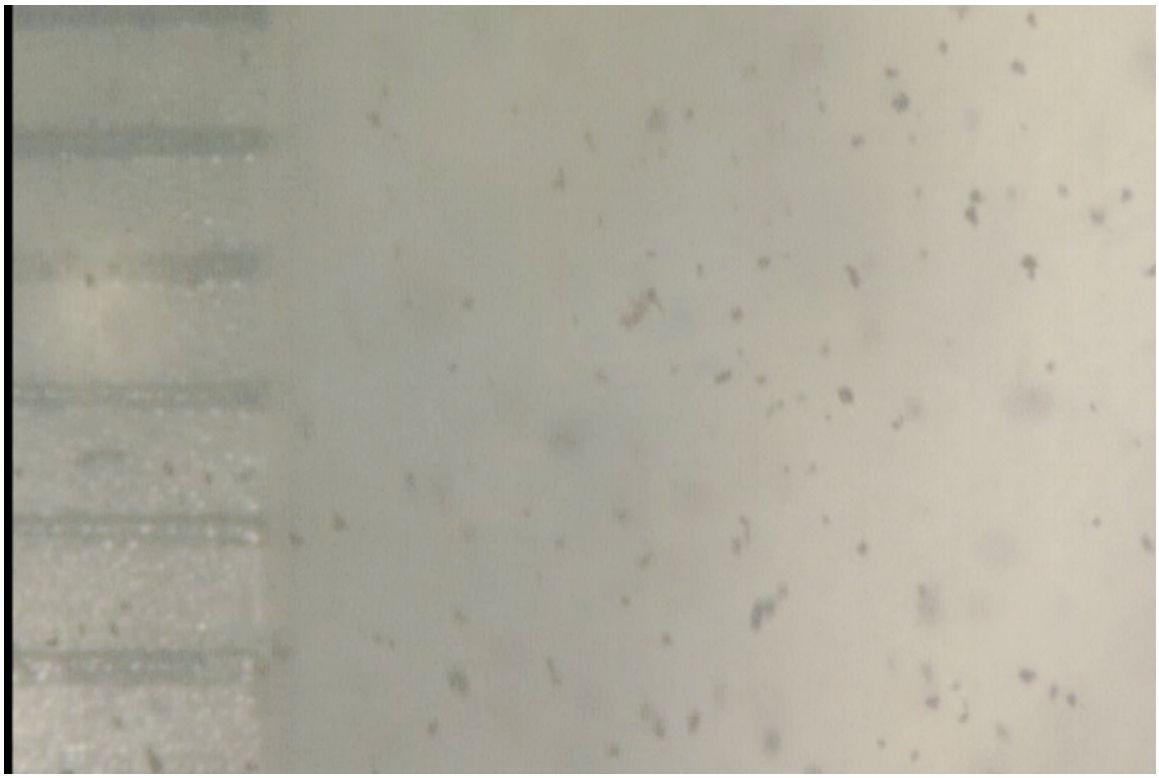

Figure A.2: Sample image of aggregates produced from mixing at 1000 RPM for 2 min before processing.

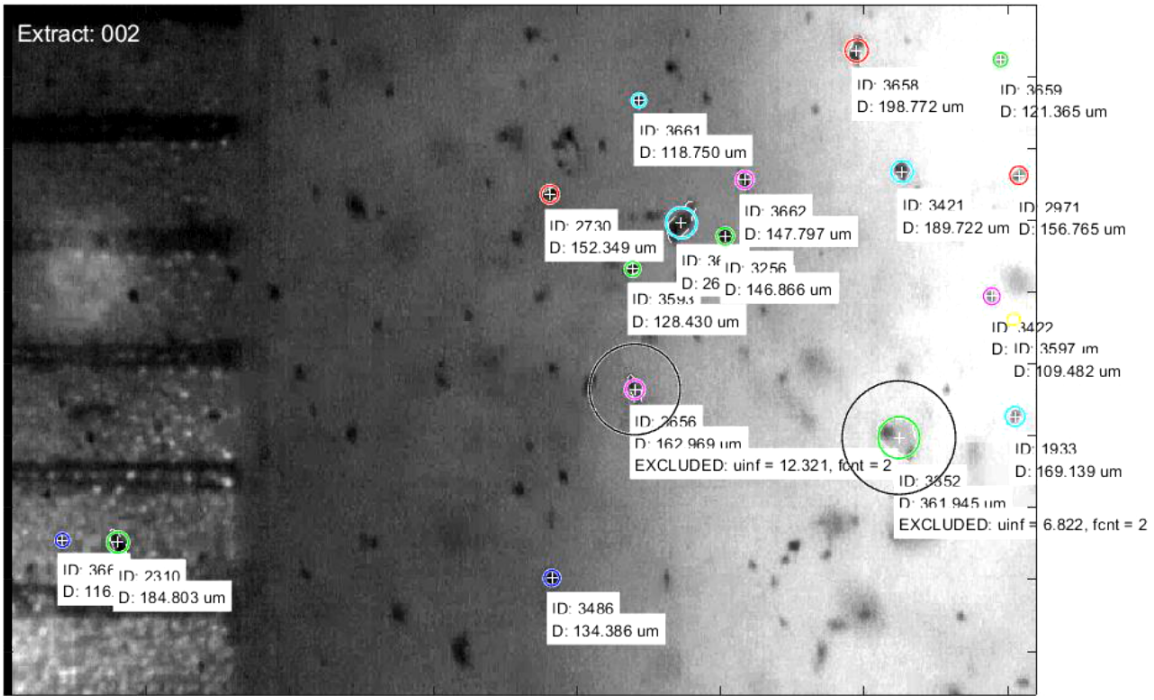

Figure A.3: Sample image of aggregates produced from mixing at 1000 RPM for 2 min after processing.

Overall, after much effort by Dr. David Breakey to minimize the errors resulting from these challenges, it was decided that the information obtained from this detection technique was only good enough to draw qualitative conclusions about the effects of mixing energy on individual aggregates and not quantitative ones. This is because varying detection parameters resulted in the technique becoming sensitive to different parts of the PSD. However, the PSDs produced from running at three different sets of parameters had considerable overlap and it proved extremely difficult to identify duplicates of the same aggregates detected from each parameter set. This prevented simply combining the results from different runs of the program. In the end, a medium filter value was chosen to minimize the issue of repeated counts of smaller aggregates while reasonably detecting them. Qualitative conclusions could still be drawn despite these challenges since the trends remained the same despite the shift in aggregate size and settling rate values observed when adjusting detection parameters.